Dopamine Release and Uptake in Animal Models of Neurological Diseases

By

Jenny L. Fulks

Submitted to the graduate degree program in Chemistry
and the Graduate Faculty of the University of Kansas in partial fulfillment of the
requirements for the degree of Doctor of Philosophy

_____

Chairperson Michael A. Johnson

_____

Carey K. Johnson

_____

Susan M. Lunte

_____

Richard S. Givens

_____

Stephen C. Fowler

Date defended: April 25th, 2011

The Dissertation Committee for Jenny L. Fulks
certifies that this is the approved version of the following dissertation:

Dopamine Release and Uptake in Animal Models of Neurological Diseases

_____

Chairperson Michael A. Johnson

Date approved: April 27th, 2011

ABSTRACT

Fast scan cyclic voltammetry (FSCV) can be utilized to detect neurotransmitter release and uptake in brain slices. When combining this technique with disease state animals models, information for therapeutic targets can be obtained. Herein, the evaluation of stimulated dopamine release and uptake in animal models was used in conjunction with pharmacological agents to assess neurological problems caused by Fragile X syndrome and chemotherapy. Fragile X Syndrome, a genetic form of mental retardation caused by a trinucleotide repeat expansion, was investigated by combining behavioral analysis and FSCV to determine alterations in dopamine release, dopamine uptake, effects of amphetamine treatments, and the functionality of the D2 autoreceptor. Side effects of chemotherapy can include alteration in neurological function and were investigated by using FSCV to monitor for effect on dopamine release and uptake patterns in the striatum of rats being dosed with Carboplatin, a chemotherapeutic drug. Finally, instrumentation was established to use caged compounds to photo release glutamate while collecting FSCV data of dopamine release to evaluate instantaneous effects of glutamate on the dopamine system in brain slices.

ACKNOWLEDGEMENTS

From the bottom of my heart I thank my parents. Throughout my life you have always encouraged me and had faith in my abilities. You have taught me the meaning of hard work and have always been my support. You taught my sisters and me to be strong, independent and capable women. I would not be the person I am today without your love and support. I will forever be grateful to have you as my parents. I love you and our whole family more than words can express. You are all such wonderful, giving people. Thank you for all your love and support and the many trips you took to Kansas to either help me move or bring my nephews to visit.

Thank you to my husband for your encouragement and support. You have always maintained your faith in me even when I have doubted myself. Thank you for spending our anniversary with me in the lab while I worked on experiments. My dear daughter Isabelle, you inspire me every day. I do my best to be a wonderful mother to you. You may only be a few months old but I have already told you many things about science. I look forward to teaching you more and more as you grow.

I am grateful to the Chemistry Department faculty at the University of Kansas. You have taught me so many things in my time at KU and have challenged and inspired me. I am especially grateful to my mentor Dr. Michael Johnson, who is a wonderful scientist and teacher. Through all the ups and down that life has brought with it over the last few years, you have provided unwavering support. I also thank all of the current and past members of the Johnson group. You have helped my love and understanding of science grow.

I am also thankful to all of those I was fortunate to meet and develop friendships with while attending Benedictine College. It was you who helped my love of chemistry develop, especially Dr. Aileen Beard who was a wonderful academic advisor and teacher. Without all of you I would not have come to this point in life. You have always encouraged and motivated me to try to become the best person possible. Your faith and love is important to me.

TABLE OF CONTENTS PAGE

CHAPTER 1 INTRODUCTION

Understanding the underlying chemical mechanisms of neurological disorders and diseases is key to being able to successfully develop therapeutic methods of treatment. It is necessary to be able to study neurological systems without causing much disturbance or damage to the system. Fast scan cyclic voltammetry (FSCV) has become a useful method for the measurement of neurochemical release both *in vitro* and *in vivo.* FSCV has long been used to evaluate dopamine release and uptake in brain slices from animal models of disease or altered brain chemistries (*1*). When pairing FSCV in brain slices with pharmacological agents, such as dopamine transporter antagonists or dopamine autoreceptor agonists, information can be obtained about the neurological system. The following sections include an introduction to FSCV, the brain dopamine system, the measurement of dopamine release and uptake, and calculating dopamine uptake parameters using modeling software. The work done using the application of the FSCV method to evaluate dopamine release and uptake in Fragile X syndrome as well as the phenomenon known as “chemobrain” are presented. Finally, a method for the combination of FSCV with photoreleased glutamate to determine immediate effects on dopamine release and uptake are discussed.

1.1 Electrochemical Methods

1.1.1 Overview of voltammetry

Voltammetry is an electroanalytical method that obtains information about an analyte by varying the potential applied to an electrode and then detecting the current produced by the electrochemical reaction of the analyte at the electrode surface. Voltammetry can be used to study various types of analytes and systems including inorganic ions and organic molecules in solution. A major shift in the use of voltammetric methods occurred in the early 1970's as Ralph N. Adams began to use voltammetry as a method for evaluating biological amines *in vivo,* thus opening a new field for electrochemical applications in evaluation of biological systems containing electroactive molecules(*2*).

In a typical electrochemical system used to collect voltammetric measurements, a working electrode, a counter electrode, and a reference electrode are employed, **Figure 1**. The working electrode is the electrode that will have an applied potential that will change based on the waveform applied by the potentiostat, thereby causing the redox reaction to occur. The potential of the working electrode is measured versus a reference electrode that will have a constant potential. A counter electrode, made up of an inert material, is often used to complete the circuit, but has little to no part in the measured redox reaction. The potentiostat controls the electrical potential between the working and reference electrodes at a preset value by forcing the necessary current to flow between the working and counter electrodes to maintain the desired potential.

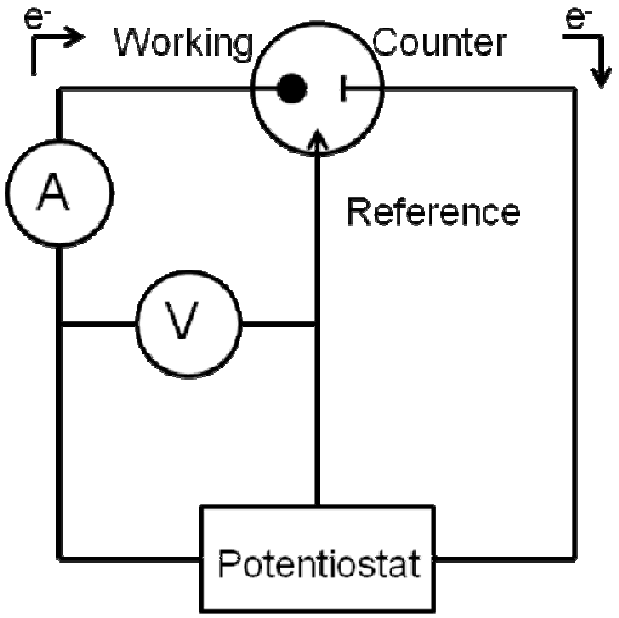

Figure 1. Diagram of a three electrode system. The working, counter and reference electrodes are labled. A represents an ammeter measuring the current, while V is representative of a voltmeter measuring the voltage difference between the reference and working electrodes.

1.1.2 Cyclic Voltammetry

Cyclic voltammetry is performed by applying a triangular waveform (**Figure 2**) to the working electrode where the electrode potential is rapidly increased linearly over time then decreased to the starting potential.

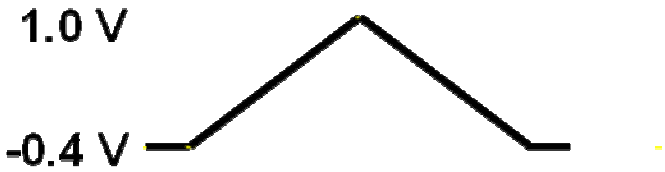

Figure 2. Triangular waveform scan from -0.4 V to 1.0 V to -0.4 V.

As the potential becomes more positive, the working electrode will become electron deficient. If a suitable electroactive analyte is present, an oxidation reaction will occur at the surface of the electrode. The oxidation reaction will cause a transfer of electrons from the molecule being oxidized to the electrode. This flow of electrons can then be measured as a current. This current, known as the anodic peak current (i_{pa}), will be proportional to the amount of analyte at the surface of the electrode. As the potential is scanned back down to the starting point, the working electrode becomes more electron rich. If the oxidation reaction is reversible, a reduction reaction can now occur at the surface of the electrode and be detected again as a current, the cathodic peak current (i_{pc}), as the electrodes are transferred to the oxidized form of the analyte, regenerating the starting analyte. When the oxidation causes the formation of a different species that will not undergo a reduction reaction when the potential is scanned back to the starting point, the oxidation reaction is not reversible, however an oxidation potential can still be detected. The potentials at which these current peaks occur as well as the ratio of the anodic and cathodic peaks can be used to determine the identity of the analyte.

Voltammetry in solutions that have attained a state of equilibrium obeys the Nernst Equation (**Equation 1)** where the reactions occurring are electrochemically reversible.

$$E = E^o + \frac{RT}{nF} \ln \frac{C_O}{C_R} \qquad \textbf{Equation 1}$$

Where E is the cell potential, E^o is the standard cell potential, C_O is the concentration of the oxidized species, C_R is the concentration of the reduced species, and n is the number of electrons involved in the redox reaction.

An electrochemical reaction is considered to be reversible if it meets the following conditions. First, the voltage separation between the anodic and cathodic peaks follows **Equation 2**,

$\Delta E = E_{p,a} - E_{p,c} = 0.059V/n$ **Equation 2**

Where n is the number of electrons transferred in the reaction. **Figure 3** is a representative voltammogram with the cathodic and anodic peaks labeled.

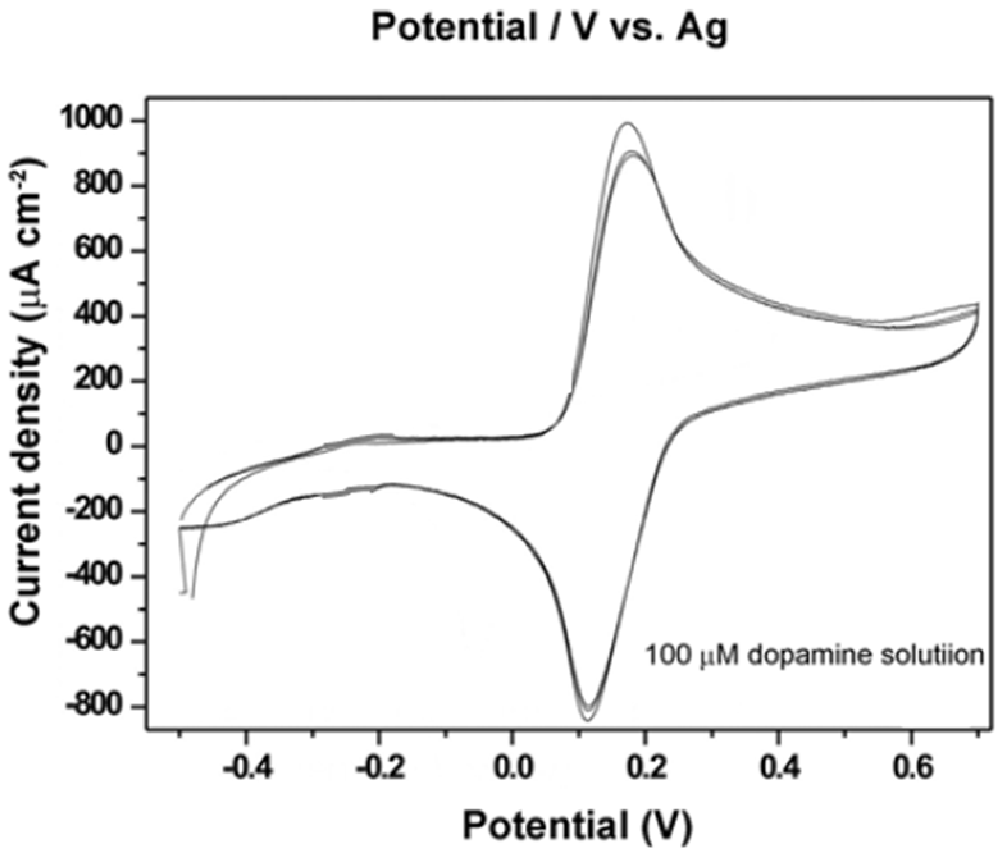

Figure 3. Depiction of a reversible slow scan cyclic voltammogram of dopamine (*3*). Figure modified from Ates *et al*. 2009.

However, when using high scan rates the electron transfer rate slows in relation to the scan rate. Due to the inability of the electron transfer to keep up with the fast scan rate a higher potential is required to cause the oxidation to happen, thus the oxidation and reduction peaks are separated, yet the reaction is still electrochemically reversible (*4*). Another criterion for reversibility is that there must be symmetry in the voltammogram between the peaks (**Equation 3**) and as shown in **Figure 3**.

$|i_{p,a}/i_{p,c}| = 1$ **Equation 3**

This property of reversibility is also dependent on the scan rates used. The relationship between scan rate and the maximum current is described by the Randles-Sevcik equation (**Equation 4**).

$i_p = 0.4463\ n\mathrm{FAC}(n\mathrm{FvD/RT})^{1/2}$ **Equation 4**

Where *n* is the number of electrons involved in the redox reaction, F is Faraday's constant, C is the concentration of the species, D is the diffusional coefficient. Increasing the scan rate will also increase the maximum current and has the same effect as increasing the rate of diffusion of the oxidized species in the case of DA. This increase in current due to an increase in scan rate is due to an increase in the flux of the analytes in the diffusional layer increase number of analyte molecules coming into contact with the electrode. It is also due to this increase in flux that the oxidized species diffuses away and is not available in the same concentration at the electrode surface to be reduced, leading to a decrease in the peak height of the reduction peak (*5*). This diffusion causes the reduction peak to be smaller than the oxidation peak and thus the ratio of the peaks is not 1, yet the reaction is still reversible, as is the case with DA using fast-scan cyclic voltammetry.

1.1.3 Fast Scan Cyclic Voltammetry (FSCV)

Fast-scan cyclic voltammetry (FSCV) is a method of voltammetry which utilizes high scan rates and can collect data on a sub-second time scale. In this work a scan rate of 300 V/s was utilized using a carbon-fiber microelectrode with a Ag/AgCl reference electrode. A plot of the current changes detected from the oxidation and reduction of the analyte versus the potential applied can be generated, creating a cyclic voltammogram. FSCV utilizes microelectrodes due to the temporal resolution and beneficial diffusional characteristics which are discussed in section 1.2.1. The sub-second time-scale of data collection associated with the high scan rates allows for the detection of very quick biological processes. FSCV also allows for the detection of very small changes (nA scale) in current due to the electrode area and based on **Equation 4**. This detection of small currents is also beneficial for biological systems where the concentrations of analytes are low (µM) (*6*).

As an electrode becomes electron deficient the negative species in the solution around the electrode will assemble next to the electrode forming the inner Helmholtz layer. From there a layer of positive charges will be attracted to the negative layer forming the outer Helmholtz layer. Another layer of opposing charges known as the Gouy-Chapman layer will form after this and then the bulk of the solution will remain heterogeneous (**Figure 4**). This is known as the double layer effect. The double layer causes a capacitance current by creating charging currents. Charging currents cause an excess or deficiency of negative charges at the surface of the electrode. Due to this difference in charge layers of opposing charges form that are different than the bulk of

the heterogeneous solution. The charges assemble adjacent to the electrode surface within a few hundred angstroms. By subtraction of the background current, the capacitance current is removed from the voltammogram and the result yields a voltammogram of the analyte of interest (*7*).

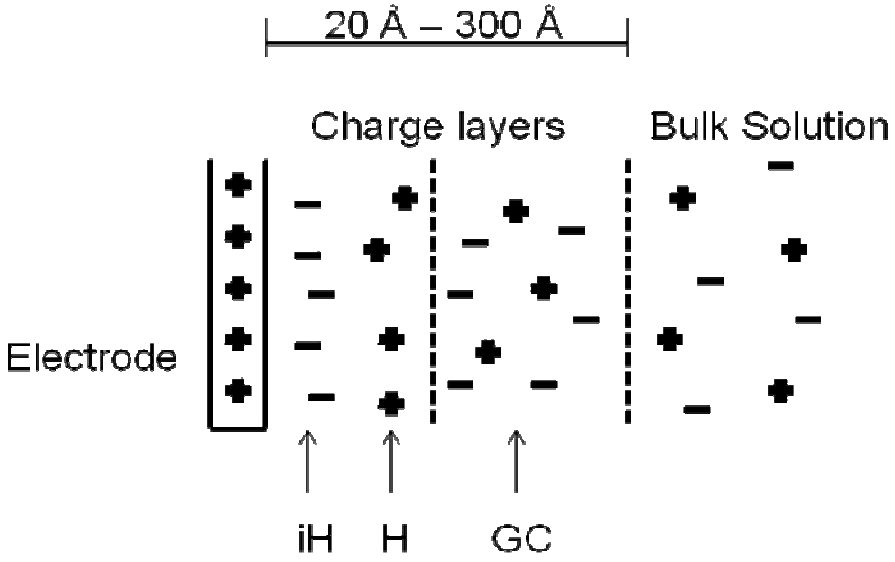

Figure 4. Depiction of how charges align creating a double layer when a potential is applied to the working electrode. iH represents the inner Helmholtz layer, H represents the outer Helmholtz layer and GC is the Gouy-Chapman layer. Figure based on information found in Bard and Faulkner(*18*).

1.1.4 Voltammetry in biological systems

Voltammetry, when coupled with microelectrodes, provides advantages over other means of chemical detection in biological systems. One popular method for biological sampling is microdialysis. While microdialysis is a powerful analytical method, the probes used are on average around 200 µm in diameter, while microelectrodes used in voltammetry can range in size from less than 10 µm to 20 µm in diameter (*7*). Microdialysis is advantageous in that it allows for the sampling of

multiple types of neurochemicals over long periods of time; however, the size of the probe may lead to increased tissue damage compared to smaller electrodes (*8*). Moreover, the use of carbon-fiber microelectrodes allows for the measurement of neurotransmitter release and uptake on sub-second timescales, compared to minute timescales when using microdialysis.

1.2 Microelectrodes

1.2.1 Microelectrodes in FSCV

Microelectrodes used in biological measurements have been constructed using a variety of configurations, such as cylindrical, disk, ring and spherical, utilizing different materials including, but not limited to, carbon fibers, platinum, and gold (*9-15*). This work has utilized the cylindrical carbon-fiber microelectrode. The surface properties of cylindrical carbon fiber microelectrodes can be easily manipulated with electrochemical pretreatments and have been shown to be less prone to surface degradation and fouling in tissues than microelectrodes made of metal, thus making them beneficial for use in biological applications (*16*).

Carbon-fiber microelectrodes are particularly useful for measuring neurotransmitter concentration changes that occur on fast timescales. Typically, in our applications, 10 CVs/s are collected using scan rates of 300 or 400 V/s, however, higher scan rates and CV collection rates may be used. The ability to collect measurements with these temporal resolutions is facilitated by the diffusional properties of microelectrodes. The diffusion that occurs around the surface of the microelectrode

yields a much greater current density around the electrode in comparison to macroelectrodes and is necessary for the analyte to reach the electrode surface and undergo an electrochemical reaction at the surface of the electrode. The diffusion occurring around a cylindrical microelectrode occurs in only one dimension, however, in the case of cylindrical microelectrodes a "quasi" steady state that follows **Equation 5 occurs** (*17-18*).

$I_{qss} = 2nFAD_oC_o^*/r_o \ln\tau$ Where $\tau = 4D_ot/r_o^2$ **Equation 5**

Where n= the number of electrons transferred in the electrochemical reaction, F= Faraday's constant, D_o= the diffusional coefficient of the oxidized species, C_o^*= the concentration of the oxidized species in the bulk solution, r_o= the radius of the electroactive surface of the electrode, and t= time.

Analysis of the equation reveals that, due to time being in the denominator of the equation, i_{qss} is in a constant decline. However, time is found in the τ equation and thus subject to the logarithmic function and when working in a time scale of seconds, this time dependent decline of i_{qss} occurs at a relatively slow rate.

Another beneficial quality of using microelectrodes is that the low charging currents. The charging current is proportional to the surface area of the electrode, thus decreases as the area of the electrode decreases as shown in **Equation 6**.

$i_c \propto 1/A$ **Equation 6**

Where i_c is the charging current and A is the area of the electrode. Lowering the charging current lowers the amount of noise in the current detection, thus decreasing the limit of detection (*15*). When a reaction occurring at the electrode surface causes a large increase in current, that excess current, when traveling through a resistive solution, creates a potential that opposes the applied potential. This potential is known

as the iR drop and can interfere with the data by distortion of the cyclic voltammogram. In order to account for the excess current, a counter electrode is used as an electron sink in a three electrode system. Microelectrodes allow for the use of a two electrode system, eliminating the need for a counter electrode. The small surface area and small concentration of analyte produces small currents, causing the iR drop to be negligible (*4, 15*). In the two electrode cell, the working electrode both causes the reaction with the analyte to occur by application of a potential from the potentiostat and also detects the change in current caused by the redox reaction (*4*).

1.2.2 Fabrication of cylindrical carbon-fiber microelectrodes

Carbon fiber microelectrodes are constructed by aspirating a single carbon fiber through a glass capillary tube. The capillary is then pulled with a glass puller to form a glass seal around the carbon fiber. The carbon fiber is then cut to the desired length beyond the glass seal under a microscope using a scalpel (**Figure 5**). Once the fibers are cut to the appropriate length, the tips of the electrodes are dipped in an epoxy resin. By capillary action the resin fills in any gaps in the glass seal around the carbon fiber. The excess resin is rinsed off of the fiber with toluene to ensure that no resin remains on the surface of the carbon fiber. The resin is then cured by heat in an oven.

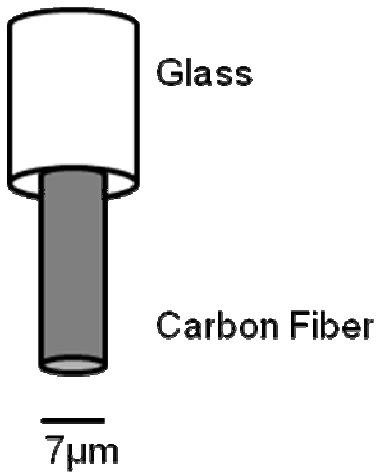

Figure 5. Depiction of a carbon fiber microelectrode tip. The glass seal is shown around a cylindrical carbon fiber which is cut extending beyond the glass seal.

1.2.3 Electrode Calibration

Carbon fiber microelectrodes are calibrated in a flow cell to determine their response to a specific concentration of analyte. The potential waveform and all other electrochemical parameters that will be used during data collection are used when calibrating the electrodes. Artificial cerebral spinal fluid (aCSF) is continuously flowed across the surface of the electrode. Since FSCV is a background subtracted method, the aCSF is allowed to flow for 3 to 5 seconds before introducing the dopamine containing solution. An HPLC injection valve is used to switch the flow solution from aCSF to aCSF containing a known concentration of dopamine. The electrode is exposed to the dopamine solution for 5 seconds and then the valve is switched back to the plain aCSF. The peak current from the DA exposure is measured and used to determine the nA/µM calibration factor for the electrode.

1.2.4 Dopamine detection using FSCV at carbon-fiber microelectrodes

Dopamine has been identified as a major catecholamine neurotransmitter that plays a role in many important neurologic functions, including locomotor activity (*19-20*), memory (*21-22*), motivation and reward (*23*), cognition (*24*), food intake and emotion(*21, 25*). Alterations in dopamine release and uptake have been characterized in various neurological disorders including a decrease in stimulated release in mice models of Huntington's disease (*1*), the loss of dopaminergic neurons in both postmortem human examinations and animal models of Parkinson's disease, and post-mortem analysis of human tissue has revealed high levels of dopamine in schizophrenia (*26*). The use of voltammetry has allowed for the determination of alterations in dopamine responses in the brain with little damage to the system being evaluated (*2, 27-28*).

Because dopamine readily gives up 2 electrons, it can be easily oxidized. The dopamine-o-quinone that forms from the oxidation reaction can then be converted back to dopamine by a reduction reaction. Using FSCV with a triangular waveform (-0.4 V to +1.0 V) and a scan rate of 300 V/s, when the potential applied to the electrode reaches +0.6 V the dopamine at the surface of the electrode will lose two electrons and produce a detectable current. As the potential is scanned back down to the starting potential, when -0.2 V is reached the dopamine-o-quinone will accept two electrons (**Figure 6**) and thus a dip in current will be detected as the reduction reaction occurs.

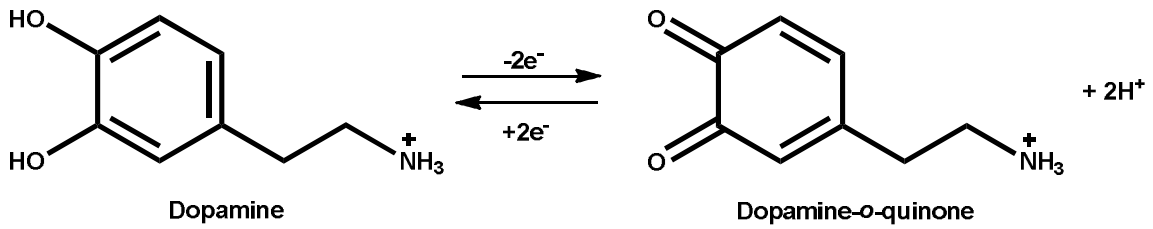

Figure 6. Dopamine is oxidized, losing two electrons, to form dopamine-*o*-quinone. The dopamine-*o*-quinone can then accept two electrons to reform dopamine.

1.3 Dopamine synthesis, release, and uptake

1.3.1 Dopamine Synthesis and metabolism

Dopamine, which does not cross the blood brain barrier, is synthesized in the brain from the amino acid precursor tyrosine. Tyrosine crosses the blood brain barrier and is taken up into dopaminergic cells in the brain. The tyrosine is then converted to DOPA by tyrosine hydroxylase. DOPA decarboxylase then converts DOPA to dopamine (**Figure 7**). The dopamine can then be packaged into vesicles by the vesicular monoamine transporter (VMAT) for release (*29-30*).

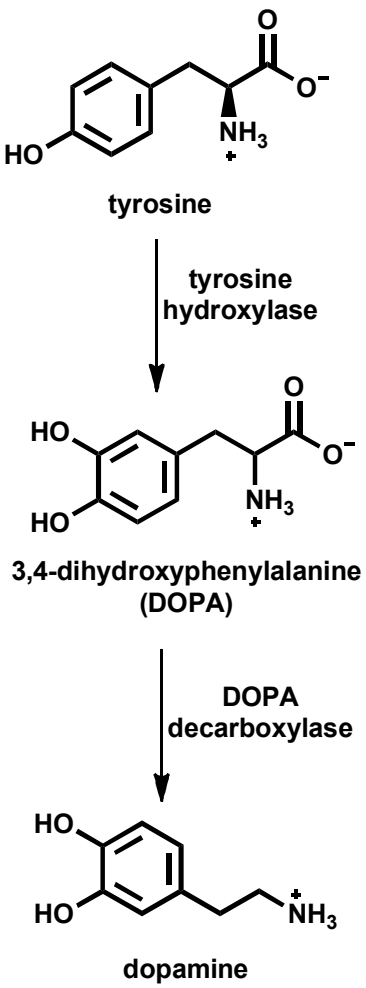

Figure 7. The synthesis of dopamine in the presynaptic terminal.

Metabolism of DA can happen both inside the dopaminergic cell and in the extracellular space. Inside of the cell, monoamine oxidase (MAO) can act on the DA converting it to 3,4-Dihydroxyphenylacetic acid (DOPAC), which can then be transformed to homovanillic acid (HVA) by catechol-*O*-methyltransferase (C*O*MT) (**Figure 8**). Extracellularly, a portion of the released DA can be transformed by C*O*MT to 3-methoxytyramine (3-MT) which can then be converted to HVA by MAO. DA can also be converted to norepinepherine by dopamine-β-hydroxylase (*31*).

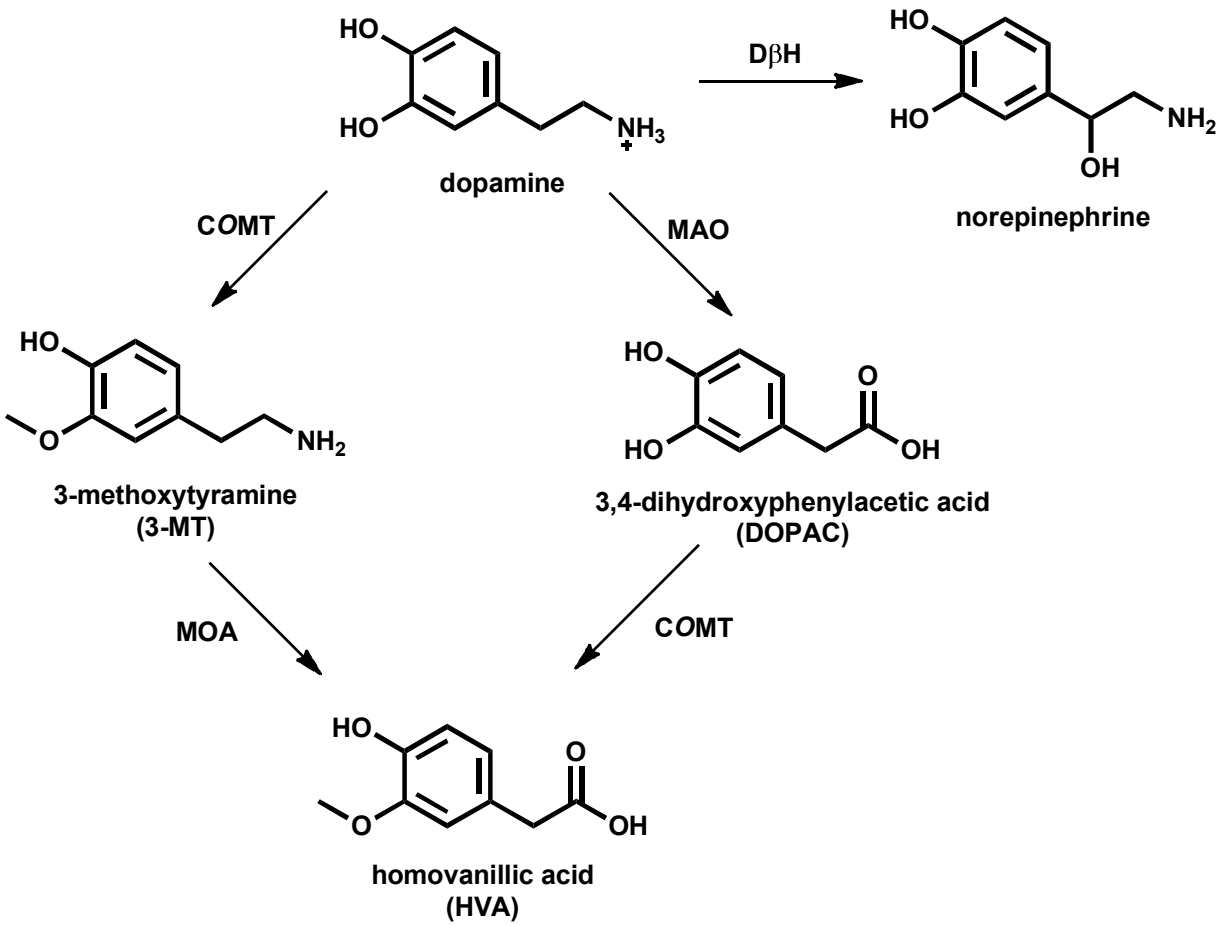

Figure 8. The metabolism of dopamine and its metabolites. Where C*O*MT is catechol-O-methyl transferase, DβH is dopamine beta hydroxylase and MOA is monoamine oxidase.

1.3.2 Detection of Dopamine and its Metabolites by HPLC

HPLC, when paired with an electrochemical detector, can be utilized in the separation and detection of electroactive species. It has been previously used to detect DA and its metabolites in samples prepared from brain homogenate (*32-33*). Samples can be obtained from specific brain regions, in this work the striatum was removed, and homogenized to evaluate total DA content in the striatum and compare DA concentrations between animal models of neurological diseases to their wildtype counterparts.

Briefly, the chromatographic separations were carried out isocratically with a mobile phase containing 10% organic phase (acetonitrile) and 90% aqueous phase (75 mM sodium dihydrogen phosphate monohydrate, 100 µL/L triethylamine, 25 µM EDTA tetrasodium tetrahydrate and 1.7 mM 1-octanesulfonic acid sodium salt) at a flow rate of 0.4 mL/min. The column used for compound separation was a C 18 column, utilizing reverse phase chromatography allowing the separation to occur based on molecular polarity where the most polar molecules are eluted first. A calibration standard chromatogram is shown in **Figure 9** indicating good separation and detection of norepinephrine (NE), DHBA (the internal standard), DOPAC, DA and homovanillic acid (HVA).

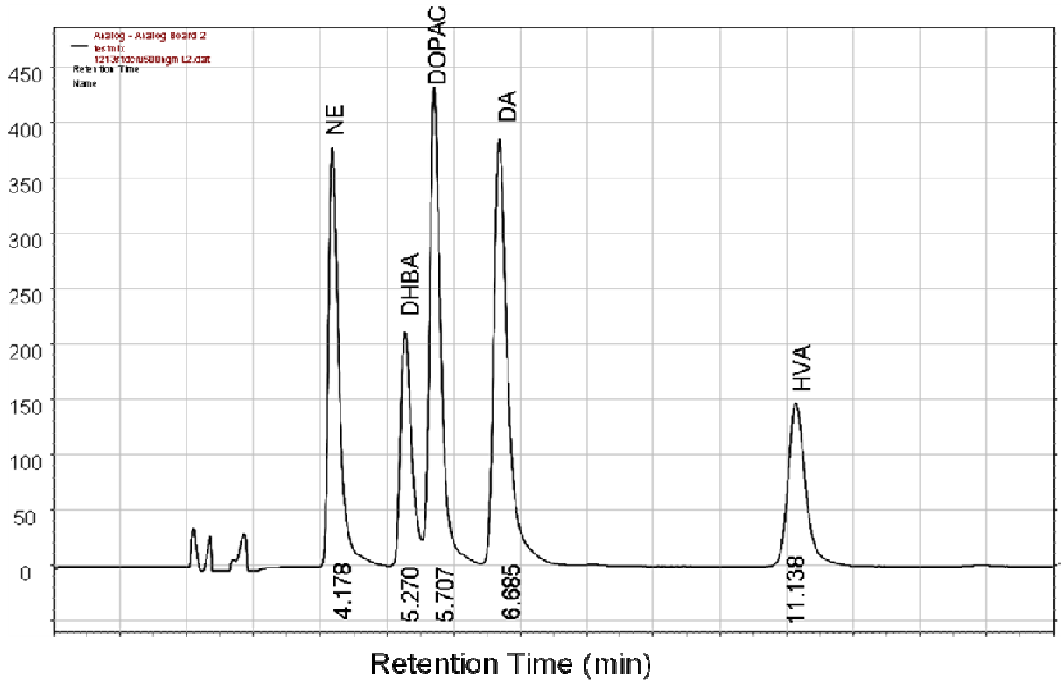

Figure 9. HPLC chromatogram of a calibration standard for the quantification of DA and its metabolites in the striatum of mice.

1.3.3 Dopamine release

1.3.3.1 The synapse

The synapse is the junction formed between two neurons and is the site at which neurotransmitters are released and communications between the two cell bodies takes place. The release of neurotransmitters from the presynaptic terminal occurs with the depolarization of the terminal due to an action potential. When neurotransmitters are released they can either act on the presynaptic receptors, cross to the postsynaptic terminal where they can act on postsynaptic receptors, be taken back into the presynaptic terminal by a transmitter specific transporter, or can diffuse out of the synaptic cleft to act on receptors on other neurons.

1.3.3.2 Vesicular release

Neurotransmitter release occurs by exocytosis of synaptic vesicles at the membrane surface of the synapse. After DA is synthesized in the presynaptic terminal it is packaged into vesicles by VMAT2, the neuronal vesicular monoamine transporter. The vesicles near the surface of the synaptic membrane, considered the active zone, then undergo docking and priming, preparing them for an action potential that will cause them to release their contents into the synaptic cleft. When an action potential occurs, voltage-gated Ca^{2+} channels are opened and the neurotransmitters are released by fusion of the vesicular membrane with the neuronal membrane, followed by endocytosis of the vesicle. (*34*).

Three different modes or vesicular recycling have been observed in single cell preparations (*35*). The first and fastest mode has been termed “kiss and run” in which

the vesicle quickly binds, releases its contents and is quickly retrieved from the membrane to be recycled, occurring on a time scale between 400 and 860 ms. The second type, compensatory, takes between 10 to 30 seconds for the fusion and recycling of the vesicle to occur. The third mode of recycling, stranded, occurs when the vesicle fuses and releases its contents, but remains attached to the membrane until another action potential occurs. DA has been shown to be released under all three of the mentioned modes of vesicular release and recycling (*36*).

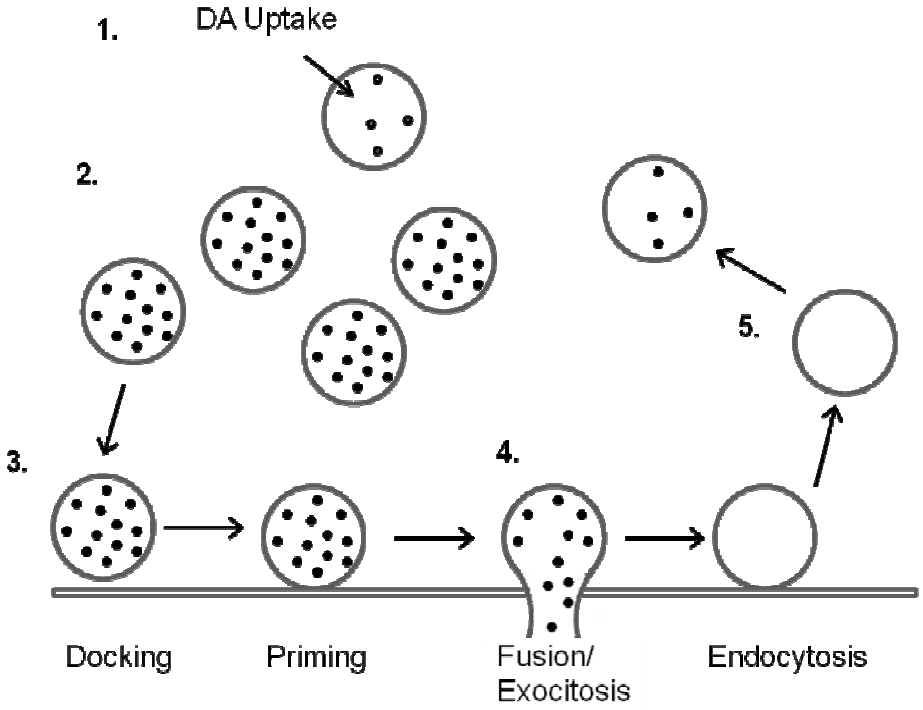

Figure 10. Vesicular release of DA into the extracellular space. 1. DA is packaged into vesicles by VMAT2, the vesicular monoamine transporter, which then become a part the vesicles ready for release (2). 3. The vesicles then dock with the membrane and are primed. 4. After in influx of Ca^{2+} the exocytosis of DA occurs. The vesicle then separates from the membrane and is recycled back (5) to be refilled with DA.

Vesicles have been classified as being a part of three distinct categories: the readily releasable pool (RRP), the recycling pool and the reserve pool (*37-40*). The RRP consists of the vesicles that are near the synaptic membrane and exocytose upon mild stimulation. The recycling pool is made up of those vesicles that will replace the RRP after exocytosis. The reserve pool vesicles, the largest pool in the presynaptic terminal, is only mobilized after long periods of synaptic activity (*41*).

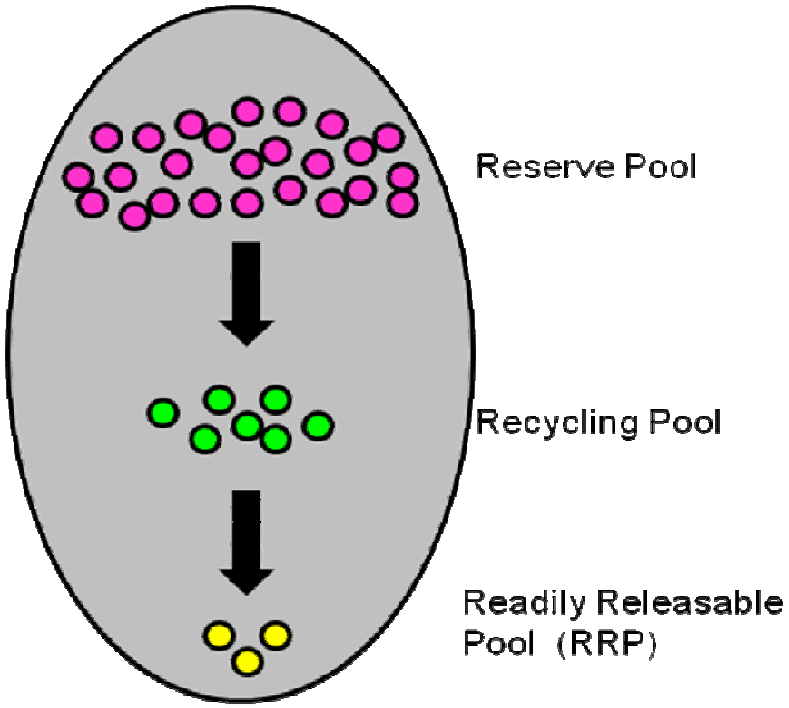

Figure 11. The three pools of DA. The most abundant pool is the reserve pool, however it takes intense stimulation to activate this pool.

1.3.4 Neurotransmitter diffusion

Most neurotransmission occurs within the synaptic cleft between the presynaptic and postsynaptic terminals where the released neurotransmitter acts upon the receptors within that cleft. DA transmission in the striatum has been shown to diffuse outside of the synaptic cleft of release and acts upon other target receptors distances of over 12

μm away (*42-44*). The ability of DA to diffuse outside of the synaptic cleft allows DA to cause an effect on a much larger number of target cells.

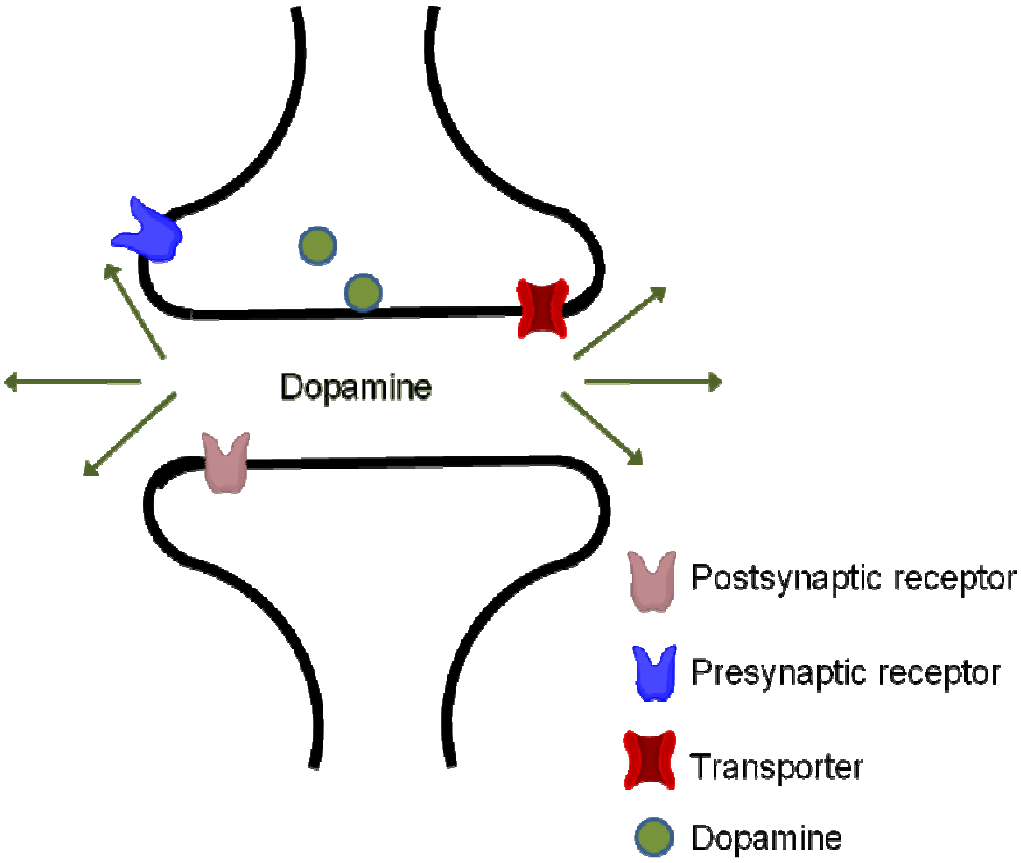

Figure 12. Simplification of the diffusion of DA in the synaptic cleft after vesicular release. DA can be taken up back into the presynaptic terminal by the DA transporter, it can diffuse to one of the DA receptors or it can diffuse out of the synaptic cleft.

1.3.5 Dopamine Receptors

Dopamine receptors were classified into two categories when discovered. These groups are now known as D1-like and D2-like. The DA receptors are G protein-coupled metabotropic receptors that primarily function through affecting cyclic adenosine monophosphate (cAMP) levels (*25*). The D1-like receptors, which include the D1 and D5 receptors, increase cAMP levels by increasing adenylyl cyclase (AC) activity, while

the activation of D2-like receptors, including D2, D3 and D4 receptors cause a decrease in cAMP by inhibition of AC.

The activity of the D2 receptor is of particular interest when it comes to regulation of DA release in DA neurons. Activation of the D2 receptor has been shown to decrease DA release (*45-48*). The stimulation of presynaptic D2 receptors causes a feedback mechanism that lowers DA levels by inhibiting DA synthesis and release (*49-50*). The D2 receptor agonist quinpirole has been shown to deplete stimulated DA release in the striatum (*51*).

Table 1. Dopamine Receptors and their functions (*25, 48, 52-58*).

D1-Like	D1	Stimulatory effect – activates adenylyl cyclase Most abundant DA receptor Regulates D2 responses Predominately postsynaptic
	D5	Stimulatory effect – activates adenylyl cyclase Expressed in limbic regions Predominately postsynaptic
D2-Like	D2	Regulate DA release by inhibiting DA synthesis, storage and release Autoreceptor for Dopamine Presynaptic and postsynaptic receptor
	D3	Inhibits adenylyl cyclase Postsynaptic receptor Possible autoreceptor
	D4	Function not well characterized

1.3.6 Dopamine Transporter (DAT)

The dopamine transporter (DAT) is a transmembrane protein located on the plasma membrane of the presynaptic nerve terminal to transport extracellular DA into the neuron from the extracellular space. DAT is a key element in termination of neurotransmission by DA by removing it from the extracellular space where it can act on DA receptors (*59-61*). DAT is made up of 12 transmembrane domains with alternating

extracellular and intracellular loops with both the C- and N- terminus located inside the cell. The transporter is Na^+/Cl^- dependant, requiring a sodium ion to bind extracellularly in order for DA to bind and the transporter to undergo a conformational change and move both the sodium and dopamine into the intracellular space (*62*).

1.4 Measuring Dopamine Release and Uptake in Brain Slices

1.4.1 Neuroanatomy

The area of dopaminergic activity of interest in this work is the Caudate-Putamen (CPu), also known as the striatum. The CPu receives a substantial amount of dopaminergic input from two distinct populations of DA neurons, the dorsal tier neurons and the ventral tier neurons (**Figure 13**). The dorsal tier neurons have their cell bodies located in the dorsal substantia nigra pars compacta (SNc), while the ventral tier neuron cell bodies are located in the ventral SNc (*63*). These neurons extending from the SNc to the CPu maintain their topographical pattern between the two regions (*64-65*). These projections of neurons that begin in the SNc and terminate in the CPu are known as the nigrostriatal pathway. The nigrostriatal pathway is involved in motor control by involvement in the basal ganglia loop and it is the destruction of the nigrostriatal pathway that plays a major role in causing Parkinson's disease and the loss of motor control associated with the disease (*64*).

Movement is triggered from the SNc by the nigrostriatal pathway causing activation of DA receptors in the striatum. The activation of these receptors is fundamental in maintaining normal posture and the origin of normal movements (*58*). A

loss of DA activity in the striatum has been shown in both Huntington's chorea and in Parkinson's disease (*1, 66*).

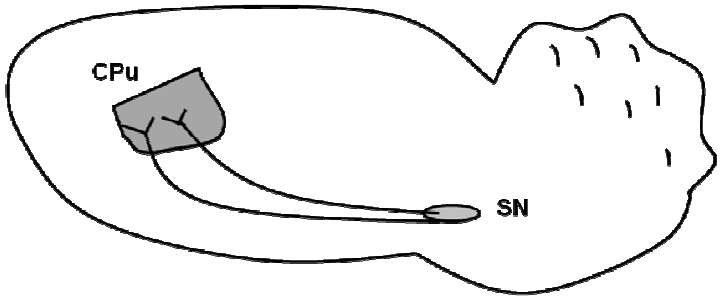

Figure 13. Depiction of the substantia nigra pathway in a mouse brain. Dopamine neurons project from the substantia nigra to the caudate putamen.

1.4.2 Brain Slices

Brain slices have long been accepted as an appropriate method of evaluation of neurobiology and activity (*67-69*). By perfusion with artificial cerebral spinal fluid, slices made from brain tissue can be kept functioning (*27, 70*). There are several advantages associated with performing experiments in vitro as opposed to in vivo. Drugs can be applied directly to the slices by perfusion, thus allowing the effects of specific concentrations to be evaluated. It is also advantageous to be able to visually place electrodes in specific locations when performing voltammetry experiments and to be able to move the electrodes to various locations with little damage to the tissue.

1.4.3 Pharmacological Agents that Alter Release and Uptake

Pharmacological agents that alter DA release and uptake can be used to evaluate neurological diseases and disorders in FSCV brain slice experiments. Some

of the common drugs used include amphetamine and cocaine. Other Drugs used in this study include GBR 12909, quinpirole and alpha-methyl-p-tyrosine (αMPT).

Amphetamine (AMPH), a psychostimulant commonly used for the treatment of attention deficit, narcolepsy and obesity, was first synthesized in 1887 by Lazar Edeleanu. The stimulating effects of the drug were not known until 1910 when it was tested in animals by Gordon Alles who was searching for a decongestant (*71*). The stimulating effects of AMPH have been shown to be due to the release of catecholamines caused by AMPH working by two mechanisms. First, AMPH causes excess DA to be released into the extracelluar space by binding to DAT and reversing its orientation, allowing outward transport of DA (*72-74*). AMPH also crosses through the plasma membrane by lipophilic diffusion (*74-76*). Once inside of the synapse, AMPH causes the depletion of vesicular DA by binding interaction with VMAT2, causing more extracellular DA, which can be outwardly transported by DAT (*77*).

Cocaine, an addictive stimulant found in the leaves of the coca plant, has been shown to bind to DAT and inhibit DA uptake, thus increasing extracellular levels of DA and causing a stimulating effect (*61, 78-80*). It has also been shown that cocaine can affect DA release by activating synapsin dependant reserve pools of DA (*81*). Once DA synthesis has been halted and its release depleted, administration of cocaine can restore DA release.

GBR 12909 has been shown to be a highly selective DAT inhibitor, thus effectively blocking presynaptic DA uptake (*82*). Because of the selectivity of GBR 12909 for DAT, it is advantageous to use it as a DAT inhibitor over cocaine and AMPH, both of which will act on transporters for different monoamines as well as DAT (*83*).

Activation of the D2 autoreceptor provides a negative feedback mechanism inhibiting adenylyl cyclase activity, halting DA synthesis and thus diminishing DA release and uptake (*84*). This mechanism of action prevents too much DA from being released into the extracellular space. Quinpirole, a D2 agonist, has been shown to activate the D2 autoreceptor and inhibit DA release in the striatum (*85*).

DA release can also be altered by preventing the synthesis of DA in the presynaptic terminal. Alpha-methyl-para-tyrosine is a tyrosine hydroxylase inhibitor (*86*). Tyrosine hydroxylase is involved in the production of DA. Once it is function is inhibited, tyrosine is no longer converted to L-DOPA which is a precursor of DA. Thus the synthesis of DA is halted and its packaging and release will be diminished.

1.4.4 Modeling Stimulated Release Plots

Dopamine uptake has been shown to follow Michaelis-Menten kinetics (*27, 87-88*). Based on previous experiments, **equation 7** is accepted (*89*):

$$(DA)_o + T \rightleftharpoons (DA)T \longrightarrow (DA)_i + T \qquad \textbf{Equation 7}$$

where $(DA)_o$ is extracellular DA, T is the DA transporter and $(DA)_I$ is intracellular DA. where $(DA)_o$ is extracellular DA, T is the dopamine transporter and $(DA)_I$ is intracellular DA. The Michaelis-Menten kinetic behavior of the DAT allows us to model the raw data to obtain information about $[DA]_p$, V_{max} and K_M, where $[DA]_p$ is the peak DA release corrected for electrode performance and uptake, V_{max} is the maximum rate of DA uptake and is proportional to the number of DAT molecules, and K_M is the concentration of DA at ½ V_{max} and is considered a measure of the affinity of DA for DAT. In the absence of drugs, the accepted value for K_M is 0.2 µM (*87, 90*) which allows us to use modeling

software, developed by the Wightman group at the University of North Carolina, to then determine $[DA]_p$ and V_{max} based on **Equation 8**.

$$d[DA]/dt = [DA]_p - V_{max}/(K_M/[DA] + 1) \qquad \textbf{Equation 8}$$

Figure 12 shows our experimentally collected data, the black dots, and the model fit to our data, the red line. By adjusting the value of $[DA]_p$ in the software, the height of the model curve changes to fit the experimental data. By adjusting the V_{max} values in the software, the width of the curve changes to fit to the data and thus we can obtain a good fit to the curve. When a slice is exposed to a drug such as AMPH, which alters the uptake, the experimentally determined V_{max} in the absence of drug is used in the software and the value of K_M is adjusted to obtain a good fit to the data.

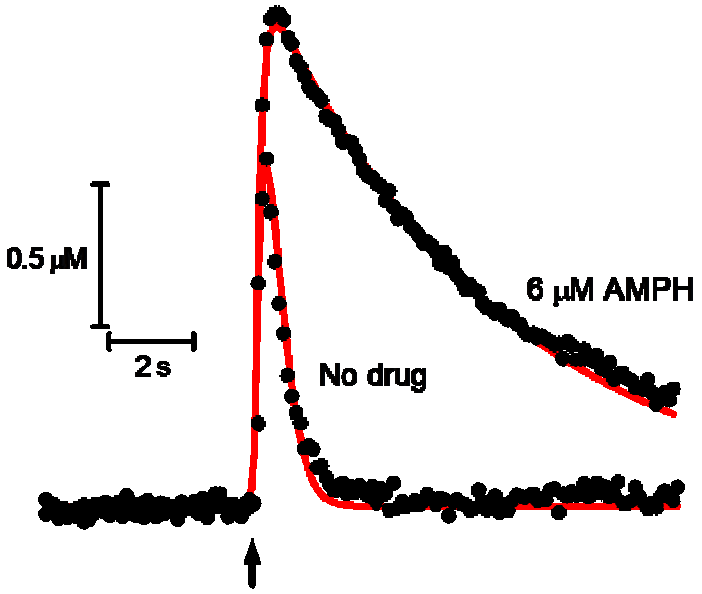

Figure 14. Modeling raw data. The experimentally collected data is shown by the black dots, the arrow indicates a stimulus pulse and the red line is the model fit curve to the data.

1.4.5 Competitive Inhibition

In the presence of a competitive inhibitor, I , the inhibition constant K_i can be determined. In the case of a competitive inhibitor the following is also occurring:

$$I + T \rightleftharpoons IT \qquad \textbf{Equation 9}$$

where K_i is the dissociation constant and follows **Equation 10.**

$$K_i = [I][T]/[IT] \qquad \textbf{Equation 10}$$

In this situation we can plot $(K_M)_{app}$ vs. [I], where $(K_M)_{app}$ is defined as $K_M(1 + [I]/K_i)$, and obtain a linear plot with a slope of K_M/K_i (*89*). In competitive inhibition, V_{max} remains unchanged due to the inhibitor binding, in most cases, to the same location as the substrate and increasing the concentration of the substrate can overcome the inhibition. K_M changes in competitive inhibition because the concentration of substrate needed to reach V_{max} has increased, thus shifting the value of K_M (**Figure 15**).

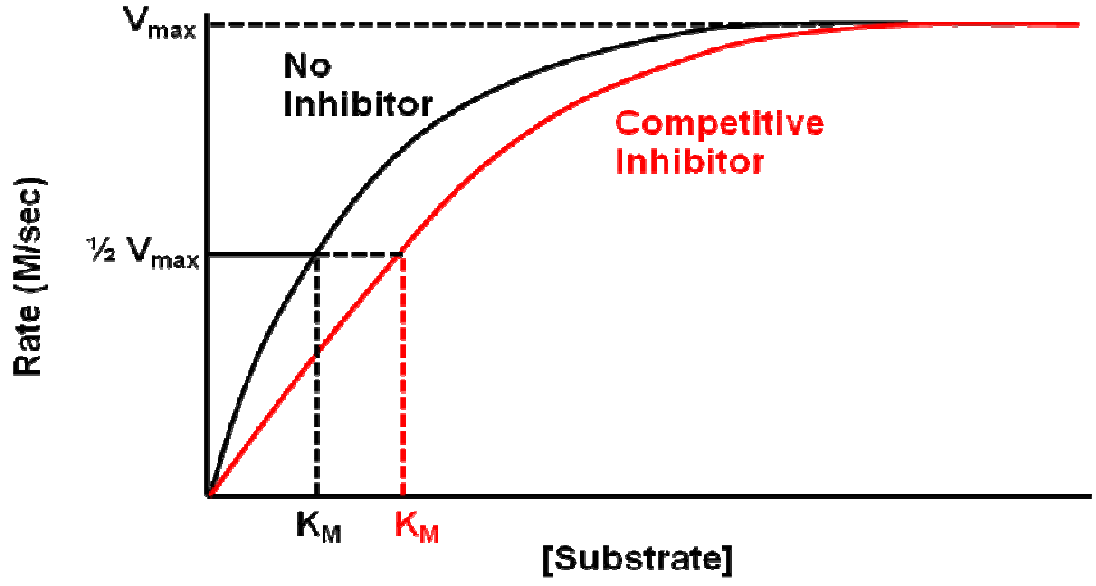

Figure 15. Representation of enzyme rates. The black line represents no inhibitor present, while the red line represents competitive inhibition. In competitive inhibition, V_{max} is unchanged, yet K_M increases due to a higher concentration of substrate being required to reach V_{max}.

1.5 The Force-Plate Actometer

The force-plate actometer was developed by Professor S.C. Fowler of the University of Kansas, has been well established for monitoring animal behavior including: locomotion, tremor, special patterning and focused stereotypy (*91*). The force-plate actometer consists of a plate with four transducers located under each corner with a cage over the plate but not touch it. The movement of the animal can then be traced in x and y directions as the animal move about the plate, as well as the z direction, detecting vertical force variation. The ability to monitor the vertical movements of the animal is important when evaluating focused stereotypy due to a decrease in locomotion that occurs while the animal experiences movement in the vertical direction. Thus, the force-plate actometer can evaluate focused-stereotypy and not mistake it for periods of paralysis.

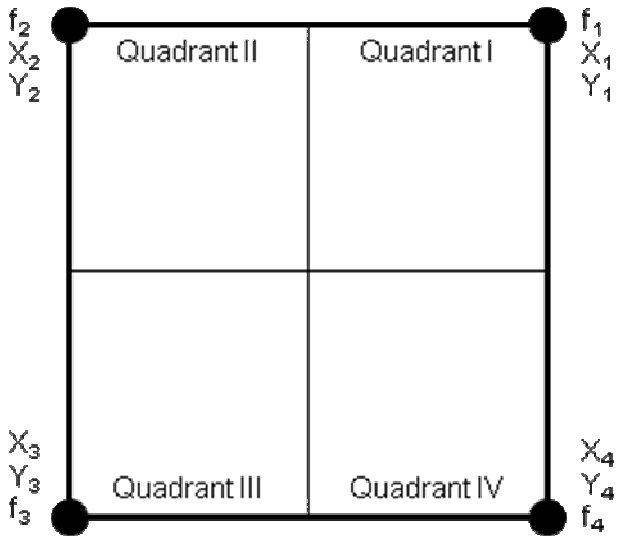

Figure 16. Coordinate system of the force plate actometer.

To track behavior the force-plate actometer has a transducer under each corner of the plate. To describe the different areas and transducers, the plate can be thought of as having four quadrants, each with a transducer in the corner given by their X,Y location , as shown in **Figure 16**. A 200 gram weight placed in the center of the plate will result in the detection of an equal distribution of forces over the transducers as shown in **Figure 17A**. When the weight is moved to a different location, the distribution of forces changes as seen in **Figure 17B**. Thus position of the object on the force-plate determines the force (f) detected at each corner of the plate.

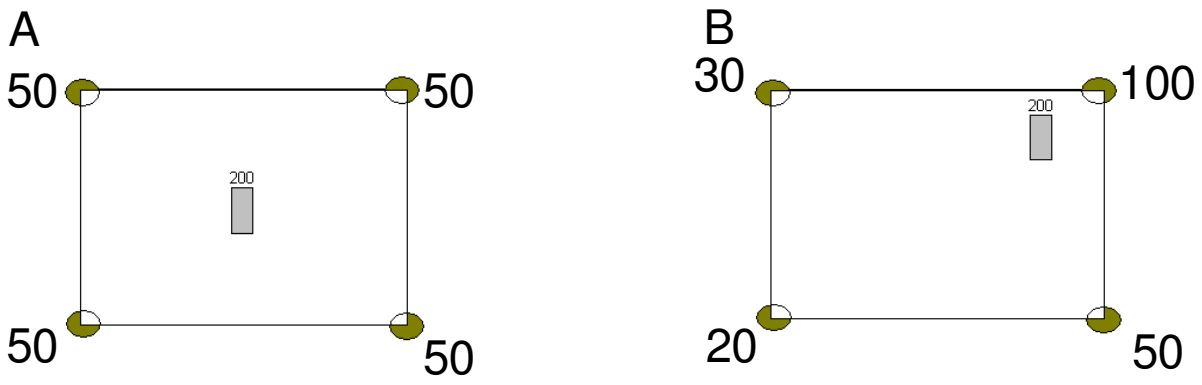

Figure 17. (A) The force plate actometer with an object in the center detecting an equal distribution of forces across the four transducers, located at the corners of the plate. (B) The change in forces detected once the object moves.

By **Equations 11** and **12**, the location of the object can be determined and thus tracked over time and its locomotor activity mapped out as shown in **Figure 18**.

$$x = (X_1f_1 + X_2f_2 + X_3f_3 + X_4f_4)/(f_1 + f_2 + f_3 + f_4) \qquad \textbf{Equation 11}$$

$$y = (Y_1f_1 + Y_2f_2 + Y_3f_3 + Y_4f_4)/(f_1 + f_2 + f_3 + f_4) \qquad \textbf{Equation 12}$$

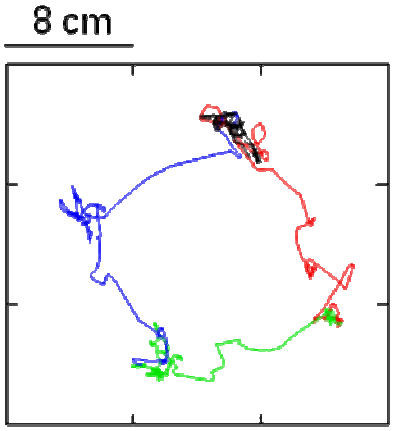

Figure 18. Depiction of the type of locomotor pattern around the plate of an animal after an actometer recording session and the determination of animal movement based on the changes of force distributions.

By recording the force measurements at a high rate over time the rhythmic variations in the animal's movement can also be detected and not just the locomotion (*91*). Since force measurements are being collected as opposed to position measurements, the rhythmic force variations caused by behaviors such as jumping, tremors or stereotypies can be detected. By use of Fourier transform these patterns of vertical frequency changes are detected as shown in **Figure 19**.

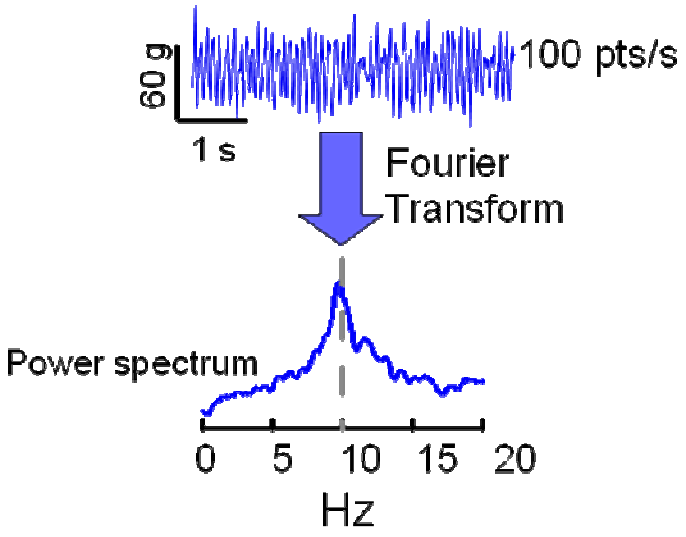

Figure 19. The use of Fourier Transform to detect rhythmic patterns in the force data. The power spectrum here represents the focused stereotypy behavior.

Amphetamine-induced focused stereotypy was evaluated in this work utilizing the force plate actometer. In order to compare the focused stereotypy occurring between the different genotypes the focused stereotypy scores (FSS) were calculated. The FSS, which is based on the amount of time and the force variance in the z direction as well as the number of sectors used, was determined for the animals based on **Equation 13** to assess the response to AMPH (*92*).

$$\text{Focused Stereotypy Score} = \frac{\Sigma(\%\text{time} \times F_z \text{ variance})}{\#\text{ of sectors used}} \qquad \textbf{Equation 13}$$

In this work, fast-scan cyclic voltammetry at carbon-fiber microelectrodes (FSCV) was used to investigate the electrically-evoked release and uptake of DA in striatal brain slices taken from *Fmr*1 KO mice and WT mice. These neurochemical measurements were compared with behavioral measurements of locomotion and focused stereotypy

obtained using a force-plate actometer, a behavioral device that measures variation in behavior-induced reactive forces even while the subject is not locomoting (*91*).

1.6 Summary of subsequent chapters

Chapter 2 describes the use of FSCV in the evaluation dopamine release in Fragile X Syndrome through the use of *Fmr*1 knockout mice. Behavioral analyses were performed using a force-plate actometer. The release and uptake of dopamine was characterized in three different age groups. Pharmacological agents were also employed to assess the functionality of the dopamine transporter, the D2 autoreceptor and dopamine reserve pools. These studies revealed information about how alterations in the dopamine system in Fragile X syndrome may impact the behavioral phenotype in Fmr1 KO mice.

Chapter 3 describes our evaluation of the effects of chemotherapy on striatal dopamine release. Many cancer patients report a significant decline in cognitive skills after chemotherapy. Male *Wistar* rats were dosed with carboplatin as an animal model for the examination of the role of dopamine in the Chemobrain phenomena. Healthy male rats were used in order to eliminate any hormonal effect or effect due to the cancerous cells on their neurochemistry. Fast scan cyclic voltammetry was used to characterize dopamine release and uptake in the striatum of the rats. Dopamine reserve pools were also evaluated using amphetamine induced dopamine efflux after inhibition of dopamine synthesis and depletion of the readily releasable and recycling pools of dopamine by electrical stimulation.

Chapter 4 introduces the experimental design and instrumentation for the assessment of immediate dopamine release alterations caused by the photorelease of caged compounds. Using caged compounds to evaluate dopamine responses in brain slices gives us the ability to introduce a biologically active molecule that is bound to a photoprotecting group, which yields the molecule inactive until photolysis removes the cage and reforms the biologically active compound. The design and setup of the instrumentation are presented with a brief introduction to its potential use in brain slices.

1.7 References

1. Johnson, M. A., Rajan, V., Miller, C. E., and Wightman, R. M. (2006) Dopamine release is severely compromised in the R6/2 mouse model of Huntington's disease, *Journal of Neurochemistry 97*, 737-746.

2. Kissinger, P. T., Hart, J. B., and Adams, R. N. (1973) Voltammetry in brain tissue--a new neurophysiological measurement, *Brain Res 55*, 209-213.

3. Ates, M., Sarac, A. S., Turhan, C. M., and Ayaz, N. E. (2009) Polycarbazole modified carbon fiber microelectrode: Surface characterization and dopamine sensor, *Fibers and Polymers 10*, 46-52.

4. Bond, A. M. (2002) *Broadening Electrochemical Horizons: Principles and Illistration of Voltammetric and Related Techniques*, Oxford University Press, New York.

5. Gosser Jr, D. K. (1994) *Cyclic Voltammetry Simulation and Analysis of Reaction Mechanisms*, VCH Publishers Inc., New York.

6. Stamford, J. A., Kruk, Z. L., Millar, J., and Wightman, R. M. (1984) Striatal dopamine uptake in the rat - invivo analysis by fast cyclic voltammetry, *Neuroscience Letters 51*, 133-138.

7. Kawagoe, K. T., Zimmerman, J. B., and Wightman, R. M. (1993) Principles of Voltammetry and Microelectrode Surface-States, *Journal of Neuroscience Methods 48*, 225-240.

8. Stenken, J. A., Church, M. K., Gill, C. A., and Clough, G. F. (2010) How Minimally Invasive is Microdialysis Sampling? A Cautionary Note for Cytokine Collection in Human Skin and other Clinical Studies, *Aaps J. 12*, 73-78.

9. Authier, L., Grossiord, C., Brossier, P., and Limoges, B. (2001) Gold nanoparticle-based quantitative electrochemical detection of amplified human cytomegalovirus DNA using disposable microband electrodes, *Analytical Chemistry 73*, 4450-4456.

10. Conyers, J. L., and White, H. S. (2000) Electrochemical characterization of electrodes with submicrometer dimensions, *Analytical Chemistry 72*, 4441-4446.

11. Demaille, C., Brust, M., Tsionsky, M., and Bard, A. J. (1997) Fabrication and characterization of self-assembled spherical gold ultramicroelectrodes, *Analytical Chemistry 69*, 2323-2328.

12. Katemann, B. B., and Schuhmann, T. (2002) Fabrication and characterization of needle-type Pt-disk nanoelectrodes, *Electroanalysis 14*, 22-28.

13. Menon, V. P., and Martin, C. R. (1995) Fabrication and evaluation of nanoelectrode ensembles, *Analytical Chemistry 67*, 1920-1928.

14. Slevin, C. J., Gray, N. J., Macpherson, J. V., Webb, M. A., and Unwin, P. R. (1999) Fabrication and characterisation of nanometre-sized platinum electrodes for voltammetric analysis and imaging, *Electrochemistry Communications 1*, 282-288.

15. Kissinger, P. T., and Heineman, W. R., (Eds.) (1996) *Laboratory Techniques in Electroanalytica Chemistry*, 2nd ed., Marcel Dekker, Inc., New York.

16. Kovach, P. M., Ewing, A. G., Wilson, R. L., and Wightman, R. M. (1984) Invitro comparison of the selectivity of electrodes for invivo electrochemistry, *Journal of Neuroscience Methods 10*, 215-227.

17. Bard, A. J., Abruna, H. D., Chidsey, C. E., Faulkner, L. R., Feldberg, S. W., Itaya, K., Majda, M., Melroy, O., Murray, R. W., Porter, M. D., Soriaga, M. P., and White, H. S. (1993) The electrode-electrolyte interface - a status-report, *J. Phys. Chem. 97*, 7147-7173.

18. Bard, A. J., and Faulkner, L. R. (2001) *Electrochemical Methods: Fundamentals and Applications*, John Wiley & Sons.

19. Beninger, R. J. (1983) The role of dopamine in locomotor-activity and learning, *Brain Research Reviews 6*, 173-196.

20. Pijnenburg, A. J. J., Honig, W. M. M., Vanderheyden, J. A. M., and Vanrossum, J. M. (1976) Effects of chemical stimulation of mesolimbic dopamine system upon locomotor activity, *European Journal of Pharmacology 35*, 45-58.

21. Berke, J. D., and Hyman, S. E. (2000) Addiction, dopamine, and the molecular mechanisms of memory, *Neuron 25*, 515-532.

22. Williams, G. V., and Goldmanrakic, P. S. (1995) Modulation of memory fields by dopamine D1 receptors in prefrontal cortex, *Nature 376*, 572-575.

23. Wise, R. A. (2004) Dopamine, learning and motivation, *Nature Reviews Neuroscience 5*, 483-494.

24. Everitt, B. J., and Robbins, T. W. (1997) Central cholinergic systems and cognition, *Annual Review of Psychology 48*, 649-684.

25. Missale, C., Nash, S. R., Robinson, S. W., Jaber, M., and Caron, M. G. (1998) Dopamine receptors: From structure to function, *Physiological Reviews 78*, 189-225.

26. Davis, K. L., Kahn, R. S., Ko, G., and Davidson, M. (1991) Dopamine in schizophrenia - a review and reconceptualization, *Am. J. Psychiat. 148*, 1474-1486.

27. Wightman, R. M., Amatore, C., Engstrom, R. C., Hale, P. D., Kristensen, E. W., Kuhr, W. G., and May, L. J. (1988) Real-Time Characterization of Dopamine Overflow and Uptake in the Rat Striatum, *Neuroscience 25*, 513-523.

28. Wightman, R. M., Strope, E., Plotsky, P., and Adams, R. N. (1978) Invivo voltammetry - monitoring of dopamine metabolites in csf following release by electrical-stimulation, *Brain Research 159*, 55-68.

29. Cartier, E. A., Parra, L. A., Baust, T. B., Quiroz, M., Salazar, G., Faundez, V., Egana, L., and Torres, G. E. (2010) A Biochemical and Functional Protein Complex Involving Dopamine Synthesis and Transport into Synaptic Vesicles, *J. Biol. Chem. 285*, 1957-1966.

30. Izumi, Y., Yamamoto, N., Kume, T., Katsuki, H., Sawada, H., and Akaike, A. (2008) Regulation of intracellular dopamine levels by dopaminergic drugs: Involvement of vesicular monoamine transporter, *European Journal of Pharmacology 582*, 52-61.

31. Qi, Z., Miller, G. W., and Voit, E. O. (2008) Computational Systems Analysis of Dopamine Metabolism, *Plos One 3*.

32. Fulks, J. L., O'Bryhim, B. E., Wenzel, S. K., Fowler, S. C., Vorontsova, E., Pinkston, J. W., Ortiz, A. N., and Johnson, M. A. (2010) Dopamine Release and Uptake Impairments and Behavioral Alterations Observed in Mice that Model Fragile X Mental Retardation Syndrome, *ACS Chemical Neuroscience 1*, 679-690.

33. Bailey, B. (2006) Monoamines and Acid Metabolites Analysis for Tissue Samples, Magellan Biosciences, esa Magellan Biosciences.

34. Sudhof, T. C. (2004) The synaptic vesicle cycle, *Annual Review of Neuroscience 27*, 509-547.

35. Gandhi, S. P., and Stevens, C. F. (2003) Three modes of synaptic vesicular recycling revealed by single-vesicle imaging, *Nature 423*, 607-613.

36. Staal, R. G. W., Mosharov, E. V., and Sulzer, D. (2004) Dopamine neurons release transmitter via a flickering fusion pore, *Nat. Neurosci. 7*, 341-346.

37. Murthy, V. N., and Stevens, C. F. (1999) Reversal of synaptic vesicle docking at central synapses, *Nat. Neurosci. 2*, 503-507.

38. Neves, G., and Lagnado, L. (1999) The kinetics of exocytosis and endocytosis in the synaptic terminal of goldfish retinal bipolar cells, *Journal of Physiology-London 515*, 181-202.

39. Rizzoli, S. O., and Betz, W. J. (2005) Synaptic vesicle pools, *Nature Reviews Neuroscience 6*, 57-69.

40. Zucker, R. S., and Regehr, W. G. (2002) Short-term synaptic plasticity, *Annual Review of Physiology 64*, 355-405.

41. Stevens, C. F., and Tsujimoto, T. (1995) Estimates for the pool size of releasable quanta at a single central synapse and for the time required to refill the pool, *Proceedings of the National Academy of Sciences of the United States of America 92*, 846-849.

42. Borland, L. M., Shi, G. Y., Yang, H., and Michael, A. C. (2005) Voltammetric study of extracellular dopamine near microdialysis probes acutely implanted in the striatum of the anesthetized rat, *Journal of Neuroscience Methods 146*, 149-158.

43. Gonon, F. (1997) Prolonged and extrasynaptic excitatory action of dopamine mediated by D1 receptors in the rat striatum in vivo, *Journal of Neuroscience 17*, 5972-5978.

44. Zoli, M., Torri, C., Ferrari, R., Jansson, A., Zini, I., Fuxe, K., and Agnati, L. F. (1998) The emergence of the volume transmission concept, *Brain Research Reviews 26*, 136-147.

45. Gonon, F. G., and Buda, M. J. (1985) Regulation of dopamine release by impulse flow and by autoreceptors as studied by invivo voltammetry in the rat striatum, *Neuroscience 14*, 765-774.

46. Jomphe, C., Tiberi, M., and Trudeau, L. E. (2006) Expression of D2 receptor isoforms in cultured neurons reveals equipotent autoreceptor function, *Neuropharmacology 50*, 595-605.

47. Starke, K., Gothert, M., and Kilbinger, H. (1989) Modulation of neurotransmitter release by presynaptic autoreceptors, *Physiological Reviews 69*, 864-989.

48. Tepper, J. M., Sun, B. C., Martin, L. P., and Creese, I. (1997) Functional roles of dopamine D-2 and D-3 autoreceptors on nigrostriatal neurons analyzed by antisense knockdown in vivo, *Journal of Neuroscience 17*, 2519-2530.

49. Benkert, O., Grunder, G., and Wetzel, H. (1992) Dopamine autoreceptor agonists in the treatment of schizophrenia and major depression, *Pharmacopsychiatry 25*, 254-260.

50. Sokoloff, P., Giros, B., Martres, M. P., Bouthenet, M. L., and Schwartz, J. C. (1990) Molecular-cloning and characterization of a novel dopamine receptor (D3) as a target for neuroleptics, *Nature 347*, 146-151.

51. Maina, F. K., and Mathews, T. A. (2010) Functional Fast Scan Cyclic Voltammetry Assay to Characterize Dopamine D2 and D3 Autoreceptors in the Mouse Striatum, *Acs Chemical Neuroscience 1*, 450-462.

52. Beaulieu, J. M., and Gainetdinov, R. R. (2011) The Physiology, Signaling, and Pharmacology of Dopamine Receptors, *Pharmacological Reviews 63*, 182-217.

53. Clark, D., Hjorth, S., and Carlsson, A. (1985) Dopamine receptor agonists - mechanisms underlying autoreceptor selectivity .2. theoretical considerations, *Journal of Neural Transmission 62*, 171-207.

54. Seeman, P. (1980) Brain dopamine-receptors, *Pharmacological Reviews 32*, 229-313.

55. Seeman, P., and Tallerico, T. (2003) Link between dopamine D-1 and D-2 receptors in rat and human striatal tissues, *Synapse 47*, 250-254.

56. Seeman, P., Tallerico, T., and Ko, F. (2003) Dopamine displaces H-3 domperidone from high-affinity sites of the dopamine D2 receptor, but not H-3 raclopride or H-3 spiperone in isotonic medium: Implications for human positron emission tomography, *Synapse 49*, 209-215.

57. Usiello, A., Baik, J. H., Rouge-Pont, F., Picetti, R., Dierich, A., LeMeur, M., Piazza, P. V., and Borrelli, E. (2000) Distinct functions of the two isoforms of dopamine D-2 receptors, *Nature 408*, 199-203.

58. Fuxe, K., Agnati, L. F., Kalia, M., Goldstein, M., Andersson, K., and Harfstrand, A. (1985) Dopaminergic Systems in the Brain and Pituitary, In *The Dopaminergic System. Basic and Clinical Aspects of Neuroscience* (Fluckiger, E., Ed.), Springer-Verlag, Berlin.

59. Giros, B., Jaber, M., Jones, S. R., Wightman, R. M., and Caron, M. G. (1996) Hyperlocomotion and indifference to cocaine and amphetamine in mice lacking the dopamine transporter, *Nature 379*, 606-612.

60. Iversen, L. L. (1971) Role of transmitter uptake mechanisms in synaptic neurotransmission, *British Journal of Pharmacology 41*, 571.

61. Jones, S. R., Gainetdinov, R. R., Jaber, M., Giros, B., Wightman, R. M., and Caron, M. G. (1998) Profound neuronal plasticity in response to inactivation of the dopamine transporter, *Proceedings of the National Academy of Sciences of the United States of America 95*, 4029-4034.

62. Sonders, M. S., Zhu, S. J., Zahniser, N. R., Kavanaugh, M. P., and Amara, S. G. (1997) Multiple ionic conductances of the human dopamine transporter: The actions of dopamine and psychostimulants, *Journal of Neuroscience 17*, 960-974.

63. Smith, Y., and Kieval, J. Z. (2000) Anatomy of the dopamine system in the basal ganglia, *Trends Neurosci. 23*, S28-S33.

64. Nolte, J. (1988) *The Human Brain. An Introduction to its Functional Anatomy*, Second ed., C.V. Mosby Company, St. Louis.

65. Smeets, W., and Gonzalez, A. (2000) Catecholamine systems in the brain of vertebrates: new perspectives through a comparative approach, *Brain Research Reviews 33*, 308-379.

66. Pisani, A., Centonze, D., Bernardi, G., and Calabresi, P. (2005) Striatal synaptic plasticity: Implications for motor learning and Parkinson's disease, *Movement Disorders 20*, 395-402.

67. Dingledine, R. (1984) *Brain Slices*, Plenum Press, New York.

68. Dingledine, R., Dodd, J., and Kelly, J. S. (1980) The invitro brain slice as a useful neurophysiological preparation for intracellular-recording, *Journal of Neuroscience Methods 2*, 323-362.

69. Nicholson, C., and Hounsgaard, J. (1983) Diffusion in the slice microenvironment and implications for physiological-studies, *Federation Proceedings 42*, 2865-2868.

70. Kelly, R. S., and Wightman, R. M. (1987) Detection of dopamine overflow and diffusion with voltammetry in slices of rat-brain, *Brain Research 423*, 79-87.

71. Fleckenstein, A. E., Volz, T. J., Riddle, E. L., Gibb, J. W., and Hanson, G. R. (2007) New insights into the mechanism of action of amphetamines, *Annu Rev Pharmacol Toxicol 47*, 681-698.

72. Fischer, J. F., and Cho, A. K. (1979) Chemical-release of dopamine from striatal homogenates - evidence for an exchange diffusion-model, *Journal of Pharmacology and Experimental Therapeutics 208*, 203-209.

73. Liang, N. Y., and Rutledge, C. O. (1982) Evidence for carrier-mediated efflux of dopamine from corpus striatum, *Biochemical Pharmacology 31*, 2479-2484.

74. Liang, N. Y., and Rutledge, C. O. (1982) Comparison of the release of H-3 dopamine from isolated corpus striatum by amphetamine, fenfluramine and unlabeled dopamine, *Biochemical Pharmacology 31*, 983-992.

75. Mack, F., and Bonisch, H. (1979) Dissociation-constants and lipophilicity of catecholamines and related-compounds, *Naunyn-Schmiedebergs Archives of Pharmacology 310*, 1-9.

76. Zaczek, R., Culp, S., Goldberg, H., McCann, D. J., and Desouza, E. B. (1991) Interactions of H-3 amphetamine with rat-brain synaptosomes .1. saturable sequestration, *Journal of Pharmacology and Experimental Therapeutics 257*, 820-829.

77. Floor, E., and Meng, L. H. (1996) Amphetamine releases dopamine from synaptic vesicles by dual mechanisms, *Neuroscience Letters 215*, 53-56.

78. Nestler, E. J. (2001) Molecular basis of long-term plasticity underlying addiction, *Nature Reviews Neuroscience 2*, 119-128.

79. Koob, G. F., and Le Moal, M. (2001) Drug addiction, dysregulation of reward, and allostasis, *Neuropsychopharmacology 24*, 97-129.

80. Heikkila, R. E., Orlansky, H., and Cohen, G. (1975) Studies on distinction between uptake inhibition and release of H-3 dopamine in rat-brain tissue-slices, *Biochemical Pharmacology 24*, 847-852.

81. Venton, B. J., Seipel, A. T., Phillips, P. E., Wetsel, W. C., Gitler, D., Greengard, P., Augustine, G. J., and Wightman, R. M. (2006) Cocaine increases dopamine release by mobilization of a synapsin-dependent reserve pool, *J Neurosci 26*, 3206-3209.

82. Andersen, P. H. (1989) The dopamine uptake inhibitor GBR 12909 - selectivity and molecular mechanism of action, *European Journal of Pharmacology 166*, 493-504.

83. Sivam, S. P. (1995) GBR-12909-induced self-injurious-behavior - role of dopamine, *Brain Research 690*, 259-263.

84. Pothos, E. N., Przedborski, S., Davila, V., Schmitz, Y., and Sulzer, D. (1998) D-2-like dopamine autoreceptor activation reduces quantal size in PC12 cells, *Journal of Neuroscience 18*, 5575-5585.

85. O'Neill, C., Evers-Donnelly, A., Nicholson, D., O'Boyle, K. M., and O'Connor, J. J. (2009) D-2 receptor-mediated inhibition of dopamine release in the rat striatum in vitro is modulated by CB1 receptors: studies using fast cyclic voltammetry, *Journal of Neurochemistry 108*, 545-551.

86. Moore, K. E., and Dominic, J. A. (1971) Tyrosine hydroxylase inhibitors, *Federation Proceedings 30*, 859-&.

87. Jones, S. R., Garris, P. A., and Wightman, R. M. (1995) Different effects of cocaine and nomifensine on dopamine uptake in the caudate-putamen and nucleus accumbens, *J Pharmacol Exp Ther 274*, 396-403.

88. Kawagoe, K. T., Garris, P. A., Wiedemann, D. J., and Wightman, R. M. (1992) Regulation of transient dopamine concentration gradients in the microenvironment surrounding nerve-terminals in the rat striatum, *Neuroscience 51*, 55-64.

89. Mathews, C. K., and van Holde, K. E. (1996) *Biochemistry*, 2nd ed., Benjamin/Cummings, Menlo Park, CA.

90. Garris, P. A., Christensen, J. R. C., Rebec, G. V., and Wightman, R. M. (1997) Real-time measurement of electrically evoked extracellular dopamine in the striatum of freely moving rats, *Journal of Neurochemistry 68*, 152-161.

91. Fowler, S. C., Birkestrand, B. R., Chen, R., Moss, S. J., Vorontsova, E., Wang, G., and Zarcone, T. J. (2001) A force-plate actometer for quantitating rodent behaviors: illustrative data on locomotion, rotation, spatial patterning, stereotypies, and tremor, *J Neurosci Methods 107*, 107-124.

92. Fowler, S. C., Covington, H. E., and Miczek, K. A. (2007) Stereotyped and complex motor routines expressed during cocaine self-administration: results from a 24-h binge of unlimited cocaine access in rats, *Psychopharmacology 192*, 465-478.

CHAPTER 2

DOPAMINE RELEASE AND UPTAKE IMPAIRMENTS AND BEHAVIORAL ALTERATIONS IN MICE THAT MODEL FRAGILE X SYNDROME

Fulks, J. L., O'Bryhim, B. E., Wenzel, S. K., Fowler, S. C., Vorontsova, E., Pinkston, J. W., Ortiz, A. N., and Johnson, M. A. (2010) Dopamine Release and Uptake Impairments and Behavioral Alterations Observed in Mice that Model Fragile X Mental Retardation Syndrome, *ACS Chemical Neuroscience 1*, 679-690.

A clear understanding of the underlying the neurochemical mechanisms of neurological disease is vital in the search for therapeutic treatments. This work addresses potential alterations in dopamine (DA) release and uptake mechanisms associated with fragile X syndrome (FXS), the most common known genetic cause of mental retardation. We have studied the behavioral effects of amphetamine injections in *Fmr*1 knockout (*Fmr*1 KO) mice, which model FXS, and have evaluated the DA release and uptake characteristics in brain slices in order to study the relationship between the behavior and neurochemistry. Behavioral analysis was carried out with the use of a force-plate actometer, a device that collects movement information at millisecond temporal resolution and 2 mm spatial resolution. Behavioral analyses revealed that, injection with 10 mg/kg (ip) amphetamine, *Fmr*1 KO mice expressed a lower degree of focused stereotypy compared to wild type (WT) control mice. Brain slice experiments using fast scan cyclic voltammetry (FSCV) at carbon-fiber microelectrodes were performed to identify differences in electrically evoked DA release and uptake between KO and WT mice to identify potential mechanisms that would

explain the differences seen in the behavioral data. At 10 weeks of age DA per pulse, a measure of dopamine release corrected for electrode performance and reuptake, was unchanged between KO and WT mice. However, at 15 weeks and 20 weeks of age there were decreases seen in DA per pulse and in the rate of DA uptake in the KO mice compared to the WT mice. Direct application of amphetamine to the brain slices in increasing concentrations showed that there was equal affinity of amphetamine for the DA transporter in both the KO and WT mice. Brain slices were also treated with the mGluR5 antagonist 2-methyl-6-(phenylethynyl)-pyridine (MPEP) revealing no immediate effect in the recovery of dopamine release in the KO mice. The D2 autoreceptor function was evaluated in slices by application of quinpirole, a D2 agonist, showed that there is no change in D2 autoreceptor sensitivity in FXS. A direct comparison of predrug and post drug DA release in the presence of amphetamine showed an increased response to amphetamine by the KO mice. These data support a scenario in which inferior extracellular dopamine levels in the striatum explain the diminished focused stereotypy in the *Fmr*1 KO mice.

2.1 INTRODUCTION

2.1.1 Fragile X Syndrome

Fragile X syndrome (FXS), the most common known genetic cause of mental retardation and autism occurring in approximately 1 in 1250 males and 1 in 2500 females (*1*), is caused by a repeat expansion of greater than 200 CGG repeats on the fragile X mental retardation 1 (FMR1) gene located on the X chromosome (*2*). The repeat expansion leads to a silencing of the transcription of the fragile X mental retardation protein (FMRP) (*3-4*), resulting in neurological impairments. FMRP plays a role in mRNA transport and regulation of their translation (*5-8*).

The behavioral manifestation of FXS commonly includes ADHD-like symptoms along with communication and motor control disturbances (*9-12*). Symptoms that occur in FXS are often the same as those that common in cases of autism including repetitive behaviors that appear like those of obsessive-compulsive disorder (OCD), anxiety in social settings and an increase in sensitivity to sensory stimuli (*9-10, 13*). Individuals with FXS lack communications skills as is apparent by their lack of eye contact and turning their heads and bodies away from others or by attempting to block their eyes with their hands and arms (*14*).

2.1.2 Animal Model of FXS

In order to investigate FXS and the pathological mechanisms that lead to the symptoms of the disorder, an *Fmr*1 knockout (KO) mouse model was developed in which the *Fmr*1 gene is inactivated (*15*). These mice have been used in various studies

to evaluate cognition, behavior and therapeutic treatments. The *Fmr*1 KO mice have been shown to be susceptible to seizure (*16-18*); however, behavioral measurements that utilize spatial learning tasks, such as the Morris water maze, have only been able to show mild deficits (*19-24*). The maze evaluations could likely show only mild deficits because these tasks evaluate learning and memory, but not attention and inhibitory control, which are major contributing factor to cognitive deficits in FXS (*25*). In more recent studies, when presented with attention based tasks, the *Fmr*1 KO mice exhibited a higher rate of premature responses indicating impaired inhibitory control during times of stress or arousal (*26*).

2.1.3 Neurological Manifestations of FXS

The mutation in FXS may manifest under several different neurological mechanisms, influencing brain development. In recent studies it has been suggested that neural development in FXS is impaired as a result of excessive induction of hippocampal and cerebellar long-term depression (LTD) (*27-28*). The dorsal striatum is heavily laden with dopaminergic neurons (*29*) where the activation of D2 receptors, acting in combination with group I mGluRs, CBI cannabinoid receptors and L-type calcium channels, is required for the induction of a form of LTD (*30-33*). Due to the high density of DA in the striatum, an alteration in DA regulation may influence synaptic plasticity and brain development (*34-35*). Behavioral disorders, such as stereotypy and hyperactivity, have been treated by use of DA receptor blockers (*36*) and are associated with FXS (*37-38*) and autism (*39-42*). Thus DA signaling abnormalities are a potential neurological disturbance associated with FXS.

2.1.4 Dopamine Release Altered by Amphetamine

The DA system can be challenged by the psychostimulant AMPH to cause an excess of extracellular DA (*43*). AMPH is often used to evaluate differences in behavior between KO mice and their WT counterparts (*44-48*). There are dose dependent responses to AMPH when evaluating the behavioral response of the animals. When given a low dose (1-2 mg/kg), locomotor stimulation occurs; at a higher dose (8-10 mg/kg) an excited state of small repetitive movements of the head, forelimbs and trunk, referred to as a focused stereotypy, occur (*45, 49*). At very high doses (over 15 mg/kg), self-mutilation is sometimes seen (*50-51*). Previous studies performed with AMPH doses on *Fmr*1 KO mice were done with doses well below the focused stereotypy range (*47-48*).

The doses of AMPH used in this work were within the ranges for increased locomotor activity and focused stereotypy, but below the threshold for self-mutilation. There is a wide acceptance that the focused stereotypy behavior caused by AMPH is in part due to increased levels of DA in the dorsal striatum (*52-53*). The behavioral changes caused by the AMPH injections were measured using a force-plate actometer, described in Chapter 1 of this work, which is capable of distinguishing between locomotor activity and focused stereotypy.

2.2 EXPERIMENTAL PROCEDURES

2.2.1 Animals

All animal procedures were conducted in accordance with protocols approved by the Animal Care and Use Committee of the University of Kansas. Fragile X knockout mice FVB.129P2-***Fmr1***^{tm1Cgr}/J (*19*) and wild-type control mice were obtained from The Jackson Laboratory (Bar Harbor, ME, USA). These mice were received at approximately 8 weeks of age and were housed in the University of Kansas Animal Care Unit (ACU) under a temperature-regulated, humidity-controlled environment. The mice had unrestricted access to food and water and were housed with 12 hour light/dark cycles.

2.2.2 Drugs

d-Amphetamine sulfate, GBR12909, quinpirole, and cocaine were purchased from Sigma-Aldrich (St. Louis, MO).

2.2.3 Behavior

Behavioral Apparatus. Behavioral data were collected during the light phase of the housing light/dark cycle. Eight force-plate actometers (*54*) were utilized in the collection of behavioral data for the comparison of behavioral characteristics between KO and WT mice. Each actometer measured 28 cm X 28 cm and in order to prevent alterations in behavior due to outside noises, the actometers were placed in sound-attenuating chambers. In order to provide ventilation, a silent, vibration free ventilation system was

utilized. Animal activity was tracked by force measurements being recorded at a rate of 100 pts/s with a spatial resolution less than 2 mm. Vertical forces both associated with locomotion and non-locomotor movements were also recorded and analyzed. Locomotor activity in rodents is commonly reported in the form of distance traveled, which was determined by summing the distances between consecutive center of force coordinate 0.5 s apart. By utilizing this measuring system the locomotion is accentuated and the contribution to the distance variable of small, high-frequency movements is reduced. The force-plate method has been used to measure the mouse behavior even while the animal is "staying in place" allowing the quantitation on focused stereotypy (*49*) induced by central nervous system stimulants, such as amphetamine (*55*) or cocaine (*56*). A combination of the animal remaining in one location (spatial confinement) in combination with the vigor of head, limb and trunk activity (while confined) was used to determine the FS score. In order to determine the FS score, the floor area of the actometer was divided into 256 equal-sized square sectors. One minute intervals were used to calculate the percent of time the animal spent in each sector. Computation of the FS score was then done by the following: 1) multiplying the variance in the vertical force in a sector by the percent time in the same sector; 2) the products across all of the 256 sectors were summed; and 3) this sum of the products was then divided by the number of sectors used during the 1-min time period to obtain the FS score. The average of 60 1-min FS scores was taken to obtain the FS score for a 60-min time period.

Behavioral Procedures. Fifteen-week old *Fmr*1 KO mice and age-matched WT control mice were placed in the actometers for two 1-hr recording sessions conducted 10 days apart. A few seconds before sessions, separate groups of n = 6 mice each received ip injections of saline vehicle, 1.0, 3.3, or 10.0 mg/kg of d-amphetamine sulfate. In experimental design terminology this was an analysis of variance (ANOVA) with 2 genotypes, 4 doses, and 2 injections as a repeated measures variable. Therefore, the procedure dictated the use of 24 WT and 24 KO mice. Doses of amphetamine were selected to produce locomotor stimulation at the two lower doses and focused stereotypy at the highest dose in WT mice.

2.2.4 Brain slice preparation

Striatal brain slices were prepared as described previously (*57*). Briefly, mice were anesthetized by inhalation of isoflurane gas and decapitated. The brain was removed immediately and placed into ice-cold artificial cerebrospinal fluid (aCSF) saturated with 95%O_2/5%CO_2 The aCSF solution consists of (in mM) 126 NaCl, 22 HEPES, 1.6 NaH_2PO_4, 2.5 KCl, 25$NaHCO_3$, 2.4 $CaCl_2$, 1.2 $MgCl_2$, and 11 D-glucose, and was adjusted to a pH of 7.4. For support while slicing, a 1 cm^3 block of agar gel was glued to the support block. The cerebellum was removed with a razor blade and the brain was bisected. Next, the brain was glued to the support block with Roti®coll 1 (Carl Roth, Karlsruhe, Germany), a quick-setting glue, and the buffer tray was then filled with ice-cold aCSF. The remaining half of the brain was dissected and the striatum removed and placed on dry ice and stored at -80℃ for HPLC analysis. Coronal slices 300µm thick were made using a Leica VT1000 S vibrating-blade microtome (Leica

Microsystems, Nussloch, Germany). Striatal slices obtained between 0.4mm and 1.60mm anterior to bregma were used for voltammetry analyses. The brain slices were stored in ice-cold aCSF saturated with 95%O_2/5%CO_2 until needed for use. Prior to experimentation, slices were placed in a perfusion chamber with aCSF continuously flowing (1 mL/min) and kept at a temperature of 34°C. Slices were allowed to equilibrate in the perfusion chamber for at least 90 minutes before data collection. Drugs were introduced to slices through a three-way valve that allowed aCSF containing the chosen drug to flow from a separate reservoir to the slice chamber.

2.2.5 Fast-Scan Cyclic Voltammetry

Microelectrodes, with the exposed carbon-fiber tip having a diameter of 7 µm and a length of 30 µm, were constructed as previously described (*58*). Electrodes were calibrated before and after use by exposure to known DA concentrations in a flow cell. The stimulation electrodes were made by gluing two tungsten electrodes (A-M Systems Inc, Carlsborg, WA, USA) and adjusting the distance between the two tips using heat shrink (3M Electronics, Austin, TX, USA) until they were 200 µm apart. Electrochemical measurements were obtained using an Axopatch 200B amplifier (Molecular Devices, Sunnyvale, CA) interfaced with a computer through a locally constructed breakout box and custom designed software written by M.L.A.V. Heien and R. M. Wightman, Department of Chemistry, University of North Carolina, Chapel Hill, NC.

For brain slice experiments, carbon fiber microelectrodes were inserted 100 µm below the surface of the brain slice between the two stimulus electrodes, situated in the dorsolateral caudate. To obtain most measurements, DA release was evoked by the

application of a single, biphasic, electrical pulse (4 ms duration, 350 μA current). A series of 50 stimulus pulses applied at 10 Hz was used when evaluating the effects of quinpirole and cocaine. To detect released DA, a triangular waveform was applied to the carbon fiber microelectrode in which the potential was linearly scanned from a holding potential of -0.4 V to +1.0 V and back to -0.4 V at a scan rate of 300 V/sec and an update rate of 10 Hz. A Ag/AgCl reference electrode was used. Currents measured prior to stimulation were subtracted from those measured during and immediately after stimulation to yield a cyclic voltammogram for DA. To measure DA release in the absence of drugs, recordings were collected from four different locations within the dorsolateral caudate region of each slice and averaged (*57*). This averaging approach decreased variability caused by the heterogeneous nature of dopaminergic innervation in the striatum.

Stimulated release plots were modeled using software written by R. M. Wightman, University of North Carolina, Chapel Hill, NC. From this modeling operation, kinetic parameters associated with dopamine release and uptake were calculated. These parameters include dopamine per pulse $[DA]_p$, which is peak dopamine release corrected for electrode performance and reuptake, K_M, and V_{max}. The approach used here is similar to that applied previously to FSCV data obtained using brain slices (*57*).

2.2.6 High Performance Liquid Chromatography

High Performance Liquid Chromatography (HPLC) analyses of catecholamine content were carried out using a Shimadzu Model LC 20 AD, (Shimadzu Corporation, Kyoto, Japan) with a dual reciprocating pump and a DGV 20A3 degasser and a model

CBM 20A system controller. An ESA Coulochem II electrochemical detector (ESA, Inc., Chelmsford, MA, USA), consisting of a guard cell and two analytical cells, was used for detection of catecholamines in striatal lysates. The guard cell was set at 350 mV. The analytical cells were set at -150mV for the first detector and +220 mV for the second detector. Mobile phase consisted of 10% organic phase (acetonitrile) and 90% aqueous phase (containing 75 mM sodium dihydrogen phosphate monohydrate, 0.01% trietheylamine, 25µM EDTA tetrasodium tetrahydrate, and 1.7mM 1-Octanesulfonic acid sodium salt) adjusted to a pH of 2.8 with 80% phosphoric acid. Chromatographic separations were carried out isocratically using a 150mm × 3.2 mm ESA MD-150 column. The flow rate was set to 0.4 mL/min.

Animals were euthanized and the striata removed and stored at -80°C until analysis. For analysis, tissue was prepared by homogenizing in 0.500 ml of 0.2N perchloric acid containing 200ng/ml DHBA as internal standard. Homogenate was centrifuged at 14,000 rpm for 20 minutes at 4°C. Supernatant was removed and filtered through a 0.2 micron syringe filter prior to injection in the HPLC instrument. Standard curve solutions were prepared immediately prior to each HPLC run by dissolving pure substance in 0.2 N perchloric acid containing 200ng/ml internal standard and diluting by serial dilution. Nine concentrations were used for each compound (1000, 500, 200, 100, 50, 25, 10, 5 and 1 ng/ml).

2.2.7 Genotype verification

Tail snips were saved from each mouse to use in genotyping to verify each animals genotype. A DNeasy Blood and Tissue kit (QIAGEN, Valencia, CA, USA) was used for DNA extraction. Primer sequences were made according to the design on the Jackson Laboratory website and were purchased from Invitrogen (Carlsbad, CA, USA). A 5 mM cresol Red diluted in a 60% sucrose solution was used as the loading dye. After DNA extraction and PCR, samples were loaded onto a 1.5% agarose gel with 5 µL of ethidium bromide and were run in a TAE buffer. Each mouse DNA sample was separated into two different PCR reactions; A and B. Where a band detected in lane A indicated WT and a band in lane B indicated KO. All genotypes were proved to be correctly labeled.

2.2.8 Statistical Analyses

Statistical analyses were performed using either student's t-test or ANOVA. A value of $p < 0.05$ was considered significant. Values are expressed as average ± SEM.

2.3 RESULTS AND DISCUSSION

2.3.1 Behavioral Results

2.3.1.1 Locomotor activity

Locomotor activity, expressed as distance traveled shown in **Figure 2** (panels A & B), was significantly higher in the Fmr1 KO mice in the absence of AMPH after both vehicle injections. Our results are consistent with previous studies reporting on locomotor activity in *Fmr*1 KO mice (*48-49, 59-65*). Methods utilized in these prior studies included multiple brands of photobeam actometers, manual counting of line crossings, and computer scored video tracking. Some studies report a non significant difference between the KO and WT mice (*62-64*); however, the data reported indicated that the *Fmr*1 KO mice were numerically higher than the WT mice. It appears that the lesser differences in locomotor activity are associated with shorter recording times.

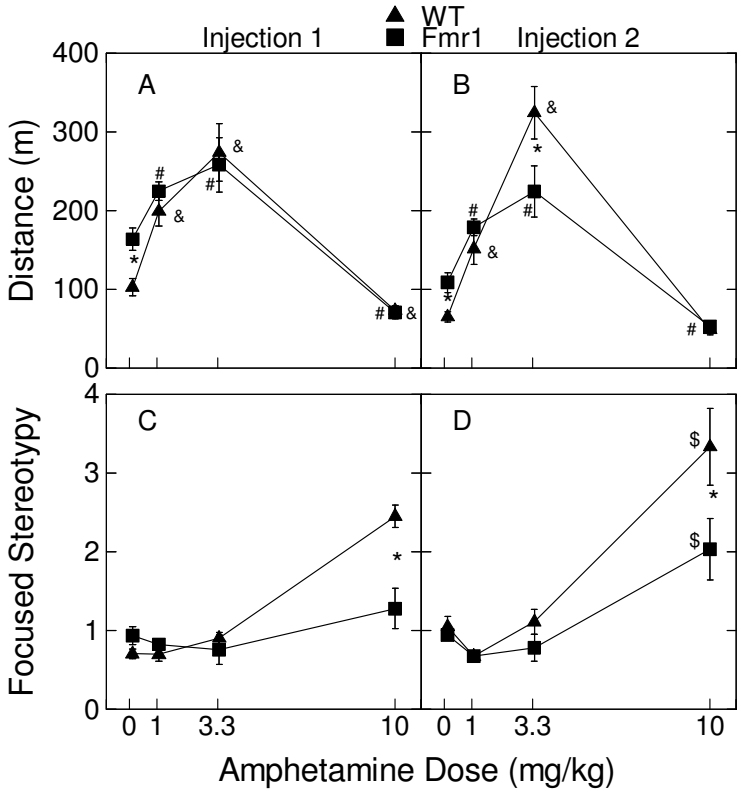

Figure 2. Induction of locomotor activity and focused stereotypy by d-amphetamine sulfate in *Fmr*1 knockout and WT control mice. Separate groups of mice (n=6) were used at each dose. Data points are group means and the brackets indicate ± SEM. The four symbols, asterisks (*), ampersands (&), pound signs (#), and dollar sign($) reflect significant differences between means as determined by t-tests conducted after initial 3-way ANOVA's. *'s indicate significant differences between Wild type (WT) and *Fmr*1 knockout mice at the indicated doses. &'s designate significant differences between vehicle and each dose of amphetamine for WT mice for a given injection, while #'s mark differences between vehicle and each amphetamine dose administered to the *Fmr*1 mice. $'s, used in Panel D only, designate differences between injection 1 and injection 2 for a given genotype. **(A) Distance traveled-Injection 1:** * WT vs *Fmr*1KO at dose 0: t_{10}=4.16, p<0.01. **&**: WT: 0 vs 1.0 mg/kg, t_{10}=4.42, p<0.01; 0 vs 3.3 mg/kg, t_{10}=4.50, p<0.01; and 0 vs 10.0 mg/kg, t_{10}=2.34, p<0.05 (a decrease). # *Fmr*1: 0 vs 1.0 mg/kg, t_{10}=3.24, p<0.01; 0 vs 3.3 mg/kg, t_{10}=2.53, p<0.05; and 0 vs 10.0 mg/kg, t_{10}=5.50, p<0.01. **(B) Distance-Injection 2**: * WT vs *Fmr*1 KO at dose 0: t_{10}=2.98, p<0.01; WT vs *Fmr*1 at dose 3.3 mg/kg, t_{10}=6.29, p<0.001. **&**: WT: 0 vs 1.0 mg/kg, t_{10}=4.12, p<0.01; 0 vs 3.3 mg/kg, $t_{10=}$7.69, p<0.01. # *Fmr*1: 0 vs 1.0

mg/kg, t_{10}=4.25, p<0.01; 0 vs 3.3, t_{10}=3.32, p<0.01; 0 vs 10.0 mg/kg, t_{10}=4.25, p<0.01 (a decrease). **(C) Focused Stereotypy-Injection 1**: ***** WT vs *Fmr*1 at dose 10.0 mg/kg, t_{10}=2.897, p<0.05. **(D) Focused Stereotypy-Injection 2**: * WT vs *Fmr*1 at dose 10.0 mg/kg, t_{10}=3.33, p<0.01; **$** Injection 2 vs injection 1: Wt: t_{10}=2.60, p<0.05; *Fmr*1: t_{10}=3.04, p<0.05 (*66*). Figure taken from Fulks *et al*. 2010.

AMPH stimulated locomotor activity at the two lower doses but decreased locomotor activity at the 10 mg/kg dose. Each dose group for injection 1, regardless of genotype, showed a significant dose response to AMPH, either by an increase in locomotion at the lower doses, or with a decrease in the high dose. The dose effect pattern for injection 2 was similar to the pattern in Injection 1 with two exceptions. In the 3.3 mg/kg AMPH dose the *Fmr*1 KO mice were significantly lower than the WT mice, and at the 10 mg/kg dose the WT mice were not significantly lower than the WT mice under vehicle conditions, likely due to the low distance traveled by the WT mice receiving the vehicle after the second injection. Previous studies have reported that at 2.0 mg/kg AMPH there was no significant increase in locomotor activity (*48-49*), however, this discrepancy may due to the enhanced temporal and spatial resolution of the force-plate method.

2.3.1.2 Focused Stereotypy

Focused stereotypy data for AMPH dose-effect are shown in **Figure 2** (Panels C and D). The 3-way ANOVA of focused stereotypy measurements indicated significant main effects of mouse type, dose and injection number. A significant dose interaction was seen with both injection number and mouse type. A 2-way post hoc, type x injection # ANOVA at the 10.0 mg/kg dose showed significantly greater focused

stereotypy in the WT mice than in the *Fmr*1 KO mice on both injection days. Focused stereotypy for both KO and WT mice was significantly higher after injection 2 compared to injection 1. These data suggest that the *Fmr*1 KO mice have a diminished high-dose response to AMPH. For the focused stereotypy measure, AMPH dose effects were not detected when the 10.0 mg/kg dose groups were removed from the analysis, showing that the WT-KO differences in focused stereotypy was primarily at the 10.0 mg/kg dose.

2.3.2 DA Release in the Dorsal Striatum

Previous evidence suggests that focused stereotypy expression is strongly influenced by increased extracellular DA levels in the dorsal striatum (*53*). Therefore, the differences in AMPH-induced stereotypic behavior between KO and WT mice prompted us to determine DA release and uptake characteristics in striatal brain slices from *Fmr*1 KO and WT mice. FSCV was used to generate plots of stimulated DA release and uptake **Figure 3**.

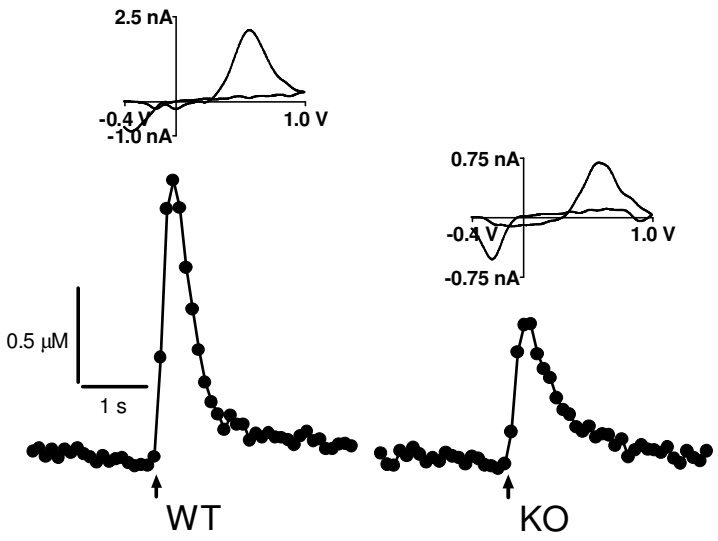

Figure 3. DA release is impaired in 15 week-old *Fmr*1 KO mice. Representative plots of electrically stimulated DA release obtained in brain slices from a 15 week-old *Fmr*1 KO mouse and an age-matched WT control mouse. The application of a single, biphasic electrical stimulus pulse (4 ms total duration, 350 µA current) is denoted by the arrow under each plot. Cyclic voltammograms, provided above each plot, confirm the presence of DA.

Curve modeling software was then used to calculate DA released per stimulus pulse ($[DA]_p$), which is peak DA release corrected for uptake and electrode performance, and V_{max}, the maximum rate of DA uptake (**Figure 4**). Values obtained from *Fmr*1 KO mice were normalized against corresponding WT values. At 10 weeks of age, no significant differences in $[DA]_p$ was noted between KO mice (n=7) and WT mice (n=7). This finding is consistent with voltammetric measurements obtained previously in *Fmr*1 KO mice (*67*). However, at 15 (KO n=6 and WT n=6) and 20 (KO n=10 and WT n=10) weeks of age, $[DA]_p$ was diminished in KO mice compared to WT mice ($p< 0.05$ and $p<0.001$ respectively). Similarly, V_{max} was the same in the KO and WT mice at 10

weeks of age, but was decreased in KO mice at 15 and 20 weeks of age. It is not known why impairments in release and uptake develop later in life in KO mice; however, this finding may imply that neurochemical changes occur into adulthood in humans with fragile X syndrome.

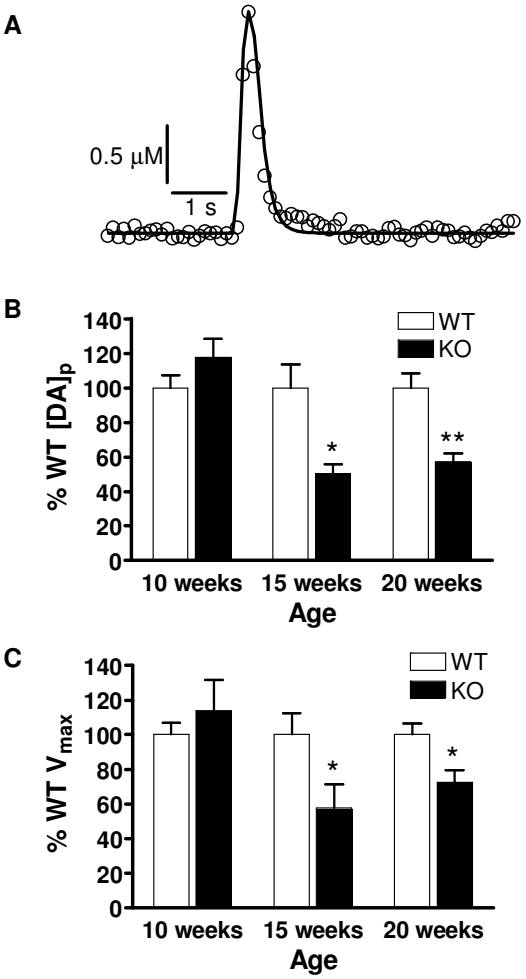

Figure 4. $[DA]_p$ and V_{max} are impaired in 15- and 20-week old KO mice compared to aged-matched WT control mice. (A) The open circles represent the experimental data, while the line shows the model fit to the data. (B) When the stimulated DA release of the KO mice were compared to the WT mice, a significant difference in the release was seen at 15 and 20 weeks of age. (C) By modeling the data, V_{max} was also determined and the KO compared to the WT. A significant decrease in V_{max} was seen in the 15 and 20 week old mice.

A potential underlying cause for the decrease in $[DA]_p$ noted in the older KO mice is a diminishment in the amount of DA available for release. Therefore, striatal catecholamine content was measured using high performance liquid chromatography (HPLC) with electrochemical detection (*68*). Total DA content was the same between age groups and genotype (n=4 to 7 mince; **Table 1**). Moreover, no differences were noted in the striatal content of 3,4-dihydroxyphenylacetic acid (DOPAC) and homovanillic acid (HVA), two metabolites of DA. Therefore, even though sufficient DA stores are present in the KO striatum, these stores are not released as effectively as in the WT mice.

Table 1. Catacholamine content in striatal lysates from KO and WT mice. No significant differences in the content of DA, DOPAC, or HVA were noted between KO and WT. The n-values in parentheses indicate number of mice.

	KO			WT		
Age (weeks)	**DA(ng/g)**	**DOPAC(ng/g)**	**HVA(ng/g)**	**DA(ng/g)**	**DOPAC(ng/g)**	**HVA(ng/g)**
10	10166 ± 623 (n=5)	1077 ± 91 (n=5)	1336 ± 79 (n=5)	9529±329 (n=7)	1154 ± 91 (n=7)	1536 ± 81 (n=7)
15	9934±1051 (n=5)	764 ± 81 (n=5)	1177 ± 113 (n=5)	8796±637 (n=6)	805 ± 38 (n=6)	1483 ± 186 (n=6)
20	9375±624 (n=5)	1294 ±382 (n=5)	2546 ± 596 (n=5)	9653±967 (n=4)	1419 ± 250 (n=4)	1481 ± 111 (n=4)

2.3.3 D2 Autoreceptor Function

Presynaptic D2 autoreceptors are G-protein coupled receptors that inhibit DA synthesis and release upon activation (*69*). To determine if D2 autoreceptor over-

activation causes decreased $[DA]_p$ in KO mice, striatal brain slices from 20-week old mice were treated with increasing concentrations of quinpirole, a D2 agonist (*70*). After treatment with the maximum quinpirole concentration of 150 nM, DA release disappeared (**Figure 5**). No significant interactions between drug concentration and genotype were found (ANOVA, $p>0.05$, KO n=4 and WT n=6); therefore, over-activation of D2 autoreceptors is not a likely underlying cause of decreased release in KO mice.

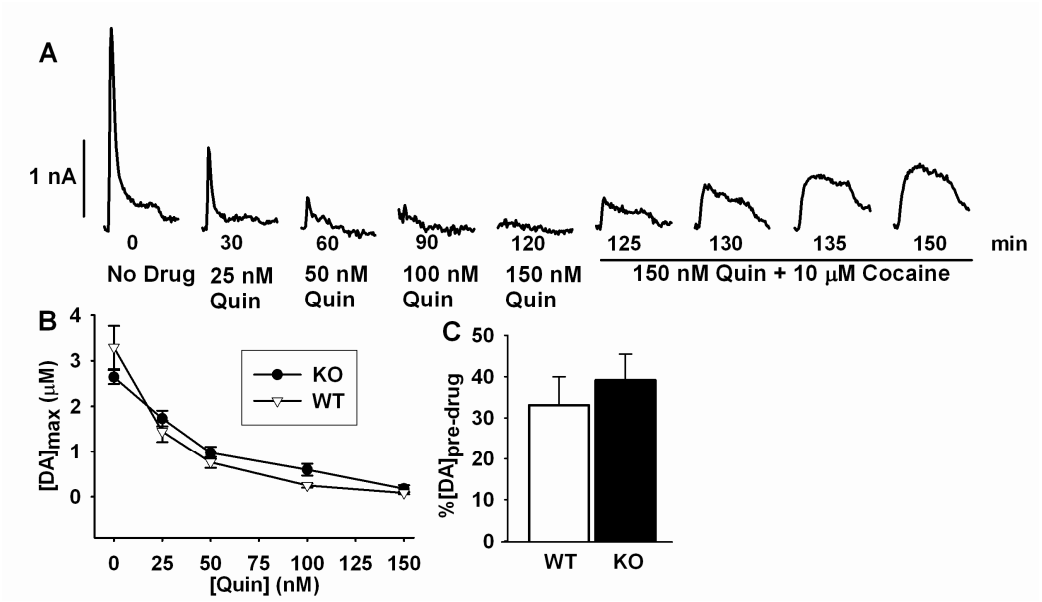

Figure 5. D2 autoreceptor activation similarly and cocaine induced reserve pool activation were similar in WT and KO mice. (A) Representative data collected in a striatal brain slice from a 20 week old WT mouse. The slice was exposed to cumulatively increasing concentrations of quinpirole while measuring electrically-evoked DA release every 5 minutes. After DA release disappeared, cocaine was added to the slice with the quinpirole to mobilize reserve pool DA. (B) Quinpirole inhibited DA release similarly in WT and KO mice (ANOVA). (C) The percent DA recovery post quinpirole and cocaine showed no difference in the KO and WT mice.

An important aspect of D2 autoreceptor function is inhibition of DA synthesis. Continuous treatment with quinpirole and concurrent application of periodic electrical stimulus pulses should deplete terminals of releasable DA, leaving only reserve pool DA. To identify potential differences in reserve pool mobilization and content, cocaine (10 µM) was added to the slices in addition to the quinpirole (150 nM) already present, and the stimulation regiment of a series of 50 pulses applied at 10 Hz every 5 minutes was continued. The purpose of using the extended pulse sequences opposed to single pulses was to facilitate the depletion of releasable DA. Cocaine has been shown to mobilize a synapsin dependent DA reserve pool (*71-72*). Therefore, as expected, within 5 minutes, the reserve pool vesicles were mobilized and the stimulated release peak reappeared. After 30 minutes of cocaine exposure, KO and WT stimulated release peaks, expressed as a percentage of the pre-drug peak, were compared (**Figure 5C**). These values did not differ significantly (student's t-test, KO n=4 and WT n=6, $p > 0.05$), indicating that similar amounts of reserve pool DA were mobilized in KO and WT mice.

2.3.4 Neurochemical Response to AMPH

To compare the DA uptake efficiencies between KO and WT mice, brain slices from both genotypes were treated with successively increasing concentrations of AMPH, which inhibits DA uptake through the DA transporter (DAT). Drug response curves were then obtained by plotting the average K_M values against [AMPH]. Linear regression analyses reveal that the slopes for the KO and WT curves both deviate significantly from zero ($p < 0.001$, n=4 KO and 4 WT mice) and analyses by 2-way ANOVA show that there is no significant interaction between genotype and AMPH

concentration (**Figure 6**). Therefore, differences in behavioral activation due to AMPH administration likely do not arise from differences in the affinity of AMPH for DAT.

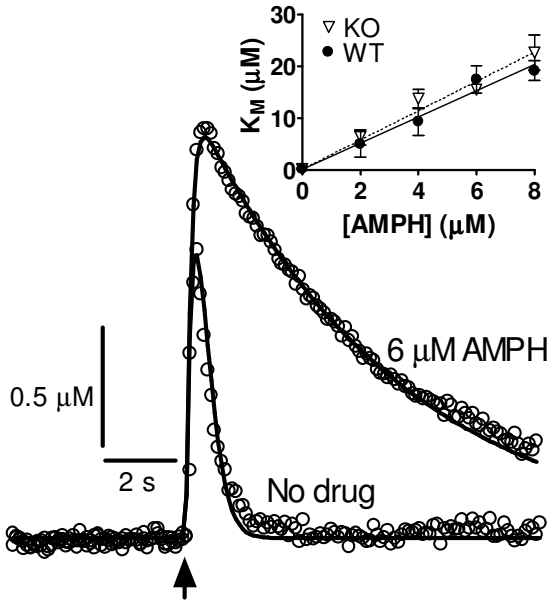

Figure 6. DA uptake is similarly inhibited in the KO and WT striatum. The stimulated release plots (open circles) were modeled (solid line) to determine K_M for DA uptake during a cumulative treatment regimen. Average values of K_M at each AMPH concentration were determined and plotted (inset). There was no significant interaction between genotype and K_M or between genotype and [AMPH] (ANOVA).

Further analyses of these data revealed no differences in $[DA]_p$ between KO and WT mice at any given concentration of AMPH (**Figure 7**); however, a concern with these release values was that genotype-related differences in $[DA]_p$ could be masked by the high degree of heterogeneity of dopaminergic innervations within the striatum. To account for this variability, we used a separate experimental approach in which DA

release was sampled from four locations in the dorsolateral caudate and averaged, both before and after treating the slice with 6 µM AMPH (a concentration that provided a large increase in K_M but did not appear to cause diminished release). However, DA release plots obtained in this way were not amenable to modeling because V_{max} changes when the working electrode is moved to different locations within the striatum. Because curves generated from these measurements were not modeled, the DA release values were uncorrected for uptake. For each slice, the peak DA release values after AMPH treatment were expressed as a percentage of average release prior to treatment (% no drug release). Slices were averaged to obtain a value for each mouse. These data revealed that % no drug release was significantly greater in the KO mice than in the WT mice ($p < 0.01$, t-test, n=4 WT and 4 KO mice; **Figure 7**) and indicate that AMPH treatment enhanced DA release in slices from KO mice, but not in slices from WT mice. The raw values of DA release following AMPH treatment were 1.50 ± 0.31 µM in KO mice and 0.58 ± 0.46 µM in WT mice ($p < 0.05$, t-test, n=4 WT and 4 KO mice).

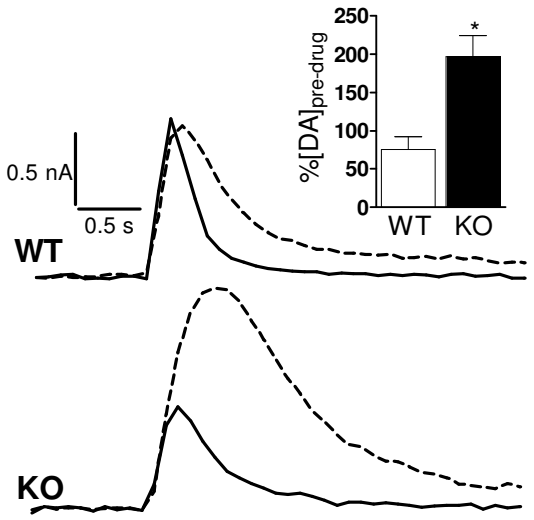

Figure 7. AMPH enhances stimulated DA release in brain slices from KO mice, but not in those from WT mice. Representative plots of stimulated DA release are shown for WT and KO mice before (solid lines) and after (dashed lines) treatment with 6 μM AMPH. After AMPH administration, stimulated DA release increased, relative to pre-drug values in KO mice, but not in WT mice (inset). Statistics: $*p < 0.01$, t-test, n = 4 WT and 4 KO mice.

AMPH empties DA from presynaptic terminals and vesicles. To do this, it first enters terminals either through membrane-bound DAT protein molecules or by lipophilic diffusion through the membrane. AMPH that enters through the DAT causes allosteric translocation of the protein and induces the reverse transport of DA from the cytosol to the extracellular space (*73-75*). Additionally, AMPH displaces vesicular DA into the cytoplasm where it can then be released by reverse transport (*73, 76*). Thus, the availability of DAT protein molecules for both AMPH entrance and for DA reverse transport should impact extracellular DA levels in AMPH-injected mice.

Our data show a decrease in V_{max} in KO mice at 15 and 20 weeks of age. According to Michaelis-Menton kinetics, V_{max} is directly proportional to the number of

functioning DAT protein molecules (*77*) ($V_{max} – k_{cat}[E]_t$ where k_{cat} is a rate constant and $[E]_t$ is the total enzyme concentration). This means that less transporter protein molecules function properly in KO mice compared to WT mice. Logically, our voltammetric data are consistent with a scenario in which AMPH cannot enter, and DA cannot leave, terminals in the *Fmr*1 KO striatum as readily as in the WT striatum. Therefore, DA is able to reside within the terminals and vesicles for a longer period of time in the KO striatum and is, therefore, available for release in the event of an action potential. These neurochemical results are consistent with those of Ventura et al. (*47*), who found that AMPH induces a smaller increase in extracellular striatal DA levels in KO mice compared to WT mice. More importantly, however, these neurochemical results agree with our behavioral data in the case of 15 week old KO mice which showed diminished expression of focused stereotypy compared to age matched WT mice.

2.3.5 DA response to GBR12909

The effect of slice exposure to GBR12909 (GBR) was also evaluated. Unlike AMPH, GBR is a selective DAT blocker thus inhibiting DA uptake and has been shown to cause an increase in extracellular DA levels (*78-80*). GBR was administered to slices by perfusion in increasing concentrations (25, 50 and 100µM) over time, while collecting stimulated DA release data. The data were modeled to determine K_M values for each concentration (**Figure 8**). A plot of K_M vs. concentration of GBRsuggests that the affinity of GBR for DAT is the same in both the WT and KO mice (**Figure 8**).

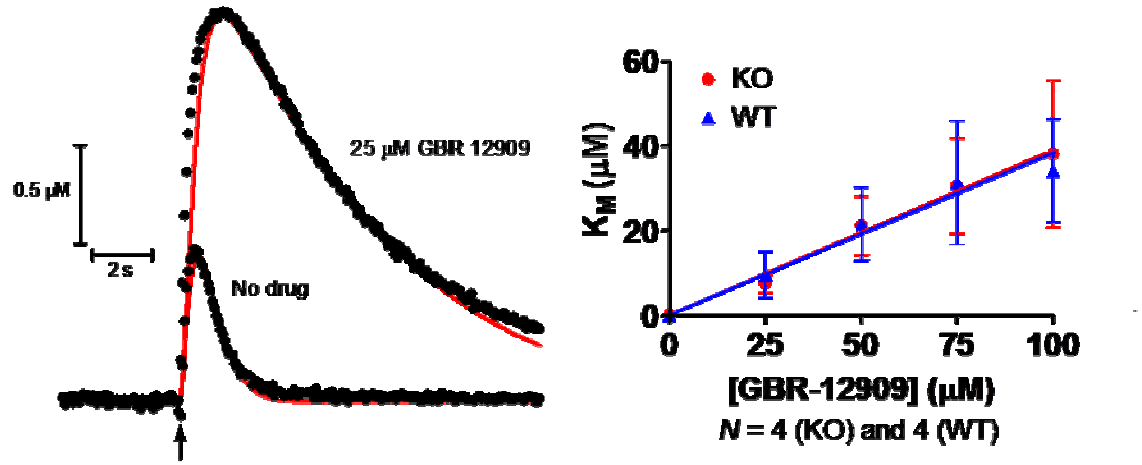

Figure 8. GBR-12909 brain slice data. The data was modeled using modeling software and values of K_M were plotted against the concentration of GBR-12909 showing no alterations in the affinity of GBR-12909 for DAT in the KO mice.

2.3.7 DA release and the mGluR Theory

Metabotropic glutamate receptors (mGluR) and FMRP are important in the regulation of mRNA transcription (*8, 81*). Evidence indicates a hypersensitivity of mGluR's in FXS which contributes to the phenotype (*5, 82-83*). The use of an mGluR antagonist 2-methyl-6-(phenylethynyl)pyridine (MPEP) has been shown to recover some of the phenotypic behavior associated with FXS when given to *Fmr*1 mutant *Drosophila* over time (*84*). We have shown that FXS has diminished stimulated release in the 15 and 20 week old age groups likely connected to the behavioral differences seen between the KO and WT mice. To evaluate the effect of antagonizing the mGluR's on DA release, we exposed slices to MPEP to determine if it would recover stimulated DA release in the KO mice. Slices from 10 week and 20 week old mice were exposed to 46 µM & 30 µM MPEP respectively. Stimulated release data was collected from four locations in each slice before and after MPEP exposure. The data were

reported as a % of the predrug release (**Figure 9**). We were unable to detect any immediate effect on stimulated DA release when exposing the slices to MPEP ($p > 0.05$, n=6 for 10 week old and n=3 for 20 week old).

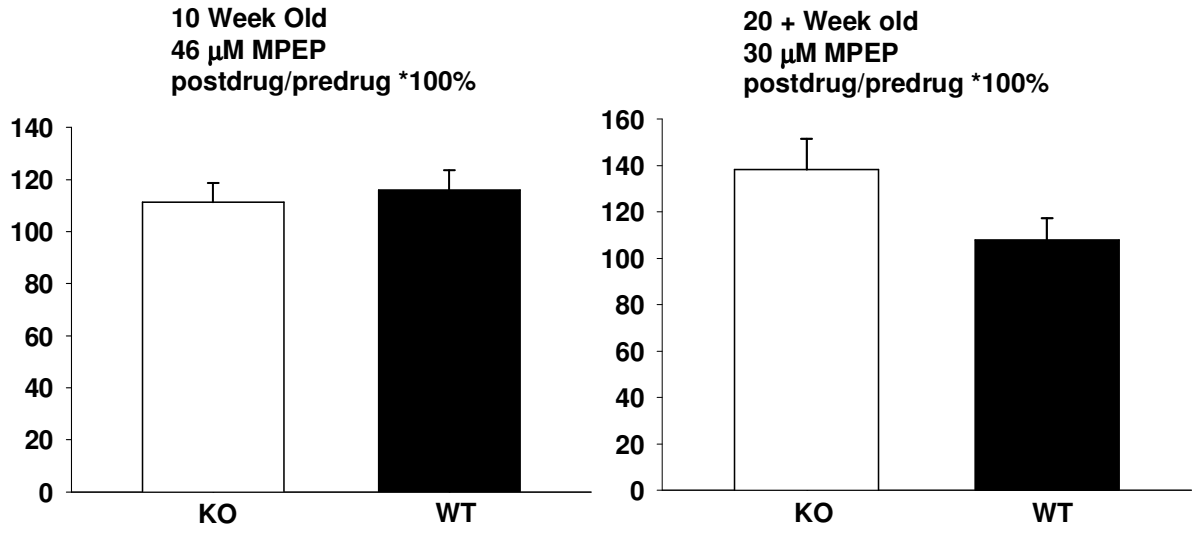

Figure 9. Stiumulated DA response to MPEP exposure on slices. No significant difference was seen in either the 10 week or 20 week old groups. ($p>0.05$, n=6 for 10 week old mice and n=3 for 20 week old mice)

2.4 CONCLUDING REMARKS

To our knowledge, this is the first published study to use the force-plate actometer to provide quantitative measurements of behavior in *Fmr1* KO mice in comparison to WT control mice. This method has the utility of being able to identify and quantify rodent behavior even when the animal is not locomoting. Our results reveal a significant difference in behavioral response to AMPH injection. In particular, *Fmr1* KO mice are resistant to the expression of AMPH-induced focused stereotypy. Our DA release plots support the concept that this resistance is potentially influenced not only by an impairment in the ability of these mice to release DA, but also by decreased AMPH-induced efflux of DA from terminals in the *Fmr1* KO striatum. Moreover, because these neurochemical differences were found only in mice 15 weeks of age or older, it may be that changes in DA release and uptake occur into adulthood of individuals with fragile X syndrome.

ACKNOWLEDGMENT

This project was funded by: the National Institutes of Health (NIH) from the IDeA Network of Biomedical Research Excellence (INBRE) Program of the National Center for Research Resources under the award P20 RR016475 (MAJ); the Kansas City Area Life Sciences Institute and TEVA Neuroscience, Inc. (MAJ); and by the Life Span Institute (P30-HD02528) at the University of Kansas (SCF).

2.5 REFERENCES

1. Webb, T. P., Bundey, S., Thake, A., and Todd, J. (1986) The frequency of the fragile X chromosome among schoolchildren in Coventry, *J Med Genet 23*, 396-399.

2. Verkerk, A. J., Pieretti, M., Sutcliffe, J. S., Fu, Y. H., Kuhl, D. P., Pizzuti, A., Reiner, O., Richards, S., Victoria, M. F., Zhang, F. P., and et al. (1991) Identification of a gene (FMR-1) containing a CGG repeat coincident with a breakpoint cluster region exhibiting length variation in fragile X syndrome, *Cell 65*, 905-914.

3. Feng, Y., Zhang, F. P., Lokey, L. K., Chastain, J. L., Lakkis, L., Eberhart, D., and Warren, S. T. (1995) Translational suppression by trinucleotide repeat expansion at FMR1, *Science 268*, 731-734.

4. Oberle, I., Rousseau, F., Heitz, D., Kretz, C., Devys, D., Hanauer, A., Boue, J., Bertheas, M. F., and Mandel, J. L. (1991) Instability of a 550 base pair DNA segment and abnormal methylation in FRAGILE X-syndrome, *Science 252*, 1097-1102.

5. Bear, M. F., Huber, K. M., and Warren, S. T. (2004) The mGluR theory of fragile X mental retardation, *Trends Neurosci 27*, 370-377.

6. Huot, M. E., Bisson, N., Davidovic, L., Mazroui, R., Labelle, Y., Moss, T., and Khandjian, E. W. (2005) The RNA-binding protein fragile X-related 1 regulates somite formation in Xenopus laevis, *Molecular Biology of the Cell 16*, 4350-4361.

7. Siomi, H., and Dreyfuss, G. (1997) RNA-binding proteins as regulators of gene expression, *Curr. Opin. Genet. Dev. 7*, 345-353.

8. Siomi, H., Siomi, M. C., Nussbaum, R. L., and Dreyfuss, G. (1993) The protein product of the fragile X gene, FMR1, has characteristics of an RNA-binding protein, *Cell 74*, 291-298.

9. Cornish, K., Sudhalter, V., and Turk, J. (2004) Attention and language in fragile X, *Mental Retardation and Developmental Disabilities Research Reviews 10*, 11-16.

10. Hagerman, R. J., and Hagerman, P. J. (2002) The fragile X premutation: into the phenotypic fold, *Curr Opin Genet Dev 12*, 278-283.

11. Hatton, D. D., Hooper, S. R., Bailey, D. B., Skinner, M. L., Sullivan, K. M., and Wheeler, A. (2002) Problem behavior in boys with fragile X syndrome, *Am. J. Med. Genet. 108*, 105-116.

12. Maes, B., Fryns, J. P., Vanwalleghem, M., and Vandenberghe, H. (1994) Cognitive-functioning and information-processing of adult mentally-retarded men with fragile-X syndrome, *Am. J. Med. Genet. 50*, 190-200.

13. Reiss, A. L., and Freund, L. (1992) Behavioral-phenotype of fragile-X syndrome - DSM-III-R autistic behavior in male-children, *Am. J. Med. Genet. 43*, 35-46.

14. Hagerman, R. J. (1996) Fragile X syndrome, *Child Adolesc. Psychiatr. N. Am. 5*, 895-&.

15. (1994) The Dutch-Belgian Fragile X Consortium. Fmr1 knockout mice: a model to study fragile X mental retardation. , *Cell 78*, 23-33.

16. Musumeci, S. A., Ferri, R., Scuderi, C., Bosco, P., and Elia, M. (2001) Seizures and epileptiform EEG abnormalities in FRAXE syndrome, *Clinical Neurophysiology 112*, 1954-1955.

17. Musumeci, S. A., Hagerman, R. J., Ferri, R., Bosco, P., Dalla Bernardina, B., Tassinari, C. A., De Sarro, G. B., and Elia, M. (1999) Epilepsy and EEG findings in males with fragile X syndrome, *Epilepsia 40*, 1092-1099.

18. Yan, Q. J., Rammal, M., Tranfaglia, M., and Bauchwitz, R. P. (2005) Suppression of two major Fragile X Syndrome mouse model phenotypes by the mGluR5 antagonist MPEP, *Neuropharmacology 49*, 1053-1066.

19. Bakker, C. E., Verheij, C., Willemsen, R., Vanderhelm, R., Oerlemans, F., Vermey, M., Bygrave, A., Hoogeveen, A. T., Oostra, B. A., Reyniers, E., Deboulle, K., Dhooge, R., Cras, P., Vanvelzen, D., Nagels, G., Martin, J. J., Dedeyn, P. P., Darby, J. K., and Willems, P. J. (1994) Fmr1 Knockout Mice - a Model to Study Fragile-X Mental-Retardation, *Cell 78*, 23-33.

20. Dhooge, R., Nagels, G., Franck, F., Bakker, C. E., Reyniers, E., Storm, K., Kooy, R. F., Oostra, B. A., Willems, P. J., and DeDeyn, P. P. (1997) Mildly impaired water maze performance in male Fmr1 knockout mice, *Neuroscience 76*, 367-376.

21. Dobkin, C., Rabe, A., Dumas, R., El Idrissi, A., Haubenstock, H., and Brown, W. T. (2000) Fmr1 knockout mouse has a distinctive strain-specific learning impairment, *Neuroscience 100*, 423-429.

22. Kooy, R. F., Dhooge, R., Reyniers, E., Bakker, C. E., Nagels, G., DeBoulle, K., Storm, K., Clincke, G., DeDeyn, P. P., Oostra, B. A., and Willems, P. J. (1996) Transgenic mouse model for the fragile X syndrome, *Am. J. Med. Genet. 64*, 241-245.

23. Paradee, W., Melikian, H. E., Rasmussen, D. L., Kenneson, A., Conn, P. J., and Warren, S. T. (1999) Fragile X mouse: Strain effects of knockout phenotype and evidence suggesting deficient amygdala function, *Neuroscience 94*, 185-192.

24. Peier, A. M., McIlwain, K. L., Kenneson, A., Warren, S. T., Paylor, R., and Nelson, D. L. (2000) (Over)correction of FMR1 deficiency with YAC transgenics: behavioral and physical features, *Human Molecular Genetics 9*, 1145-1159.

25. McNaughton, C. H., Moon, J., Strawderman, M. S., Maclean, K. N., Evans, J., and Strupp, B. J. (2008) Evidence for social anxiety and impaired social cognition in a mouse model of Fragile X syndrome, *Behavioral Neuroscience 122*, 293-300.

26. Moon, J., Beaudin, A. E., Verosky, S., Driscoll, L. L., Weiskopf, M., Levitsky, D. A., Crnic, L. S., and Strupp, B. J. (2006) Attentional dysfunction, impulsivity, and resistance to change in a mouse model of fragile X syndrome, *Behav Neurosci 120*, 1367-1379.

27. Koekkoek, S. K., Yamaguchi, K., Milojkovic, B. A., Dortland, B. R., Ruigrok, T. J., Maex, R., De Graaf, W., Smit, A. E., VanderWerf, F., Bakker, C. E., Willemsen, R., Ikeda, T., Kakizawa, S., Onodera, K., Nelson, D. L., Mientjes, E., Joosten, M., De Schutter, E., Oostra, B. A., Ito, M., and De Zeeuw, C. I. (2005) Deletion of FMR1 in Purkinje cells enhances parallel fiber LTD, enlarges spines, and attenuates cerebellar eyelid conditioning in Fragile X syndrome, *Neuron 47*, 339-352.

28. Nosyreva, E. D., and Huber, K. M. (2006) Metabotropic receptor-dependent long-term depression persists in the absence of protein synthesis in the mouse model of fragile X syndrome, *J Neurophysiol 95*, 3291-3295.

29. Gerfen, C. R., Herkenham, M., and Thibault, J. (1987) The neostriatal mosaic .2. patch-directed and matrix-directed mesostriatal dopaminergic and nondopaminergic systems, *Journal of Neuroscience 7*, 3915-3934.

30. Centonze, D., Picconi, B., Gubellini, P., Bernardi, G., and Calabresi, P. (2001) Dopaminergic control of synaptic plasticity in the dorsal striatum, *Eur J Neurosci 13*, 1071-1077.

31. Gerdeman, G. L., Ronesi, J., and Lovinger, D. M. (2002) Postsynaptic endocannabinoid release is critical to long-term depression in the striatum, *Nat Neurosci 5*, 446-451.

32. Giuffrida, A., Parsons, L. H., Kerr, T. M., de Fonseca, F. R., Navarro, M., and Piomelli, D. (1999) Dopamine activation of endogenous cannabinoid signaling in dorsal striatum, *Nat. Neurosci. 2*, 358-363.

33. Kreitzer, A. C., and Malenka, R. C. (2005) Dopamine modulation of state-dependent endocannabinoid release and long-term depression in the striatum, *J Neurosci 25*, 10537-10545.

34. Calabresi, P., Saiardi, A., Pisani, A., Baik, J. H., Centonze, D., Mercuri, N. B., Bernardi, G., and Borrelli, E. (1997) Abnormal synaptic plasticity in the striatum of mice lacking dopamine D2 receptors, *J Neurosci 17*, 4536-4544.

35. Jones, S. R., Gainetdinov, R. R., Jaber, M., Giros, B., Wightman, R. M., and Caron, M. G. (1998) Profound neuronal plasticity in response to inactivation of the dopamine transporter, *Proc Natl Acad Sci U S A 95*, 4029-4034.

36. Young, J. G., Kavanagh, M. E., Anderson, G. M., Shaywitz, B. A., and Cohen, D. J. (1982) Clinical neurochemistry of autism and associated disorders, *J Autism Dev Disord 12*, 147-165.

37. Baranek, G. T., Danko, C. D., Skinner, M. L., Bailey, D. B., Jr., Hatton, D. D., Roberts, J. E., and Mirrett, P. L. (2005) Video analysis of sensory-motor features in infants with fragile X syndrome at 9-12 months of age, *J Autism Dev Disord 35*, 645-656.

38. Einfeld, S. L., Tonge, B. J., and Florio, T. (1994) Behavioural and emotional disturbance in fragile X syndrome, *Am J Med Genet 51*, 386-391.

39. Aman, M. G., and Langworthy, K. S. (2000) Pharmacotherapy for hyperactivity in children with autism and other pervasive developmental disorders, *J Autism Dev Disord 30*, 451-459.

40. Bartak, L., and Rutter, M. (1976) Differences between mentally retarded and normally intelligent autistic children, *J Autism Child Schizophr 6*, 109-120.

41. Campbell, M., Locascio, J. J., Choroco, M. C., Spencer, E. K., Malone, R. P., Kafantaris, V., and Overall, J. E. (1990) Stereotypies and tardive dyskinesia: abnormal movements in autistic children, *Psychopharmacol Bull 26*, 260-266.

42. Meiselas, K. D., Spencer, E. K., Oberfield, R., Peselow, E. D., Angrist, B., and Campbell, M. (1989) Differentiation of stereotypies from neuroleptic-related dyskinesias in autistic children, *J Clin Psychopharmacol 9*, 207-209.

43. Fleckenstein, A. E., Volz, T. J., Riddle, E. L., Gibb, J. W., and Hanson, G. R. (2007) New insights into the mechanism of action of amphetamines, *Annu Rev Pharmacol Toxicol 47*, 681-698.

44. Gainetdinov, R. R., Wetsel, W. C., Jones, S. R., Levin, E. D., Jaber, M., and Caron, M. G. (1999) Role of serotonin in the paradoxical calming effect of psychostimulants on hyperactivity, *Science 283*, 397-401.

45. Jinnah, H. A., Gage, F. H., and Friedmann, T. (1991) Amphetamine-induced behavioral-phenotype in a hypoxanthine guanine phosphoribosyltransferase deficient mouse model of lesch-nyhan syndrome, *Behavioral Neuroscience 105*, 1004-1012.

46. Sallinen, J., Haapalinna, A., Viitamaa, T., Kobilka, B. K., and Scheinin, M. (1998) D-amphetamine and L-5-hydroxytryptophan-induced behaviours in mice with genetically-altered expression of the alpha(2C)-adrenergic receptor subtype, *Neuroscience 86*, 959-965.

47. Ventura, R., Pascucci, T., Catania, M. V., Musumeci, S. A., and Puglisi-Allegra, S. (2004) Object recognition impairment in Fmr1 knockout mice is reversed by amphetamine: involvement of dopamine in the medial prefrontal cortex, *Behav Pharmacol 15*, 433-442.

48. Zupan, B., and Toth, M. (2008) Wild-type male offspring of fmr-1(+/-) mothers exhibit characteristics of the fragile X phenotype, *Neuropsychopharmacology 33*, 2667-2675.

49. Rebec, G. V., and Segal, D. S. (1980) Apparent tolerance to some aspects of amphetamine stereotypy with long-term treatment, *Pharmacology Biochemistry and Behavior 13*, 793-797.

50. Brien, J. F., Peachey, J. E., Rogers, B. J., and Kitney, J. C. (1977) Amphetamine-induced stereotyped behavior and brain concentrations of amphetamine and its hydroxylated metabolites in mice, *Journal of Pharmacy and Pharmacology 29*, 49-50.

51. Kasim, S., and Jinnah, H. A. (2002) Pharmacologic thresholds for self-injurious behavior in a genetic mouse model of Lesch-Nyhan disease, *Pharmacology Biochemistry and Behavior 73*, 583-592.

52. Cho, A. K., Melega, W. P., Kuczenski, R., Segal, D. S., and Schmitz, D. A. (1999) Caudate-putamen dopamine and stereotypy response profiles after intravenous and subcutaneous amphetamine, *Synapse 31*, 125-133.

53. Creese, I., and Iversen, S. D. (1974) The role of forebrain dopamine systems in amphetamine induced stereotyped behavior in the rat, *Psychopharmacologia 39*, 345-357.

54. Fowler, S. C., Birkestrand, B. R., Chen, R., Moss, S. J., Vorontsova, E., Wang, G., and Zarcone, T. J. (2001) A force-plate actometer for quantitating rodent behaviors: illustrative data on locomotion, rotation, spatial patterning, stereotypies, and tremor, *J Neurosci Methods 107*, 107-124.

55. Fowler, S. C., Pinkston, J. W., and Vorontsova, E. (2007) Clozapine and prazosin slow the rhythm of head movements during focused stereotypy induced by d-amphetamine in rats, *Psychopharmacology 192*, 219-230.

56. Fowler, S. C., Covington, H. E., and Miczek, K. A. (2007) Stereotyped and complex motor routines expressed during cocaine self-administration: results from a 24-h binge of unlimited cocaine access in rats, *Psychopharmacology 192*, 465-478.

57. Johnson, M. A., Rajan, V., Miller, C. E., and Wightman, R. M. (2006) Dopamine release is severely compromised in the R6/2 mouse model of Huntington's disease, *Journal of Neurochemistry 97*, 737-746.

58. Kawagoe, K. T., Zimmerman, J. B., and Wightman, R. M. (1993) Principles of Voltammetry and Microelectrode Surface-States, *Journal of Neuroscience Methods 48*, 225-240.

59. Hayashi, M. L., Rao, B. S. S., Seo, J. S., Choi, H. S., Dolan, B. M., Choi, S. Y., Chattarji, S., and Tonegawa, S. (2007) Inhibition of p21-activated kinase rescues symptoms of fragile X syndrome in mice, *Proceedings of the National Academy of Sciences of the United States of America 104*, 11489-11494.

60. Mineur, Y. S., Sluyter, F., de Wit, S., Oostra, B. A., and Crusio, W. E. (2002) Behavioral and neuroanatomical characterization of the Fmr1 knockout mouse, *Hippocampus 12*, 39-46.

61. Moy, S. S., Nadler, J. J., Young, N. B., Nonneman, R. J., Grossman, A. W., Murphy, D. L., D'Ercole, A. J., Crawley, J. N., Magnuson, T. R., and Lauder, J. M. (2009) Social approach in genetically engineered mouse lines relevant to autism, *Genes Brain and Behavior 8*, 129-142.

62. Spencer, C. M., Serysheva, E., Yuva-Paylor, L. A., Oostra, B. A., Nelson, D. L., and Paylor, R. (2006) Exaggerated behavioral phenotypes in Fmr1/Fxr2 double knockout mice reveal a functional genetic interaction between Fragile X-related proteins, *Human Molecular Genetics 15*, 1984-1994.

63. Yan, Q. J., Asafo-Adjei, P. K., Arnold, H. M., Brown, R. E., and Bauchwitz, R. P. (2004) A phenotypic and molecular characterization of the fmr1-tm1Cgr fragile X mouse, *Genes Brain Behav 3*, 337-359.

64. Yan, Q. J., Rammal, M., Tranfaglia, M., and Bauchwitz, R. P. (2005) Suppression of two major Fragile X Syndrome mouse model phenotypes by the mGluR5 antagonist MPEP, *Neuropharmacology 49*, 1053-1066.

65. Zupan, B., and Toth, M. (2008) Inactivation of the Maternal Fragile X Gene Results in Sensitization of GABA(B) Receptor Function in the Offspring, *Journal of Pharmacology and Experimental Therapeutics 327*, 820-826.

66. Fulks, J. L., O'Bryhim, B. E., Wenzel, S. K., Fowler, S. C., Vorontsova, E., Pinkston, J. W., Ortiz, A. N., and Johnson, M. A. (2010) Dopamine Release and Uptake Impairments and Behavioral Alterations Observed in Mice that Model Fragile X Mental Retardation Syndrome, *ACS Chemical Neuroscience 1*, 679-690.

67. Annangudi, S. P., Luszpak, A. E., Kim, S. H., Ren, S., Hatcher, N. G., Weiler, I. J., Thornley, K. T., Kile, B. M., Wightman, R. M., Greenough, W. T., and Sweedler, J. V. (2010) Neuropeptide Release Is Impaired in a Mouse Model of Fragile X Mental Retardation Syndrome, *ACS Chemical Neuroscience*.

68. Kraft, J. C., Osterhaus, G. L., Ortiz, A. N., Garris, P. A., and Johnson, M. A. (2009) In vivo dopamine release and uptake impairments in rats treated with 3-nitropropionic acid, *Neuroscience 161*, 940-949.

69. Cooper, J. R., Bloom, F. E., and Roth, R. H. (2003) *The Biochemical Basis of Neuropharmacology*, Eighth ed., Oxford University Press, New York.

70. O'Neill, C., Evers-Donnelly, A., Nicholson, D., O'Boyle, K. M., and O'Connor, J. J. (2009) D-2 receptor-mediated inhibition of dopamine release in the rat striatum in vitro is modulated by CB1 receptors: studies using fast cyclic voltammetry, *Journal of Neurochemistry 108*, 545-551.

71. Ortiz, A. N., Kurth, B. J., Osterhaus, G. L., and Johnson, M. A. (2009) Dysregulation of intracellular dopamine stores revealed in the R6/2 mouse striatum., *J Neurochem*.

72. Venton, B. J., Seipel, A. T., Phillips, P. E. M., Wetsel, W. C., Gitler, D., Greengard, P., Augustine, G. J., and Wightman, R. M. (2006) Cocaine increases dopamine release by mobilization of a synapsin-dependent reserve pool, *Journal of Neuroscience 26*, 3206-3209.

73. Chiueh, C. C., and Moore, K. E. (1975) D-amphetamine-induced release of newly synthesized and stored dopamine from caudate-nucleus invivo, *Journal of Pharmacology and Experimental Therapeutics 192*, 642-653.

74. Fischer, J. F., and Cho, A. K. (1979) Chemical-release of dopamine from striatal homogenates - evidence for an exchange diffusion-model, *Journal of Pharmacology and Experimental Therapeutics 208*, 203-209.

75. Liang, N. Y., and Rutledge, C. O. (1982) Evidence for carrier-mediated efflux of dopamine from corpus striatum, *Biochemical Pharmacology 31*, 2479-2484.

76. Jones, S. R., Gainetdinov, R. R., Wightman, R. M., and Caron, M. G. (1998) Mechanisms of amphetamine action revealed in mice lacking the dopamine transporter, *Journal of Neuroscience 18*, 1979-1986.

77. Mathews, C. K., and van Holde, K. E. (1996) *Biochemistry*, 2nd ed., Benjamin/Cummings, Menlo Park, CA.

78. Paterson, N. E., Fedolak, A., Olivier, B., Hanania, T., Ghavami, A., and Caldarone, B. (2010) Psychostimulant-like discriminative stimulus and locomotor sensitization properties of the wake-promoting agent modafinil in rodents, *Pharmacology Biochemistry and Behavior 95*, 449-456.

79. Walker, Q. D., Morris, S. E., Arrant, A. E., Nagel, J. M., Parylak, S., Zhou, G. Y., Caster, J. M., and Kuhn, C. M. (2010) Dopamine Uptake Inhibitors but Not Dopamine Releasers Induce Greater Increases in Motor Behavior and Extracellular Dopamine in Adolescent Rats Than in Adult Male Rats, *Journal of Pharmacology and Experimental Therapeutics 335*, 124-132.

80. Rothman, R. B., Mele, A., Reid, A. A., Akunne, H. C., Greig, N., Thurkauf, A., Decosta, B. R., Rice, K. C., and Pert, A. (1991) GBR12909 antagonizes the ability of cocaine to elevate extracellular levels of dopamine, *Pharmacology Biochemistry and Behavior 40*, 387-397.

81. Zalfa, F., Giorgi, M., Primerano, B., Moro, A., Di Penta, A., Reis, S., Oostra, B., and Bagni, C. (2003) The fragile X syndrome protein FMRP associates with BC1 RNA and regulates the translation of specific mRNAs at synapses, *Cell 112*, 317-327.

82. Homayoun, H., Stefani, M. R., Adams, B. W., Tamagan, G. D., and Moghaddam, B. (2004) Functional Interaction Between NMDA and mGlu5 Receptors: Effects on Working Memory, Instrumental Learning, Motor Behaviors, and Dopamine Release, *Neuropsychopharmacology 29*, 1259-1269.

83. Vanderklish, P. W., and Edelman, G. M. (2005) Differential translation and fragile X syndrome, *Genes Brain and Behavior 4*, 360-384.

84. Chang, S., Bray, S. M., Li, Z. G., Zarnescu, D. C., He, C., Jin, P., and Warren, S. T. (2008) Identification of small molecules rescuing fragile X syndrome phenotypes in Drosophila, *Nature Chemical Biology 4*, 256-263.

CHAPTER 3

DOPAMINE RELEASE AFTER CHEMOTHERAPY: INVESTIGATING THE PHENOMENON KNOWN AS "CHEMOBRAIN"

"Chemobrain" or "Chemofog" is a persistent decline in cognitive function experienced by cancer patients following chemotherapy. Studies comparing cognitive function before and after treatment suggest that approximately 20-30% of cancer patients exhibit decreased mental capacity following treatment. Currently, the phenomenon is not well understood; however, it is important to develop an understanding of the neurological effects of chemotherapy as the survival rates of cancers continue to increase. One of the drugs associated with the cognitive decline of chemobrain is carboplatin, which is used to treat various cancers including those of the gastrointestinal tract, breast, head and neck, and bladder.

Dopamine is an abundant CNS neurotransmitter involved in cognition, motivation, reward, and memory. We hypothesized that treatment with carboplatin impairs DA system function, potentially leading to problems with cognition. Fast-scan cyclic voltammetry (FSCV) at carbon-fiber microelectrodes was used to measure electrically-evoked dopamine release in striatal brain slices from male Wistar rats. The dosing for each of the four treatment groups was: vehicle, 5 mg/kg, 20 mg/kg, and 60 mg/kg. Measurements were collected from the dorsolateral, dorsomedial, ventrolateral, and ventromedial quadrants of the striatum. Treatment with carboplatin resulted in a dose-dependent diminishment in the release of dopamine; however, uptake was unaffected. Reserve pool dopamine was quantified by sequential treatment with alpha-

methyl-para-tyrosine (50µM), which inhibits dopamine synthesis, and amphetamine (20µM), which induces dopamine efflux. The data indicate that reserve pool dopamine levels are unchanged by carboplatin treatment, suggesting that the release process is impaired.

3.1 INTRODUCTION

3.1.1 Symptoms Associated with Chemobrain

Chemotherapy treatments come with a variety of unwanted side effects as the drugs work to kill the cancer cells. As the number of cancer survivors is ever increasing with the development of new treatments and earlier cancer detection, the reports of lasting effects of chemotherapy have been rising. One adverse effect that is being reported more often, especially in cases of breast cancer, treatment of cancer in children, and in colon cancer patients (*1-3*), is the alteration and decline of cognitive function (*1, 4*). This alteration, referred to as chemobrain, has a serious impact on the quality of life experienced by sufferers (*5-6*).

Various problems with cognitive function have been reported in cases of chemobrain. These alterations include: verbal and visual memory problems, lessened mental flexibility, slowed information processing speed, attention and concentration deficits, and troubles with motor function (*5, 7*). Neuropsychological tests have shown that a large number of cancer patients and survivors experience altered cognitive function as compared to age matched control groups (*1, 5, 8-9*). A study by Furguson *et al* evaluated the cognition of monozygotic twins, where one twin underwent chemotherapy (*9*). The twin having undergone chemotherapy had significantly greater

cognitive complaints indicating that the cognitive deficits are due to chemotherapy and not simply due to aging.

The mechanisms underlying these cognitive deficits are mostly unknown; however, the drugs used in chemotherapy are toxic chemicals that can damage blood vessles (*10*), potentially causing a disruption in blood flow (*11*), which can lead to ischemic stroke and cognitive disruption. The chemo drugs may also cause problems with cognition by causing direct injury to neurons leading to an alteration in neurotransmitter function.

3.1.2 Chemotherapeutics Associated with Chemobrain

With a wide variety of chemotherapeutic agents now available to those suffering with cancer, an increase in the occurrence of cognitive decline has been seen as reviewed in many articles (*4, 12-13*). Since the principal mechanism of chemotheraputics involves either cell apoptosis or cell growth/division inhibition, it is not surprising that many of these agents are associated with chemobrain in patients. Some of the drugs that have been associated with chemobrain include tamoxifen (*14*), CAF (cyclophosphamide, doxorubicin and fluorouracil) (*10, 15*), CMF (cyclophosphamide, methotrexate and fluorouracil) (*10, 16-17*), as well as carboplatin (*16, 18-19*).

There has been controversy over whether or not chemobrain is a real neurological condition (*14, 20-22*). However, after the compilation of many studies, Argyriou *et al* determined that long term decline in cognition due to chemotherapy is real (*12*). The apparent problem for the acceptance of chemobrain is the development an objective means of evaluating cognitive function before and after chemotherapy. The

use of animal studies allows for the direct measurement of the effects of chemotherapy on neurotransmitters compared to experimental controls, which can then lead to therapeutic treatment plans for human sufferers.

3.1.3 Carboplatin

Carboplatin (cis-Diammine(1,1-cyclobutanedicarboxylato)platinum(II)), depicted **Figure 1**, was developed in the 1980's and has been used in treatment in a wide variety of cancers including: head and neck, breast, ovarian, bladder, colon and others (*23-27*). The popularity of the drug increased as trial studies showed a significantly lower amount of side effects compared to cisplatin (*28-29*). The ability of carboplatin to cross the blood brain barrier could be a key to its role in cognition deficits after therapy due to damage of neurons from its presence in the brain. Studies have shown that Carboplatin, in combination with other chemotherapeutic drugs, is associated with the occurrence of cognitive decline (*16, 30-31*).

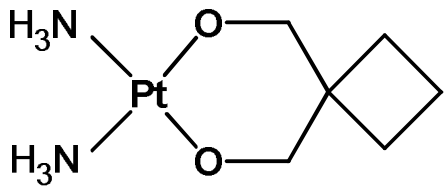

Figure 1. The structure of Carboplatin.

3.1.4 Current Treatments

Currently there are a few treatments that have shown some relief from the cognitive decline experienced by those experiencing chemobrain. One treatment that has had some successes is the use of recombinant human erythropoietin, which increases hemoglobin levels (*32*). An improvement in cognitive function and attention

has also been seen with treatments using the psychostimulant methylphenidate (*33-35*). A study by Mar Fan *et al*, however, evaluated the effects of methylphenidate on cognitive scores and verbal learning scores in women. The study found no significant improvement in the cognitive function of the methylphenidate group compared to the placebo group, indicating that methylphenidate had no major effect on cognitive function (*66*).

Methylphenidate increases extracellular levels of dopamine by binding to the dopamine transporter and blocking dopamine uptake (*36-38*). The effectiveness of a dopamine uptake inhibitor in the treatment of chemobrain led us to the hypothesis that damage is done to the dopaminergic system in chemobrain. Thus, the investigation of the effects of chemotherapy on dopamine release and uptake are well-justified.

Another drug used for treatment of cognitive impairments associated with chemobrain is modafinil, a wake-promoting drug. The benefit of utilizing modafinil is that it has a lower abuse potential compared to methylphenidate. In a study by Lundorff *et al* a double blind study was carried out for 8 days administering 200 mg doses of modafinil or placebo (*39*). The group receiving the modafinil reported a significant improvement in attention and psychomotor speed compared to the placebo group. In a separate study by Kohli *et al* it was also found that administration of modafinil enhanced memory and attention skills in cancer patients (*40*).

3.1.5 Previous Animal Studies

Few animals studies designed to assess the effects of admininistration of chemotherapeutic agents on neurological function have been published. One study performed by Mustafa et al. evaluated the effects of 5-fluorouracil (5-Fu), a common drug used in adjuvant chemotherapy, on spatial working memory and the proliferation of neurons in adult male Lister-hooded rats (*41*). They found that there was decline in the exploratory time spent by the 5-Fu treated rats when they were placed in a novel location. They also showed that the proliferating cell counts were unaffected by the administration of 5-Fu, however, the levels of brain-derived neurotrophic factor (BDNF), a protein necessary for the survival of newborn neurons and their maturation, was decreased in the 5-Fu rats compared to the vehicle treated rats.

Joshi et al. performed a study evaluating the effects of doxorubicin administered to mice to evaluate the oxidative stress caused by chemotherapy, which could lead to cognitive decline (*42*). Male B6C3 mice were dosed with either doxorubicin or saline by i.p. injection. The study found that there was a significant decrease in the GSH/GSSG ratio, a ratio that is indicative of oxidative stress, in the brains of the doxorubicin treated mice compared to vehicle treated mice. It was also shown that there were significant increases in glutathione-S-transferase (GST), glutathione peroxidase (GPx) and glutathione reductase (GR), which also indicates an increase in oxidative stress which may contribute to the neurological problems experienced by patients receiving or who have received chemotherapy.

In another mouse study, C57 mice were dosed with 5FU and methotrexate. After evaluation of the animal learning and memory skills with a after chemotherapy

administration for three weeks, it was shown that the chemotherapeutic receiving mice had learning and memory impairments compared to the mice receiving saline injections (*43*).

Dietrich *et al* evaluated the effects of chemotherapeutic agents on CBA mice after treatment with BCNU (Carmustine), cisplatin or cytrabine injections. When compairing the mice receiving chemotherapeutic injections to the saline injected mice, it was found that there was an increase in cell death and decreased cell division in the following locations in the brain compared to the drug free mice: the subventricular zone, the dentate gyrus of the hippocampus and in the corpus callosum (*44*). A negative effect of methotrexate on cell proliferation in the hippocampus has also been shown in rats dosed with methotrexate (*45*).

3.2 EXPERIMENTAL PROCEDURES

3.2.1 Materials

Carboplatin, alpha-methyl-para-tyrosine and D-amphetamine were purchased from Sigma-Aldrich (St. Louis, MO, USA). All other reagents were purchased from Sigma Aldrich (St. Louis, MO, USA) unless otherwise noted.

3.2.2 Animals

Male Wistar rats were purchased from Charles River (Wilmington, MA, USA) and were housed in the animal care unit at the University of Kansas. Animals were allowed unrestricted access to food and water and a 12 hour light-dark cycle was used. The Institutional Animal Care and Use committee approved all procedures prior to experimentation.

3.2.3 Chemotherapy Administration

Solutions containing carboplatin dissolved in biological saline were made in concentrations of 2.5 mg/mL, 15 mg/mL and 26.6 mg/mL. Male Wistar rats were given doses of carboplatin by intravenous (IV) injections. Four experimental groups, consisting of two rats each, received one of the following doses of carboplatin: 0 mg/kg, 5.0 mg/kg, 20.0 mg/kg, and 60 mg/kg. Injections were given through the tail vein once a week for four consecutive weeks.

3.2.4 Brain Slice Preparation

A previously describe procedure was used to prepare brain slices (*46*). To summarize the procedure, rats were decapitated using a guillotine after being anesthetized by isoflurane inhalation in a closed chamber. After immediate removal from the skull, the brain was immediately placed in a beaker with ice-cold, oxygenated artificial cerebrospinal fluid (aCSF). The aCSF solution was made to contain the following concentrations: 2.5 mM KCl, 126 mM NaCl, 1.2 mM NaH_2PO_4, 25 mM $NaHCO_3$, 2.4 mM $CaCl_2$, 1.2 mM $MgCl_2$, 20 mM HEPES, 11 mM D-glucose. The pH was then adjusted to the physiological pH of 7.4. In order to provide a constant supply of oxygen to the tissue, the solution was oxygenated with 95% O_2/5% CO_2 through bubbling. The brain tissue was cooled in the aCSF solution for one minute prior to bisection. One half of the brain was glued to a plate with a small block of agar also glued to the plate for support while slicing the tissue. 300 µm thick coronal slices containing the striatum were made using a vibratome (Leica, Wetzlar, Germany). The slices were then placed in a perfusion chamber and equilibrated for 60 minutes by a continuous flow of oxygenated aCSF heated to 34 ºC. Slice exposure to αMPT and AMPH was carried out by switching the aCSF flow to a reservoir containing the 50 µM αMPT. After diminishing DA release a solution containing 50 µM αMPT and 20 µM AMPH was used to cause DA efflux.

3.2.5 FSCV to Detect Dopamine Release in Brain Slices

Carbon fiber microelectrodes, 7 µm in diameter and cut to 30 µm in length, were fabricated following a previously described protocol (*47*). To summarize, a single carbon fiber (Goodfellow Cambridge Ltd, Huntingdon, UK) was aspirated by vacuum pump through a 4 inch glass capillary tube (1.2 mm outer diameter, 0.68 mm inner diameter, A-M Systems, Carlsborg, WA, USA). To create a glass seal around the carbon fiber, the capillary was pulled using a heated coil puller (Narishige International USA, East Meadow, NY, USA). The electrodes were cut to length using a scalpel under a microscope and the glass seal was reinforced by dipping the electrode tips into epoxy resin (EPON resin 815C, EPIKURE 3234 curing agent, Miller-Stephenson, Danbury, CT, USA), rinsing the excess resin with toluene, and cured at 100 ºC for one hour. Potassium acetate was used to back-fill the electrode in order to establish an electrical connection between the carbon fiber and an inserted silver wire.

The carbon fiber microelectrodes were calibrated prior to use by exposure to a known concentration of dopamine in a flow cell. The carbon fiber was positioned in the brain slice using micromanipulators under a microscope such that the tip of the electrode was approximately 100 µm below the surface of the brain slice and between two stimulating electrodes. A triangular waveform was applied to the carbon fiber microelectrode beginning at -0.4 V scanning up to +1.0 V and back down to -0.4 V at a scan rate of 300 V/sec and an update rate of 10 Hz. The voltammetry data was collected using an Ag/AgCl reference electrode. Data was collected in this manner in four different locations in each of the four quadrants of the striatum. The stimulating electrodes were made in house by gluing two tungsten electrodes (A-M Systems Inc,

Carlsborg, WA, USA) and adjusting the distance of the tips using heat shrink (3M Electronics, Austin, TX, USA) until they were 200 µM apart. A single biphasic stimulation pulse (60 Hz, 4 msec pulse width, 350 µA) was used to evoke dopamine release. The current was measured at the maximum dopamine oxidation potential, which occurs at about +0.6 V versus a Ag/AgCl reference. Using the predetermined calibration factor for each electrode, the maximum dopamine release was calculated.

To evaluate DA efflux, single pulses were applied every five minutes while the slice was exposed to 50 µM αMPT until DA release diminished. Once DA release disappeared, 20 µM AMPH was added to the aCSF with the 50 µM αMPT. DA efflux caused by AMPH exposure was detected over 25 minutes without the use of electrical stimulation. An update rate of 5 Hz was used for the 25 minute file in order to limit to file size and not exceed memory limitations (*48*).

3.2.6 Data Analysis

Data was analyzed following a similar approach previously used (*46*). Modeling software written by R.M. Wightman (University of North Carolina, Chapel Hill, NC) was used to evaluate stimulated release plots. By modeling the plots, parameters associated with the kinetics of dopamine release and uptake were determined, including dopamine per pulse, $[DA]_p$, which is the peak dopamine release corrected for electrode performance and uptake, V_{max}, the maximum rate of dopamine uptake, and K_M, dopamine concentration at $½V_{max}$.

3.3 RESULTS

3.3.1 Peak Stimulated Dopamine Release in the Striatum

Peak stimulated DA release data was collected from the dorsolateral (DL), dorsomedial (DM), ventrolateral (VL), and ventromedial (VM) quadrants of the striatum and are shown in **Figure 2**. Four data points were collected from each quadrant and averaged together. Our investigation of the role of DA release in chemobrain revealed a significant dose effect in all regions of the striatum ($p=0.0002$, $F_{3,53} = 7.79$, 2-way ANOVA, n = 4 to 5). There were no differences seen within a dose between the different quadrants of the striatum.

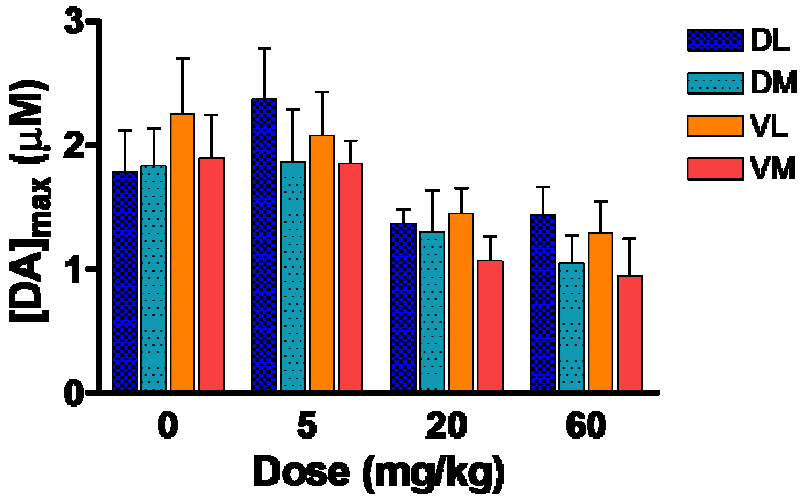

Figure 2. Maximum DA release upon stimulation after chemotherapy. Peak release data is shown for each dose in all four quadrants of the striatum.

3.3.2 Modeled Striatal Dopamine Release

The data collected was modeled using software to obtain additional information about the effects of carboplatin treatment on DA release in the striatum. Dopamine per pulse, $[DA]_p$, which is the peak dopamine release corrected for electrode performance and uptake, also showed a significant dose effect across all regions of the striatum ($p=0.0025$, $F_{3,52} = 5.45$, 2-way ANOVA, n = 4 to 5) and is shown in **Figure 3**. There was no effect seen within a dose across the different regions of the striatum.

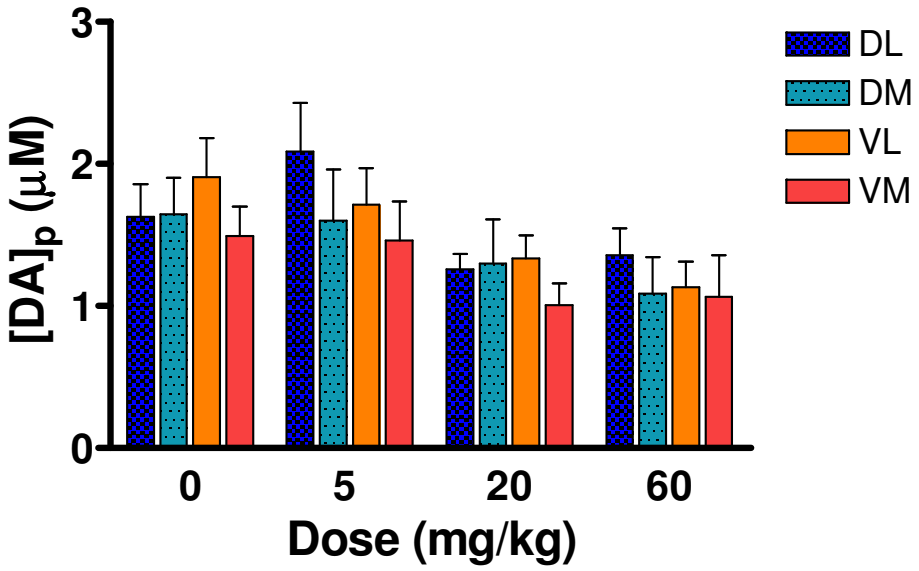

Figure 3. Dopamine per pulse data in the four quadrants of the striatum. A significant dose effect was seen ($p=0.0025$, $F_{3,52} = 5.45$, 2-way ANOVA, n = 4 to 5).

V_{max} was also determined from modeling the data also gave information about the uptake of dopamine after treatment with carboplatin. Data analysis showed that there was no difference in the uptake rates between the different doses of carboplatin, **Figure 4**. There was also no difference in the uptake rates between the different regions of the brain within a dose.

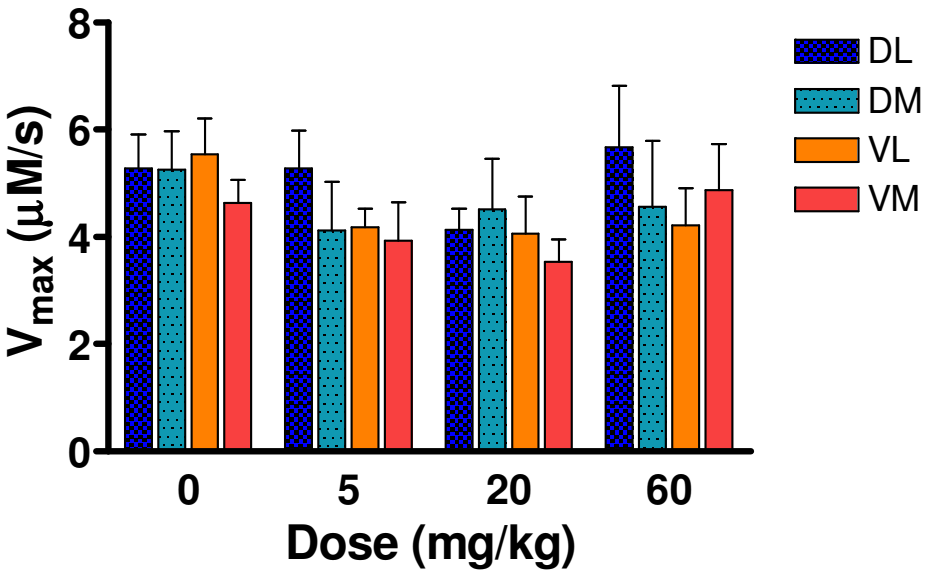

Figure 4. DA uptake data. V_{max} data for each dose of carboplatin throughout the striatum (n = 4 to 5).

3.3.3 Dopamine Reserve Pools

We also evaluated the reserve pools of DA in the DL region of the striatum. After the stimulated DA release data was collected, the electrode was placed in the dorsolateral region and the slice was exposed to αMPT to inhibit DA synthesis. The slice was stimulated until the DA release was eliminated. The raw data (**Figure 5**) shows how we began with a good DA signal and how αMPT caused the elimination of DA release and the efflux of DA caused by the addition of AMPH.

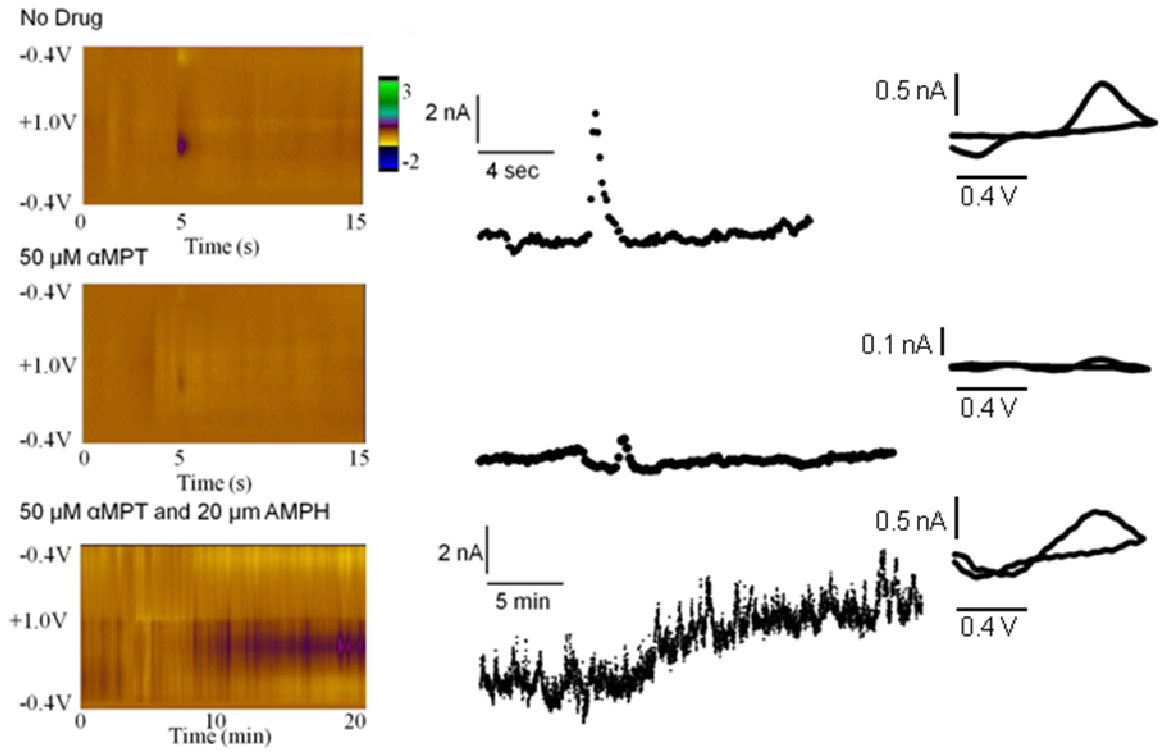

Figure 5. Raw data showing DA release, the elimination of DA release by αMPT and the efflux of DA caused by AMPH. Cyclic voltammograms show next to each plot verify the detection of DA.

The maximum amount of DA released by efflux due to AMPH exposure was calculated based on the electrode calibration and the peak current from the AMPH exposure data. The DA efflux data for each carboplatin dose group was averaged and is shown in **Figure 6**. There was no difference observed in the amount of reserve pool DA efflux due to AMPH between the different doses of carboplatin.

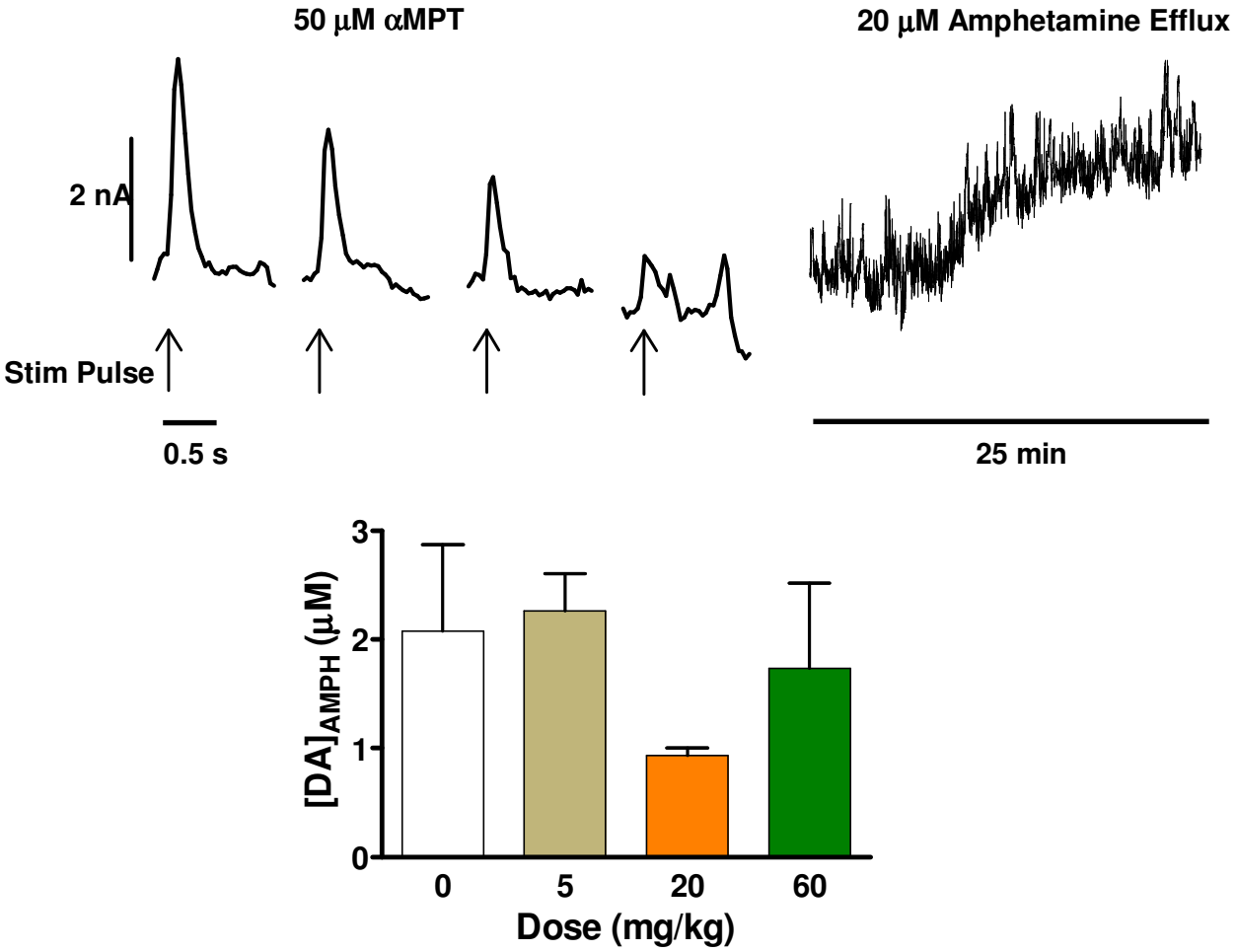

Figure 6. DA efflux caused by AMPH. Stimulated DA release was eliminated by slice exposure to αMPT followed by AMPH, which caused DA efflux. The maximum DA concentration caused by AMPH is shown for each dose group (n=3).

3.4 DISCUSSION

In this study the effects of carboplatin chemotherapy on the DA system were examined. We evaluated DA release in each of the four main quadrants of the striatum because they are associated with different areas of cognition. The dorsal region is commonly associated with motor control as well as motivation and reward (*38, 49*), while the ventral region is associated with learning memory (*50*). Since the cognitive decline is experienced in chemobrain, it was important to evaluate the effects of carboplatin on each region to determine if one region was more strongly affected than others. Our results showed that there was a generalized effect on DA release throughout the striatum, finding no difference between any regions within a dose.

The stimulated DA release in brain slices after carboplatin injections showed a significant dose effect on the amount of DA released upon stimulation in the striatum. We have also shown a significant dose effect on dopamine per pulse. The higher doses of carboplatin having a negative influence on DA release could explain the higher incidence of chemobrain associated with higher doses of chemotherapy (*31, 51*). Moreover, we found that V_{max} was unchanged between the doses, which indicates that carboplatin treatment does not cause alterations in the function of DAT (*52*).

Stimulated DA release causes the exocytosis of DA from the readily releasable pool (RRP). The RRP only contributes about 1-2% of the total DA vesicles in the presynaptic terminal Since DA release (*53*). As the RRP is depleted, the recycling pool is mobilized (*54-56*). The largest pool of DA is the reserve pool, which makes up 80-90% of the DA stores and is thought to be mobilized under conditions of high synaptic activity (*53, 57-58*). Evidence also suggests that this pool can also be mobilized

experimentally by intense electrical stimulation (*56, 59-62*). Reserve pools can also be examined through the use of pharmacological agents by first depleating the RRP and recycling pool by inhibiting DA synthesis in the presynaptic terminal by first exposing the slice to αMPT and stimulating the slice until DA release was depleted (*48*). Once the stimulated dopamine release was eliminated, AMPH was added to the perfusion aCSF to cause DA efflux by reverse transport, which is caused by allosteric translocation of the DAT such that dopamine transport into the extracellular space is facilitated (*63-65*). We were unable to detect any differences in reserve pool dopamine measure by maximum current after DA efflux caused by AMPH; however, more experiments are necessary to confirm this finding. Nevertheless, the finding that DA reserve pools are unchanged implies that the decrease in DA release with increasing carboplatin dose may be due to an alteration in the RRP release mechanism.

Our findings may also provide insight into the reason why methylphenidate has been shown to be a useful treatment in some chemobrain patients (*35*). Methylphenidate causes an increase in extracellular DA which helps alleviate symptoms associated with decreased DA release. Collectively, these data suggest that enhancement of dopamine release may represent a viable therapeutic option in the treatment of cognitive deficits associated with chemobrain.

3.5 CONCLUDING REMARKS

These initial studies have investigated the effects of a commonly used chemotherapeutic agent, carboplatin, on DA release in the striatum. The results here have shown a significant dose effect of carboplatin on stimulated DA release in all regions of the striatum. Our results also indicate that reserve pools of DA are unaltered by carboplatin. This work and future work in this area have the potential to reveal therapeutic treatment strategies that could ultimately aid in the management and treatment of the cognitive impairments associated with chemobrain in patients. We are currently pursuing the further investigation of other chemotherapeutics on DA release and the evaluation of the effects of the drugs on total DA content as well.

ACKNOWLEDGEMENTS

We thank the National Science Foundation REU program for financial support. This work was funded in part by the R.N. Adams Institute for Bioanalytical Chemistry.

3.6 REFERENCES

1. Wefel, J. S., Saleeba, A. K., Buzdar, A. U., and Meyers, C. A. (2010) Acute and Late Onset Cognitive Dysfunction Associated With Chemotherapy in Women With Breast Cancer, *Cancer 116*, 3348-3356.

2. Winick, N. (2010) Neurocognitive outcome in survivors of pediatric cancer, *Curr Opin Pediatr*.

3. Vardy, J., and Tannock, I. (2007) Cognitive function after chemotherapy in adults with solid tumours, *Crit Rev Oncol Hematol 63*, 183-202.

4. Marin, A. P., Sanchez, A. R., Arranz, E. E., Aunon, P. Z., and Baron, M. G. (2009) Adjuvant Chemotherapy for Breast Cancer and Cognitive Impairment, *Southern Medical Journal 102*, 929-934.

5. Boykoff, N., Moieni, M., and Subramanian, S. K. (2009) Confronting chemobrain: an in-depth look at survivors' reports of impact on work, social networks, and health care response, *J Cancer Surviv 3*, 223-232.

6. Grober, S. E. (2002) Resources for treatment of chemotherapy-related cognitive difficulty, *Cancer Pract 10*, 216-218.

7. Nelson, C. J., Nandy, N., and Roth, A. J. (2007) Chemotherapy and cognitive deficits: mechanisms, findings, and potential interventions, *Palliat Support Care 5*, 273-280.

8. Ahles, T. A., Saykin, A. J., Furstenberg, C. T., Cole, B., Mott, L. A., Skalla, K., Whedon, M. B., Bivens, S., Mitchell, T., Greenberg, E. R., and Silberfarb, P. M. (2002) Neuropsychologic impact of standard-dose systemic chemotherapy in long-term survivors of breast cancer and lymphoma, *J Clin Oncol 20*, 485-493.

9. Ferguson, R. J., McDonald, B. C., Saykin, A. J., and Ahles, T. A. (2007) Brain structure and function differences in monozygotic twins: possible effects of breast cancer chemotherapy, *J Clin Oncol 25*, 3866-3870.

10. Ahles, T. A., and Saykin, A. (2001) Cognitive effects of standard-dose chemotherapy in patients with cancer, *Cancer Investigation 19*, 812-820.

11. Ramassamy, C., Averill, D., Beffert, U., Bastianetto, S., Theroux, L., Lussier-Cacan, S., Cohn, J. S., Christen, Y., Davignon, J., Quirion, R., and Poirier, J. (1999) Oxidative damage and protection by antioxidants in the frontal cortex of Alzheimer's disease is related to the apolipoprotein E genotype, *Free Radical Biology and Medicine 27*, 544-553.

12. Argyriou, A. A., Assimakopoulos, K., Iconomou, G., Giannakopoulou, F., and Kalofonos, H. P. (2011) Either Called "Chemobrain" or "Chemofog," the Long-Term Chemotherapy-Induced Cognitive Decline in Cancer Survivors Is Real, *Journal of Pain and Symptom Management 41*, 126-139.

13. Taillibert, S., Voillery, D., and Bernard-Marty, C. (2007) Chemobrain: is systemic chemotherapy neurotoxic?, *Current Opinion in Oncology 19*, 623-627.

14. van Dam, F. S., Schagen, S. B., Muller, M. J., Boogerd, W., vd Wall, E., Droogleever Fortuyn, M. E., and Rodenhuis, S. (1998) Impairment of cognitive function in women receiving adjuvant treatment for high-risk breast cancer: high-dose versus standard-dose chemotherapy, *J Natl Cancer Inst 90*, 210-218.

15. Wieneke, M. H., and Dienst, E. R. (1995) Neuropsychological assessment of cognitive-functioning following chemotherapy for breast-cancer, *Psycho-Oncol. 4*, 61-66.

16. Schagen, S. B., Muller, M. J., Boogerd, W., Rosenbrand, R. M., van Rhijn, D., Rodenhuis, S., and van Dam, F. S. (2002) Late effects of adjuvant chemotherapy on cognitive function: a follow-up study in breast cancer patients, *Ann Oncol 13*, 1387-1397.

17. Schagen, S. B., van Dam, F., Muller, M. J., Boogerd, W., Lindeboom, J., and Bruning, P. F. (1999) Cognitive deficits after postoperative adjuvant chemotherapy for breast carcinoma, *Cancer 85*, 640-650.

18. Schagen, S. B., Muller, M. J., Boogerd, W., Mellenbergh, G. J., and van Dam, F. (2006) Change in cognitive function after chemotherapy: a prospective longitudinal study in breast cancer patients, *Journal of the National Cancer Institute 98*, 1742-1745.

19. Hensley, M. L., Correa, D. D., Thaler, H., Wilton, A., Venkatraman, E., Sabbatini, P., Chi, D. S., Dupont, J., Spriggs, D., and Aghajanian, C. (2006) Phase I/II study of weekly paclitaxel plus carboplatin and gemcitabine as first-line treatment of advanced-stage ovarian cancer: pathologic complete response and longitudinal assessment of impact on cognitive functioning, *Gynecol Oncol 102*, 270-277.

20. Vardy, J., and Dhillon, H. (2010) The fog hasn't lifted on "chemobrain" yet: ongoing uncertainty regarding the effects of chemotherapy and breast cancer on cognition, *Breast Cancer Research and Treatment 123*, 35-37.

21. Zukerman, J. M., Guidotti, L. M., Hook, J. N., Stebbins, G. T., Gregory, S. A., and Han, S. (2010) Effects of Chemotherapy on Cognition and Quality of Life in Older Adults with Cancer, *Clin. Neuropsychol. 24*, 615-615.

22. Hermelink, K., Untch, M., Lux, M. P., Kreienberg, R., Beck, T., Bauerfeind, I., and Munzel, K. (2007) Cognitive function during neoadjuvant chemotherapy for breast cancer: results of a prospective, multicenter, longitudinal study, *Cancer 109*, 1905-1913.

23. Eisenberger, M., Van Echo, D., and Aisner, J. (1989) Carboplatin: the experience in head and neck cancer, *Semin Oncol 16*, 34-41.

24. Gray, H., Mandel, L., Schaad, D., Wolf, F., and Goff, B. (2010) "Chemobrain" in ovarian cancer: A prospective study of cognitive function and quality of life in women undergoing chemotherapy, *Gynecologic Oncology 116*, 60.

25. Kavanagh, J. J., and Nicaise, C. (1989) Carboplatin in refractory epithelial ovarian cancer, *Semin Oncol 16*, 45-48.

26. Coughlin, C. T., and Richmond, R. C. (1989) Biologic and clinical developments of cisplatin combined with radiation - concepts, utility, projections for new trials, and the emergence of carboplatin, *Seminars in Oncology 16*, 31-43.

27. Wagstaff, A. J., Ward, A., Benfield, P., and Heel, R. C. (1989) Carboplatin - a preliminary review of its pharmacodynamic and pharmacokinetic properties and therapeutic efficacy in the treatment of cancer, *Drugs 37*, 162-190.

28. Calvert, A. H., Harland, S. J., Newell, D. R., Siddik, Z. H., Jones, A. C., McElwain, T. J., Raju, S., Wiltshaw, E., Smith, I. E., Baker, J. M., Peckham, M. J., and Harrap, K. R. (1982) Early clinical-studies with cis-diammine-1,1-cyclobutane dicarboxylate platinum-II, *Cancer Chemotherapy and Pharmacology 9*, 140-147.

29. Siddik, Z. H., Newell, D. R., Boxall, F. E., and Harrap, K. R. (1987) The comparative pharmacokinetics of carboplatin and cisplatin in mice and rats, *Biochem Pharmacol 36*, 1925-1932.

30. Schagen, S. B., Hamburger, H. L., Muller, M. J., Boogerd, W., and van Dam, F. S. (2001) Neurophysiological evaluation of late effects of adjuvant high-dose chemotherapy on cognitive function, *J Neurooncol 51*, 159-165.

31. Schagen, S. B., Muller, M. J., Boogerd, W., Mellenbergh, G. J., and van Dam, F. S. (2006) Change in cognitive function after chemotherapy: a prospective longitudinal study in breast cancer patients, *J Natl Cancer Inst 98*, 1742-1745.

32. Gabrilove, J. L., Cleeland, C. S., Livingston, R. B., Sarokhan, B., Winer, E., and Einhorn, L. H. (2001) Clinical evaluation of once-weekly dosing of epoetin alfa in chemotherapy patients: improvements in hemoglobin and quality of life are similar to three-times-weekly dosing, *J Clin Oncol 19*, 2875-2882.

33. Rozans, M., Dreisbach, A., Lertora, J. J., and Kahn, M. J. (2002) Palliative uses of methylphenidate in patients with cancer: a review, *J Clin Oncol 20*, 335-339.

34. Sood, A., Barton, D. L., and Loprinzi, C. L. (2006) Use of methylphenidate in patients with cancer, *Am J Hosp Palliat Care 23*, 35-40.

35. Meyers, C. A., Weitzner, M. A., Valentine, A. D., and Levin, V. A. (1998) Methylphenidate therapy improves cognition, mood, and function of brain tumor patients, *Journal of Clinical Oncology 16*, 2522-2527.

36. Challman, T. D., and Lipsky, J. J. (2000) Methylphenidate: its pharmacology and uses, *Mayo Clin Proc 75*, 711-721.

37. Hurd, Y. L., and Ungerstedt, U. (1989) In vivo neurochemical profile of dopamine uptake inhibitors and releasers in rat caudate-putamen, *Eur J Pharmacol 166*, 251-260.

38. Volkow, N. D., Wang, G. J., Fowler, J. S., Gatley, S. J., Logan, J., Ding, Y. S., Hitzemann, R., and Pappas, N. (1998) Dopamine transporter occupancies in the human brain induced by therapeutic doses of oral methylphenidate, *Am J Psychiatry 155*, 1325-1331.

39. Lundorff, L. E., Jonsson, B. H., and Sjogren, P. (2009) Modafinil for attentional and psychomotor dysfunction in advanced cancer: a double-blind, randomised, cross-over trial, *Palliat Med 23*, 731-738.

40. Kohli, S., Fisher, S. G., Tra, Y., Adams, M. J., Mapstone, M. E., Wesnes, K. A., Roscoe, J. A., and Morrow, G. R. (2009) The effect of modafinil on cognitive function in breast cancer survivors, *Cancer 115*, 2605-2616.

41. Mustafa, S., Walker, A., Bennett, G., and Wigmore, P. M. (2008) 5-Fluorouracil chemotherapy affects spatial working memory and newborn neurons in the adult rat hippocampus, *Eur J Neurosci 28*, 323-330.

42. Joshi, G., Aluise, C. D., Cole, M. P., Sultana, R., Pierce, W. M., Vore, M., St Clair, D. K., and Butterfield, D. A. (2010) Alterations in brain antioxidant enzymes and redox proteomic identification of oxidized brain proteins induced by the anti-cancer drug adriamycin: implications for oxidative stress-mediated chemobrain, *Neuroscience 166*, 796-807.

43. Winocur, G., Vardy, J., Binns, M. A., Kerr, L., and Tannock, I. (2006) The effects of the anti-cancer drugs, methotrexate and 5-fluorouracil, on cognitive function in mice, *Pharmacol Biochem Behav 85*, 66-75.

44. Dietrich, J., Han, R., Yang, Y., Mayer-Proschel, M., and Noble, M. (2006) CNS progenitor cells and oligodendrocytes are targets of chemotherapeutic agents in vitro and in vivo, *J Biol 5*, 22.

45. Seigers, R., Schagen, S. B., Beerling, W., Boogerd, W., van Tellingen, O., van Dam, F. S., Koolhaas, J. M., and Buwalda, B. (2008) Long-lasting suppression of hippocampal cell proliferation and impaired cognitive performance by methotrexate in the rat, *Behav Brain Res 186*, 168-175.

46. Johnson, M. A., Rajan, V., Miller, C. E., and Wightman, R. M. (2006) Dopamine release is severely compromised in the R6/2 mouse model of Huntington's disease, *Journal of Neurochemistry 97*, 737-746.

47. Kawagoe, K. T., Zimmerman, J. B., and Wightman, R. M. (1993) Principles of Voltammetry and Microelectrode Surface-States, *Journal of Neuroscience Methods 48*, 225-240.

48. Ortiz, A. N., Kurth, B. J., Osterhaus, G. L., and Johnson, M. A. (2009) Dysregulation of intracellular dopamine stores revealed in the R6/2 mouse striatum., *J Neurochem*.

49. Palmiter, R. D. (2008) Dopamine signaling in the dorsal striatum is essential for motivated behaviors: lessons from dopamine-deficient mice, *Ann N Y Acad Sci 1129*, 35-46.

50. Jocham, G., Klein, T. A., and Ullsperger, M. (2011) Dopamine-mediated reinforcement learning signals in the striatum and ventromedial prefrontal cortex underlie value-based choices, *J Neurosci 31*, 1606-1613.

51. Park, S. B., Goldstein, D., Lin, C. S. Y., Krishnan, A. V., Friedlander, M. L., and Kiernan, M. C. (2009) Acute Abnormalities of Sensory Nerve Function Associated With Oxaliplatin-Induced Neurotoxicity, *Journal of Clinical Oncology 27*, 1243-1249.

52. Zhu, J., Bardo, M. T., Bruntz, R. C., Stairs, D. J., and Dwoskin, L. P. (2007) Individual differences in response to novelty predict prefrontal cortex dopamine transporter function and cell surface expression, *Eur J Neurosci 26*, 717-728.

53. Rizzoli, S. O., and Betz, W. J. (2005) Synaptic vesicle pools, *Nature Reviews Neuroscience 6*, 57-69.

54. Harata, N., Ryan, T. A., Smith, S. J., Buchanan, J., and Tsien, R. W. (2001) Visualizing recycling synaptic vesicles in hippocampal neurons by FM 1-43 photoconversion, *Proceedings of the National Academy of Sciences of the United States of America 98*, 12748-12753.

55. Kuromi, H., and Kidokoro, Y. (2003) Two synaptic vesicle pools, vesicle recruitment and replenishment of pools at the Drosophila neuromuscular junction, *Journal of Neurocytology 32*, 551-565.

56. Richards, D. A., Guatimosim, C., Rizzoli, S. O., and Betz, W. J. (2003) Synaptic vesicle pools at the frog neuromuscular junction, *Neuron 39*, 529-541.

57. Neves, G., and Lagnado, L. (1999) The kinetics of exocytosis and endocytosis in the synaptic terminal of goldfish retinal bipolar cells, *Journal of Physiology-London 515*, 181-202.

58. Zucker, R. S., and Regehr, W. G. (2002) Short-term synaptic plasticity, *Annual Review of Physiology 64*, 355-405.

59. Heien, M. L., and Wightman, R. M. (2006) Phasic dopamine signaling during behavior, reward, and disease states, *CNS Neurol Disord Drug Targets 5*, 99-108.

60. Ortiz, A. N., Kurth, B. J., Osterhaus, G. L., and Johnson, M. A. (2010) Dysregulation of intracellular dopamine stores revealed in the R6/2 mouse striatum, *Journal of Neurochemistry 112*, 755-761.

61. Ortiz, A. N., Oien, D. B., Moskovitz, J., and Johnson, M. A. (2011) Quantification of reserve pool dopamine in methionine sulfoxide reductase a null mice, *Neuroscience 177*, 223-229.

62. Venton, B. J., Seipel, A. T., Phillips, P. E., Wetsel, W. C., Gitler, D., Greengard, P., Augustine, G. J., and Wightman, R. M. (2006) Cocaine increases dopamine release by mobilization of a synapsin-dependent reserve pool, *J Neurosci 26*, 3206-3209.

63. Floor, E., and Meng, L. H. (1996) Amphetamine releases dopamine from synaptic vesicles by dual mechanisms, *Neuroscience Letters 215*, 53-56.

64. Jones, S. R., Gainetdinov, R. R., Wightman, R. M., and Caron, M. G. (1998) Mechanisms of amphetamine action revealed in mice lacking the dopamine transporter, *Journal of Neuroscience 18*, 1979-1986.

65. Sulzer, D., Maidment, N. T., and Rayport, S. (1993) Amphetamine and other weak bases act to promote reverse transport of dopamine in ventral midbrain neurons, *Journal of Neurochemistry 60*, 527-535.

66. Mar Fan, H. G., Clemons, M., Xu, W., Chemerynsky, I., Breunis, H., Braganza, S., and Tannock, I. F. (2008) A randomised, placebo-controlled, double-blind trial of the effects of d-methylphenidate on fatigue and cognitive dysfunction in women undergoing adjuvant chemotherapy for breast cancer, *Support Care Cancer 16*, 577-583.

CHAPTER 4

CAGED-COMPOUNDS AND THE BRAIN: EVALUATING THE EFFECTS OF PHOTORELEASING GLUTAMATE ON DOPAMINE RELEASE

The toxic effect of too much glutamate on brain slices poses a serious limitation in studying the role glutamate has in neurotransmitter release and reuptake. In this work an apparatus was constructed to apply a technique using glutamate with a photoactive protecting group in order to “uncage” glutamate by a light source as a method of applying a small, localized amount of glutamate on a brain slice. A mercury light source with a shutter in front of the lens was used with a fiber optic to direct controlled pulses of light on the desired area of the slice. The caged form of glutamate had no effect on the dopamine (DA) release. HPLC analysis was used to verify the incidence of ”uncaging” glutamate using the Hg light source. The “cage” byproduct also had no effect of DA release and was determined to be electroactive, thus making detection and quantification of the released glutamate possible. This work demonstrates the potential utility of caged glutamate studies on determining the effect of glutamate on neurotransmitter release in brain slices.

4.1 INTRODUCTION

The ability to administer known concentrations of biologically active agents in a spatially localized area has many advantages in evaluation of biological responses. The use of photoactive protecting groups bonded to biologically active compounds has become a popular way to evaluate the immediate response to the biological compound once the protecting group is photocleaved. These photoprotected compounds were termed “caged” compounds by Kaplan et al to describe the way in which the photoactive protecting group will render a compound biologically inert until it is photocleaved, thus releasing the biological compound (*1*).

4.1.1 Utility of Photoreleasing compounds

Caged compounds are molecules that have had a photoactive protecting group placed on the molecule such that it inactivates the molecule (*2*). When the caged compound is exposed to a specific wavelength of light, the cage will be released and the compound converted back into its original, active form and the inert protecting group (*2*). Park and Givens have shown that the protecting group used as the cage in the caged compounds they make is biologically safe so that the caged compounds they produce can be used for biological applications (*2*). Exposing the caged compounds to a certain wavelength of light for a known length of time allows for the amount released to be known (*3*).

4.1.2 Previous studies using caged compounds

The use of fast scan cyclic voltammetry (FSCV) at carbon fiber microelectrodes allows for the sub-second detection of neurotransmitter release and uptake in brain slices (*4*). These release and uptake patterns can also be examined in the presence of various pharmacological agents; however, this usually requires that the slice be exposed to a drug by perfusion for an extended period of time. This situation is often impractical given that continuous exposure to certain chemicals may have deleterious effects on cell viability. For example, glutamate is an abundant brain neurotransmitter that participates in the regulation of striatal DA release (*5-8*). Nevertheless, the excitotoxicity of glutamate makes it impractical as a perfusion agent for brain slices.

One potential solution to the problem described is to photoactivate a caged form of glutamate, thereby preventing the prolonged exposure of the tissue, and then measure DA release using FSCV. A similar approach has been previously employed using caged DA. Studies done by Lee et al. have shown that caged DA can be used in brain slices to monitor the uptake of DA by the DA transporters based on the increased extracellular concentration. In one study the DA transporters were treated with cocaine, which acts as a DA transporter blocker (*9-10*). The caged DA was hit by a pulse of light for a known length of time in a specific location. By releasing the caged compound over a known length of time it is possible to know the concentration released (*10*). The speed of the uptake of this DA could then be monitored. To further investigate the transport of DA using the caged DA, Lee et al. showed a method of quantifying the DA that is released, showing that when the DA transporter was inhibited the release of endogenous DA was lessened by the release of the caged DA (*11*). A notable

drawback with the approach of Lee et al. is that the caged DA used was also electroactive and thus required a background subtraction operation to remove the electrochemical signal from the uncaged DA still present in the sample (*11*).

4.1.3 Types of Photoactivatable Compounds

Over the last 40+ years many different compounds have been bound to photo-releasing groups for activation by light exposure. Since one of the main uses for caged compounds is in biological applications, the primary focus has been on adding cages to compounds that will elicit some sort of biological response after light exposure. Some of the molecules that have been "caged" include; ATP (*1*), calcium (*12-13*), DA (*3*), GABA and glutamate (*2, 14-15*), as well as other biological molecules.

These caged compounds have been valuable resources in obtaining spatial and temporal resolution that is not allowed by total submersion or perfusion. The light source can be focused on a small, specific area to probe and the release of the cage can be timed to detect the immediate response due to the reformation of the biologically active compound, which happens on a very short time scale.

Different molecules can be utilized as the phototrigger when synthesizing caged compounds. The four most popular groups of chromophores include: 1. 2-nitrobenzyl (2NB), 2. benzoin, 3. *p*-hydroxyphenacyl (pHP), and 4. arylmethyl derivatives (*16*). The 2NB group has been a popular choice of cage; however, the time scale of photorelease is in the millisecond to second range (*2*). Park and Givens investigated the use of pHP as an alternative to the use of 2NB providing a phototrigger that releases with a rate constant of 10^5 s^{-1} and gave a byproduct that is biologically inert (*2*). Using the pHP group, a fast and efficient means of releasing biologically active molecules with

biologically inert by-products has been achieved. The pHP group has been attached to glutamate and GABA, which have been successfully used in evaluating cellular response to the released glutamate (*17-18*).

4.1.4 Photoactivation of pHP-Glutamate

Mechanistic studies have been perfomed on the pHP photoleaving group by Givens and Lee, which have probed the way photocleaving occurs with the pHP protecting group (*19*). To briefly summarize the study, it was determined that the mechanism can be described in four primary phases once the caged compound is exposed to 300 nm light: 1) a triplet intermediate is formed after light exposure and the loss of a proton and the leaving group, 2) the diradical triplet intermediate undergoes bond reorganization, 3) a spirodienedione is formed along with a substrate-phenacyl bond cleavage, and 4) the spirodienedione undergoes hydrolysis with further bond reorganization (**Figure 1**) (*19*).

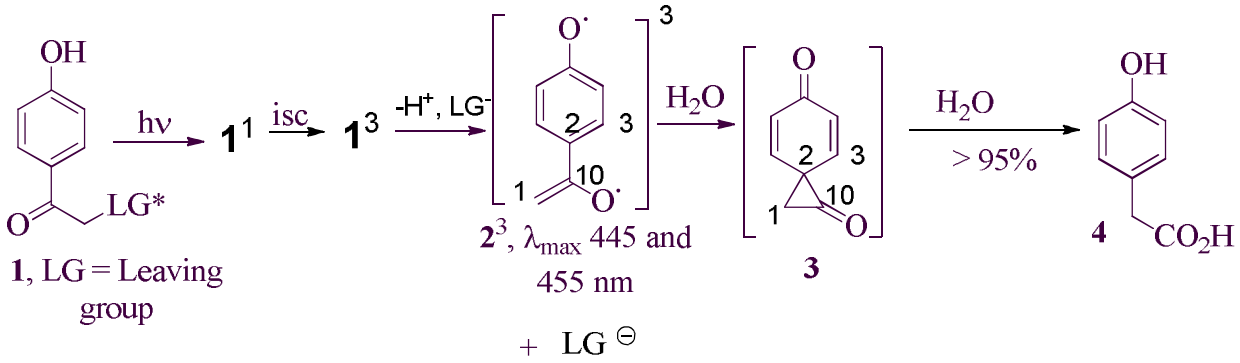

Figure 1. Reaction mechanism for the photocleaving of pHP-compounds (*19*). Figure provided by Dr. Richard S. Givens.

4.1.5 Oxidation of 4-hydroxyphenylacetic acid (4-HPAA)

It has been previously shown that an irreversible oxidation of 4-hydroxyphenylacetic acid occurs at +0.95 V vs Ag/AgCl reference at a graphite electrode under slow scan rates (50 mV/s) (*20*). Based on this previous work, it is hypothesized that the4-HPAA should oxidize at a carbon fiber electrode. By utilizing higher scan rates it is possible that either the oxidation peak may shift as an effect of the scan rate. The ability to detect the oxidation of 4-HPAA in a CV will allow for the simultaneous quantification of the glutamate which was photoreleased while quantifying DA release.

4.2 EXPERIMENTAL PROCEDURES

4.2.1 Materials

The *p*-hydroxyphenacyl glutamate (pHP-glu) was a gift from Dr. Rich Givens (University of Kansas, Department of Chemistry, Lawrence, KS). All other materials were obtained from Sigma Aldrich (St. Louis, MO) unless otherwise specified.

4.2.2 HPLC Analysis

A gradient high performance liquid chromatography (HPLC) method was used on a Shimadzu Model LC 20 AD with a dual reciprocating pump and a DGV 20A3 degasser. The detector was a Simadzu SPD-201V UV-VIS detector set to the wavelengths of 220 nm and 240 nm for the detection of the pHP-glu and 4-HPAA. The mobile phase reservoirs were as follows: (A) 99% water, 1% methanol and 0.06% formic acid; (B) 99% methanol, 1% water and 0.06%formic acid. Samples were injected by an autosampler and the gradient reached 90% B. The flow rate was set to 0.4 mL/min.

4.2.3 HPLC sample preparation

Stock solutions of caged glutamate were made by dissolving caged glutamate in 10 mL of aCSF to obtain concentrations near 10 mM. More dilute solutions of the caged glutamate were made by dilution of a portion of the stock solution into aCSF to obtain concentrations between 100 µM and 500 µM.

For verification of uncaging by our light sources, samples of the caged glutamate dissolved in aCSF were exposed to light from a Lambda DG-4 (Sutter Instruments, Novato, CA), a Mercury (Hg) lamp and natural sunlight. After light exposure samples were analyzed using HPLC.

For analysis, calibration curves were collected of the predominant byproduct, 4-hydroxyphenylacetic acid, and the caged glutamate each in aCSF. The samples of caged glutamate exposed to the different light sources were then compared to the two calibration curves to verify photorelease of the caged glutamate.

4.2.4 Voltammetry

4-HPAA release was detected using carbon fiber microelectrodes 7µm in diameter and 30µm in length, constructed following a previously described method (*21*). A triangular waveform was applied to the carbon fiber microelectrode beginning at -0.4 V scanning up to +1.3 V and back down to -0.4 V at a scan rate of 300 V/sec and an update rate of 10 Hz. The voltammetry data were collected versus a Ag/AgCl reference electrode.

4.2.6 Shutter control/light exposure

A UNIBLITZ® optical shutter (Vincent Associates, Rochester, NY, USA), controlled by a controller designed and constructed by Kenneth Ratzlaff (Instrumentation Design Laboratory, University of Kansas), was triggered by the stimulus pulse and opened by a timed delay set by the control software. The length of time the shutter remained open was also controlled by the software.

4.3 RESULTS

Monoamines, such as DA, play large roles in the brain as neurotransmitters. DA is a neurotransmitter that participates in the signaling for physical movements (*22*). There are many physiological conditions that deal with an altered level of DA, including Huntington's disease, Parkinson's disease, Tourette's syndrome and Fragile X syndrome (*4, 23-28*). The physical effects of Huntington's disease include the physical degeneration of the brain, uncontrollable physical movements and dementia (*4, 24*). The way in which DA transmission is altered in Huntington's disease and other neurological disorders has been investigated through the use of cyclic voltammetry (*4, 26, 29*). By using fast scan cyclic voltammetry and brain slices from disease model mice, extracellular concentrations of DA can be monitored (*4, 30*). The response of the DA system can be measured in real time and changes caused to DA release and uptake by glutamate can be determined using FSCV paired with the photorelease of pHP-glu, avoiding toxicity issues and maintaining high temporal and spatial resolution (*3, 11*).

4.3.1 Construction of Uncaging and FSCV Apparatus

Our original experimental design for releasing pHP-glu in brain slices was to utilize a Lambda DG-5 high speed wavelength switcher (Sutter Instruments, Novato, CA, USA) to expose the brain slice to select wavelengths of light through the microscope objective. However, our setup would not allow light less than 340 nm through to the slice, and at 340 nm the intensity was low. By HPLC analysis (**Figure 2**) we confirmed that we were not causing the photorelease of glutamate with this

experimental setup. The photorelease of caged compounds generally occurs between 250 and 360 nm (*31*), however, our original light source was not providing the intensity needed at 340 nm to photorelease the pHP-glu, thus a different light source was needed.

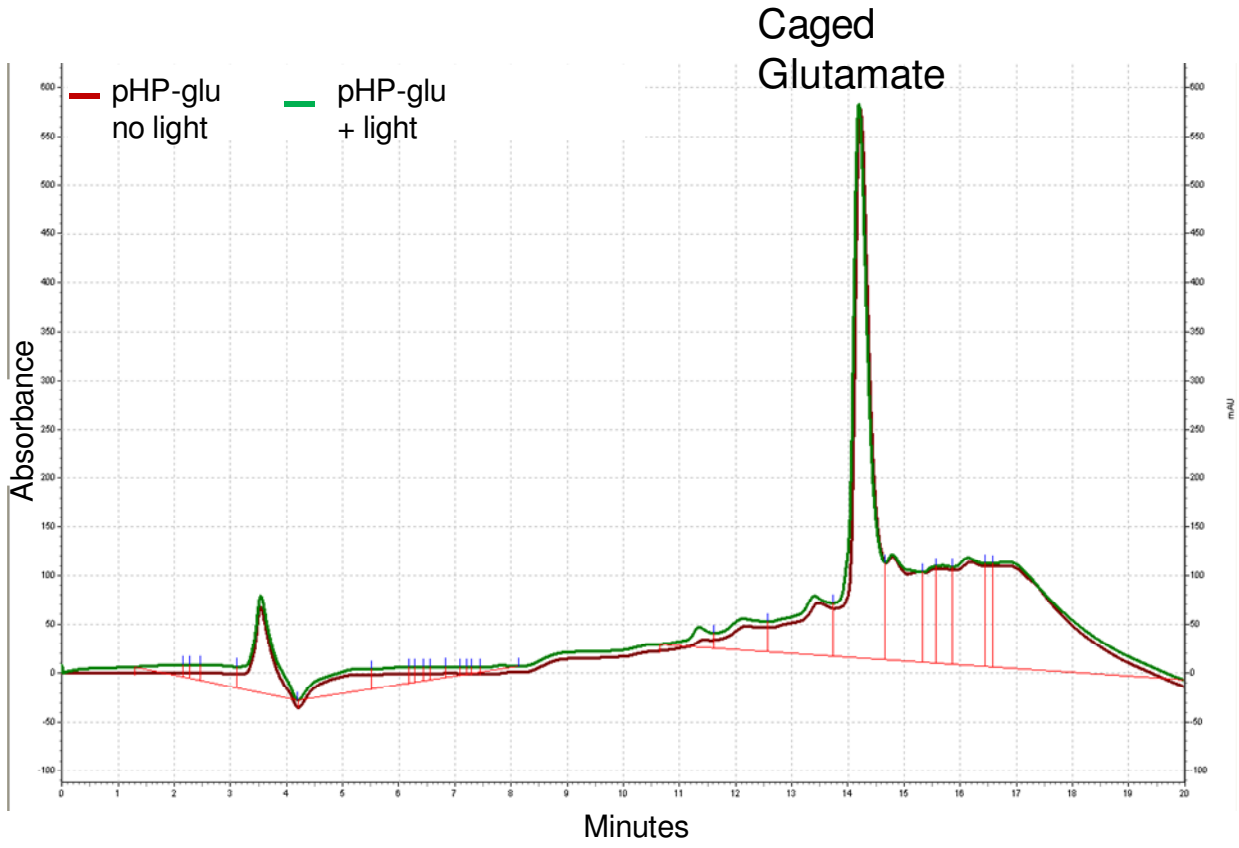

Figure 2. HPLC data of caged glutamate samples (wavelength of 220 nm). The top green trace was exposed to light from the original experimental setup, while the bottom trace was the unexposed caged glutamate sample, showing in the major peak in the chromatogram. No difference in the intensity of the caged glutamate peak was seen.

In order to achieve wavelengths around 300 nm with enough intensity to photo release the pHP-glu, a 100 W Oriel mercury (Hg) lamp (Newport Corporation, Irving,

CA, USA) was used for UV light emission. To control the length of time the samples were exposed to light, a shutter was positioned in front of the focusing lens on the Hg light source. The shutter is controlled by software produced in the Instrument Design Laboratory at the University of Kansas and can be programmed to remain open for a desired length of time. The stimulus pulse used to cause DA release can also be paired to the shutter, signaling it to open based on the software parameters. The light output was focused to an intense dot and a fiber optic was positioned such that the light was successfully transmitted to the desired location. The fiber optic was held by an adjustable holder so that's its position in front of the light source could be easily adjusted to give the most intense output through the fiber optic (**Figure 3**). The light source design was based on work previously done by Karl Kandler (*31*).

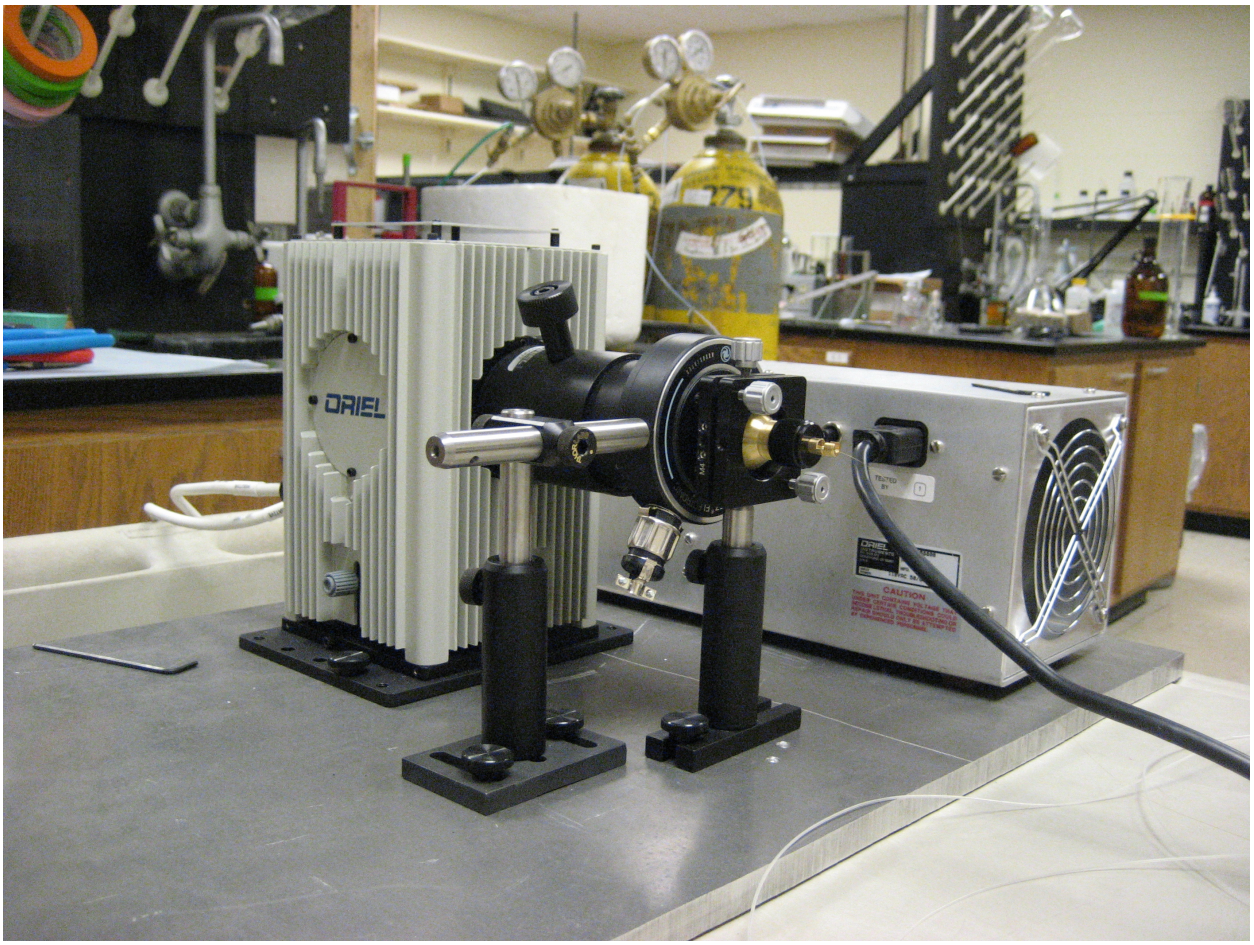

Figure 3. Mercury lamp with the shutter and fiber optic set up in front of the lens.

The light system then needed to be paired to the apparatus used for brain slice experiments. **Figure 4** depicts the resulting setup of the uncaging apparatus which is paired with a FSCV setup. The fiber optic was connected to a micromanipulator so that the position of the fiber relative to both the carbon fiber microelectrode and surface of the brain slice could easily be adjusted and moved. Micromanipulators allow us to easily move the working and stimulating electrodes to various locations in the brain slice and thus allow us to collect multiple data points from the same slice. By using a

micromanipulator with the fiber optic, it becomes possible to move the location of the light exposure to various positions throughout the brain slice as we move our stimulating and working electrodes. Since the fiber optic produces such a small area of light, it should be possible to move the electrode to a new location in the brain slice and collect more data points from unexposed locations.

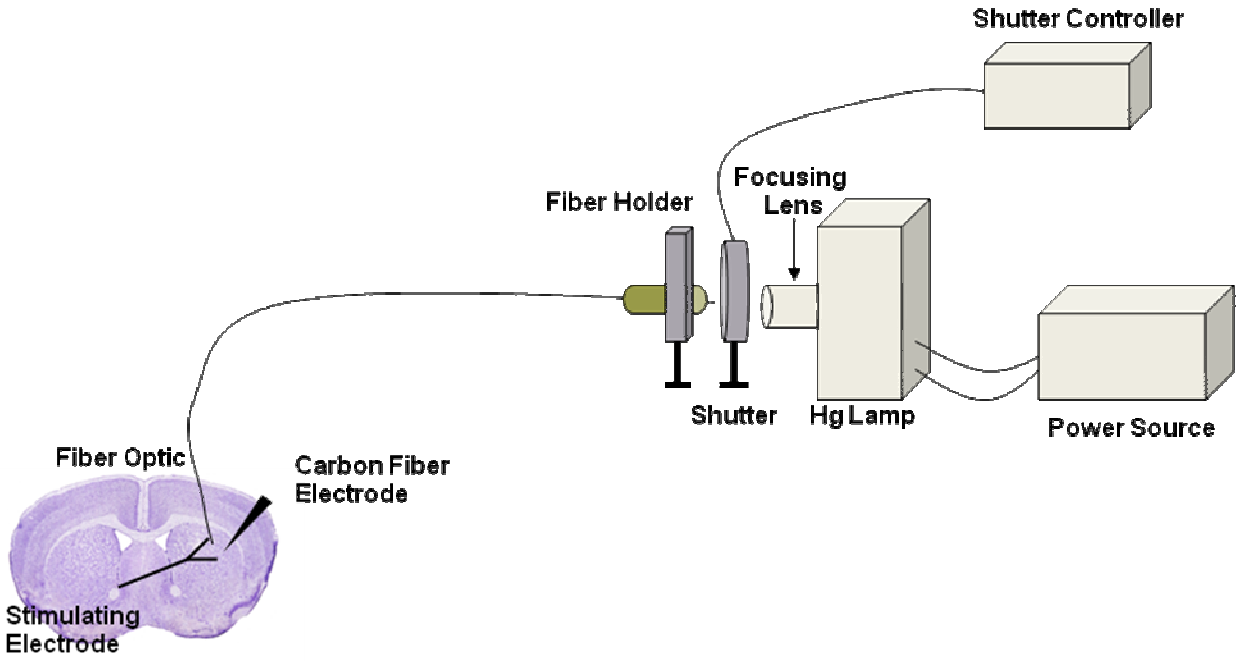

Figure 4. Experimental design for the uncaging of glutamate in slices.

We then had to verify release of caged glutamate by exposure to light from the new light source and evaluate how stable the samples were when allowed exposure to ambient light. Samples of the pHP-glu were also placed out in the room exposed to both sunlight and the room lights in order to determine if the ambient light would cause significant amounts of uncaging of the pHP-glu. After 10 minutes of expose the sample was evaluated using HPLC and no increase in the presence of the 4-HPAA byproduct was seen. To ensure glutamate release using the Hg lamp, samples of the pHP-glu

solution were exposed to light from the Hg lamp and analyzed using HPLC. **Figure 5** shows that we were able to successfully uncage glutamate using our light source. A sample containing the major release byproduct (Green) was evaluated by HPLC to confirm the peak placement. The unexposed sample (Blue) produced a large peak at a later time than the peak caused by the 4-HPAA standard. After light exposure (Red) the intensity of the caged glutamate peak greatly diminished, while a peak at the same retention time as the byproduct peak was detected confirming the release of 4-HPAA and indicating the release of glutamate. There were also other smaller peaks that were detected in the sample exposed to light from the mercury lamp. These other peaks correspond to other minor byproducts caused by photorelease (peaks were confirmed by collecting chromatograms of the other byproducts, data not shown).

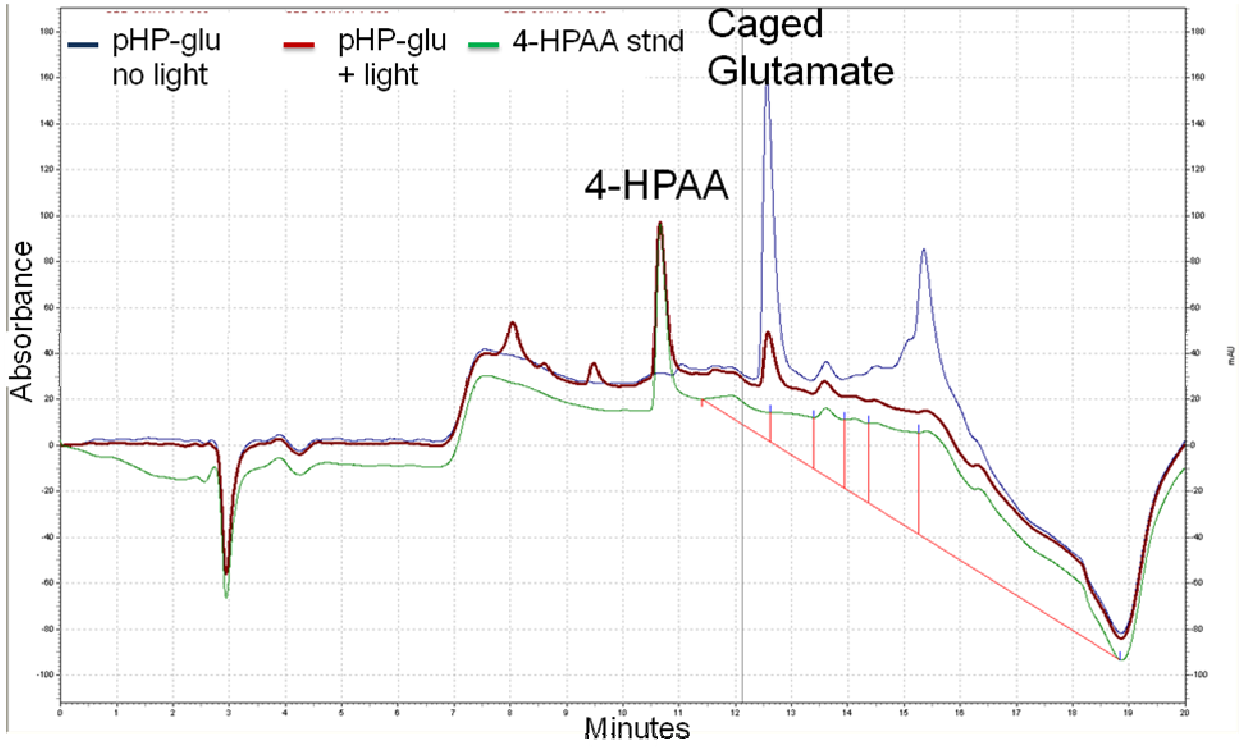

Figure 5. Confirmation of uncaging caused by light exposure from the mercury lamp. The blue trace shows the original sample with no 4-HPAA byproduct peak, which is the major byproduct from the uncaging. The green trace shows the 4-HPAA standard and the red trace shows the sample exposed to light from the mercury lamp with a major peak overlapping the 4-HPAA standard with other minor byproduct peaks detected as well. (Wavelength = 220 nm)

4.3.2 Detection of the Photorelease Byproduct

The amount of caged compound released is dependent on the concentration of the caged sample, the duration and intensity of the light exposure and the area of the light spot (*31*). The heterogeneity of the striatum paired with repositioning of the fiber optic caused a need for a method to determine how much glutamate was released. Work is being conducted in our laboratory to develop a means of quantifying the release of caged glutamate by using FSCV to detect the 4-HPAA byproduct.

4.4 DISCUSSION

Various caged compounds have been used in biological systems over the last several decades to elucidate the immediate responses to compounds one they are photoreleased (*32-33*). The utilization of *p*-hydroxyphenacyl protecting group has provided investigators with a photoreleaseing group that releases on a much faster time scale (*2*). The faster response time of the pHP photoreleasing group makes it a valuable compound for evaluation of neurotransmission.

Glutamate bound to the pHP photoprotecting group has been utilized in the evaluation of neuronal responses in brain slices using whole cell patch clamp recordings (*17, 31*). Since FSCV allows us to detect real time alterations in neurotransmitter release and uptake, combining photoreleasing compounds with FSCV opens up opportunities to evaluate the immediate effect of compounds on the release or uptake of the targeted neurotransmitter, in our case DA. There has been work done utilizing caged DA with FSCV in brain slices (*3*); however, having other compounds that cause changes to the DA system will allow greater understanding of how the DA system is functioning.

We have shown that our experimental setup works to release pHP-glu in solution and that we can detect the release of the byproduct to verify the amount of glutamate released. The use of this instrumentation will allow FSCV to be paired with photoreleasing compounds in slices for the investigation of the immediate response of the DA system in various locations of the brain and also in animal models of different neurological disease states. The information obtained by utilizing caged compounds in

FSCV brain slice experiments will elucidate important information that may provide therapeutic targets.

4.5 CONCLUDING REMARKS

To establish a means of utilizing caged compounds in FSCV brain slice experiments, a mercury lamp setup with a micromanipulator controlled fiber optic was constructed. Our original experimental design was proven to be flawed after light exposure and a failure to cause any photorelease of the pHP-glu. During the study the release of pHP-glu by the mercury lamp setup was confirmed using HPLC analysis. To determine if the pHP-glu in aCSF solution was stable in ambient light, a sample was exposed to room lighting and analyzed using HPCL, confirming that the sample was not photoreleasing due to exposure to ambient light. The ability to oxidize 4-HPAA, the photoreleasing byproduct, has also been shown by work in our laboratory. Using this method for the release and detection of compound effects on DA release will provide great insight into the dopaminergic system in different animal models.

ACKNOWLEDGMENT

I thank Dr. Rich Givens and Dr. Kenneth Stensrud of the Chemistry Department at the University of Kansas for providing the caged glutamate samples and Dr. Karl Kandler of the Department of Otolaryngology at the University of Pittsburg for assistance in building the light source apparatus. I also thank Dr. Gregory Osterhaus of the University of Kansas for assistance in performing HPLC analysis.

4.6 REFERENCES

1. Kaplan, J. H., Forbush, B., and Hoffman, J. F. (1978) Rapid photolytic release of adenosine 5'-triphosphate from a protected analog - utilization by Na-K pump of human red blood-cell ghosts, *Biochemistry 17*, 1929-1935.

2. Park, C. H., and Givens, R. S. (1997) New photoactivated protecting groups .6. p-hydroxyphenacyl: A phototrigger for chemical and biochemical probes, *Journal of the American Chemical Society 119*, 2453-2463.

3. Lee, T. H., Gee, K. R., Ellinwood, E. H., and Seidler, F. J. (1996) Combining 'caged-dopamine' photolysis with fast-scan cyclic voltammetry to assess dopamine clearance and release autoinhibition in vitro, *Journal of Neuroscience Methods 67*, 221-231.

4. Johnson, M. A., Rajan, V., Miller, C. E., and Wightman, R. M. (2006) Dopamine release is severely compromised in the R6/2 mouse model of Huntington's disease, *Journal of Neurochemistry 97*, 737-746.

5. Avshalumov, M. V., Chen, B. T., Marshall, S. P., Pena, D. M., and Rice, M. E. (2003) Glutamate-dependent inhibition of dopamine release in striatum is mediated by a new diffusible messenger, H2O2, *J. Neurosci. 23*, 2744-2750.

6. Carlsson, A., Waters, N., Holm-Waters, S., Tedroff, J., Nilsson, M., and Carlsson, M. L. (2001) Interactions between monoamines, glutamate, and GABA in schizophrenia: New evidence, *Annu. Rev. Pharmacol. Toxicol. 41*, 237-260.

7. Cartmell, J., and Schoepp, D. D. (2000) Regulation of neurotransmitter release by metabotropic glutamate receptors, *Journal of Neurochemistry 75*, 889-907.

8. Chen, B. T., and Rice, M. E. (2002) Synaptic regulation of somatodendritic dopamine release by glutamate and GABA differs between substantia nigra and ventral tegmental area, *Journal of Neurochemistry 81*, 158-169.

9. Davidson, C., Lee, T. H., and Ellinwood, E. H. (2005) Acute and chronic continuous methamphetamine have different long-term behavioral and neurochemical consequences, *Neurochemistry International 46*, 189-203.

10. Lee, T. H., Gee, K. R., Ellinwood, E. H., and Seidler, F. J. (1998) Altered cocaine potency in the nucleus accumbens following 7-day withdrawal from intermittent but not continuous treatment: voltammetric assessment of dopamine uptake in the rat, *Psychopharmacology 137*, 303-310.

11. Lee, T. H., Gee, K. R., Davidson, C., and Ellinwood, E. H. (2002) Direct, real-time assessment of dopamine release autoinhibition in the rat caudate-putamen, *Neuroscience 112*, 647-654.

12. Adams, S. R., Kao, J. P. Y., Grynkiewicz, G., Minta, A., and Tsien, R. Y. (1988) Biologically useful chelators that RELEASE Ca-2+ upon illumination, *Journal of the American Chemical Society 110*, 3212-3220.

13. Ellis Davies, G. C. R., and Kaplan, J. H. (1988) A new class of photolabile chelators for the rapid release of divalent-cations - generation of caged-ca and caged-Mg, *Journal of Organic Chemistry 53*, 1966-1969.

14. Gee, K. R., Kueper, L. W., Barnes, J., Dudley, G., and Givens, R. S. (1996) Desyl esters of amino acid neurotransmitters. Phototriggers for biologically active neurotransmitters, *Journal of Organic Chemistry 61*, 1228-1233.

15. Pirrung, M. C., and Shuey, S. W. (1994) Photoremovable protecting groups for phosphorylation of chiral alcohols - asymmetric-synthesis of phosphotriesters of (-)-3',5'-dimethoxybenzoin, *Journal of Organic Chemistry 59*, 3890-3897.

16. Givens, R. S., Lee, J.-I., and Kotala, M. (2005) Mechanistic overview of phototriggers and cage release, In *Dynamic Studies in Biology: Phototriggers, Photoswitches, and Caged Biomolecules* pp 95-129, J. Wiley, and Sons.

17. Kandler, K., Katz, L. C., and Kauer, J. A. (1998) Focal photolysis of caged glutamate produces long-term depression of hippocampal glutamate receptors, *Nat. Neurosci. 1*, 119-123.

18. Kullmann, P. H. M., Ene, F. A., and Kandler, K. (2002) Glycinergic and GABAergic calcium responses in the developing lateral superior olive, *Eur. J. Neurosci. 15*, 1093-1104.

19. Givens, R. S., and Lee, J.-I. (2003) The p-Hydroxyphenacyl Photoremovable Protecting Group, *Journal of Photoscience 10*, 37-48.

20. Silva, T. A. R., Ferreira, L. F., Souza, L. M., Goulart, L. R., Madurro, J. M., and Brito-Madurro, A. G. (2009) New approach to immobilization and specific-sequence detection of nucleic acids based on poly(4-hydroxyphenylacetic acid), *Materials Science & Engineering C-Biomimetic and Supramolecular Systems 29*, 539-545.

21. Kawagoe, K. T., Zimmerman, J. B., and Wightman, R. M. (1993) Principles of Voltammetry and Microelectrode Surface-States, *Journal of Neuroscience Methods 48*, 225-240.

22. Riddle, E. L., Fleckenstein, A. E., and Hanson, G. R. (2005) Role of monoamine transporters in mediating psychostimulant effects, *Aaps Journal 7*, E847-E851.

23. Rabinovic, A. D., Lewis, D. A., and Hastings, T. G. (2000) Role of oxidative changes in the degeneration of dopamine terminals after injection of neurotoxic levels of dopamine, *Neuroscience 101*, 67-76.

24. Charvin, D., Vanhoutte, P., Pages, C., Borelli, E., and Caboche, J. (2005) Unraveling a role for dopamine in Huntington's disease: The dual role of reactive oxygen species and D2 receptor stimulation (vol 102, pg 12218, 2005), *Proceedings of the National Academy of Sciences of the United States of America 102*, 16530-16530.

25. Vetter, J. M., Jehle, T., Heinemeyer, J., Franz, P., Behrens, P. F., Jackisch, R., Landwehrmeyer, G. B., and Feuerstein, T. J. (2003) Mice transgenic for exon 1 of Huntington's disease: properties of cholinergic and dopaminergic pre-synaptic function in the striatum, *Journal of Neurochemistry 85*, 1054-1063.

26. Fulks, J. L., O'Bryhim, B. E., Wenzel, S. K., Fowler, S. C., Vorontsova, E., Pinkston, J. W., Ortiz, A. N., and Johnson, M. A. (2010) Dopamine Release and Uptake Impairments and Behavioral Alterations Observed in Mice that Model Fragile X Mental Retardation Syndrome, *ACS Chemical Neuroscience 1*, 679-690.

27. Kish, S. J., Shannak, K., and Hornykiewicz, O. (1988) Uneven pattern of dopamine loss in the striatum of patients with idiopathic parkinsons-disease - pathophysiologic and clinical implications, *New England Journal of Medicine 318*, 876-880.

28. Feinberg, M., and Carroll, B. J. (1979) Effects of dopamine agonists and antagonists in tourettes disease, *Archives of General Psychiatry 36*, 979-985.

29. Ortiz, A. N., Kurth, B. J., Osterhaus, G. L., and Johnson, M. A. (2009) Dysregulation of intracellular dopamine stores revealed in the R6/2 mouse striatum., *J Neurochem*.

30. John, C. E., Budygin, E. A., Mateo, Y., and Jones, S. R. (2006) Neurochemical characterization of the release and uptake of dopamine in ventral tegmental area and serotonin in substantia nigra of the mouse, *Journal of Neurochemistry 96*, 267-282.

31. Kandler, K., Givens, R., and Katz, L. C. (1997) Photostimulation with Caged Glutamate, In *In Imaging Neurons: A Laboratory Manual* (Yuste, R., Lanni, F., and Konnerth, A., Eds.), Cold Spring Harbor Laboratory Press.

32. Adams, S. R., and Tsien, R. Y. (1993) Controlling cell chemistry with caged compounds, *Annual Review of Physiology 55*, 755-784.

33. McCray, J. A., and Trentham, D. R. (1989) Properties and uses of photoreactive caged compounds, *Annual Review of Biophysics and Biophysical Chemistry 18*, 239-270.

CHAPTER 5

SUMMARY OF FINDINGS AND FUTURE DIRECTIONS

Understanding the alterations caused to the dopaminergic system in disease states involving alterations in cognition and motor function will aid in the development of therapies to help improve the quality of life for sufferers. This work has presented insight into the changes to the dopamine (DA) system that occur in both a genetic neurological disorder and in neurological problems cause by drug administration. A method to evaluate the real time DA response to photoreleased neurotransmitters has also been presented. The major findings of each project and potential future research ideas are presented below.

5.1 FRAGILE X SYNDROME

5.1.1 Major Findings

Our behavioral analysis of the *Fmr*1 KO mice using the force plate actometer showed a significant difference in the locomotor activity of the KO mice compared to the WT mice, which agrees with earlier findings (*1-2*). The mice that received injections of amphetamine showed similar locomotor activity, however, the *Fmr*1 KO mice were less sensitive to amphetamine in their focused stereotypy behavioral response. At the 10 mg/kg dose, a dose in the range known for causing focused stereotypy (*3-4*), the KO mice showed a significant lesser amount of time spent in experiencing focused stereotypy.

By evaluation of DA release and uptake using brain slices from the *Fmr*1 KO and WT mice, we have shown that as the mice age, a significant difference in striatal DA release and uptake was seen in the 15 week and 20 week old mice, but no difference was found in the younger 10 week old mice. The mice that had undergone the behavioral analysis were in the 15 week group and the altered behavioral response may be explained by the impaired release. DA content analysis was done using HPLC to determine if the altered release was due to an alteration in the amount of DA present in the striatum. No differences in the concentration of DA in striatal homogenate were found.

By exposing the slices to increasing concentrations of AMPH and in another experiment GBR12909, we found that the affinity of AMPH and GBR for DAT is the same in both the KO and WT mice. Our results are consistent with the concept that

release impairments contribute to the altered behavioral response to AMPH. However, differences in the number of DAT protein molecules may also contribute.

We have also shown that there is no significant difference in the DA response after slice exposure to MPEP, an antagonist for MGluR5 receptors which are hypothesized to be hyperactive in Fragile X syndrome. The response to quinpirole, a selective D2 agonist, was also unchanged between the KO and WT mice, indicating proper D2 function in the KO mice. Data from mobilizing DA reserve pools by use of cocaine, after stimulated DA release was eliminated by D2 activation with quinpirole, indicated that reserve pools are unaltered in Fragile X syndrome.

5.1.2 Future Research Ideas

The levels of DAT are known to decrease with aging (*5*) and may decline more rapidly in FXS leading to alterations in the uptake of DA after stimulated release. In order to assess the amount of DAT present in the striatum of the *Fmr*1 KO mice compared to the WT mice, Western Blot analysis can be used.

DA release was impaired in the KO mice yet the total DA content was unchanged indicating a problem with the mechanism of release or the filling of vesicles. Since DA release is dependent on Ca^{2+} entry and studies have shown alterations in Ca^{2+} sensitivity in neurological disorders (*6*), a study evaluating the DA response to different concentrations of Ca^{2+} in the perfusion aCSF could lead to insight into the role of Ca^{2+} in the altered DA release seen in FXS. A study using Fura-2 would also provide a means to quantify calcium levels in brain slices (*7-8*).

One study has shown a potential utility of dosing Drosophila flies with small molecules to recover some of the phenotypical characteristics in FXS model Drosophila flies (*9*). One of the small molecules used was MPEP (2-Methyl-6-(phenylethynyl)pyridine). *Fmr*1 KO mice could be given MPEP in their food over time and the DA release and uptake studies done in brain slices repeated to evaluate if the administration of MPEP helps to recover the impaired DA release that we have shown.

.

5.2 "CHEMOBRAIN"

5.2.1 Summary of Findings

After dosing male *Wistar* rats with carboplatin weekly for four weeks, stimulated DA release and uptake was detected in slices. Data were collected in each of the four regions in the striatum. ANOVA analysis revealed a significant dose effect in the peak stimulated DA release as well as in the $[DA]_p$. However, V_{max} showed no significant effect over the doses. We also found no significant difference between the measurements taken in the different quadrants within a dose, showing that carboplatin had a generalized effect on DA release in all four quadrants of the striatum. DA efflux was also measured by inhibition of DA synthesis with αMPT and efflux caused by AMPH. There was no significant difference seen in the amount of DA efflux in the carboplatin treated rats.

5.2.2 Future Research Ideas

This work was done to collect preliminary data and confirm our hypothesis that the DA system undergoes alterations due to chemotherapy and contributes to the problem known as "chemobrain." There are many different prospective experiments that could advance the project and further our understanding of the neurological problems occurring during and after chemotherapy.

The experiment presented here should be repeated to confirm our findings as well as to provide more samples to use in collecting DA content data by HPLC since we

did not have enough samples to get statistically relevant data after this first study. It would also be beneficial to verify the reserve pool data.

It would also be advantageous to evaluate neurotransmitter release in other regions of the brain that are associated with cognition. One such location is the hippocampus, which may provide further insight to the chemobrain problem.

Various other chemotherapeutic drugs have been indicated in "Chemobrain" (*10-13*), especially in cases of breast cancer treatment. Since chemobrain is a post chemotherapy complaint most commonly from women who have undergone treatment for breast cancer, tailoring the drugs to match those most commonly used in breast cancer treatment would provide further insights into treatment of the cognitive issues experience by the reporting women.

After using male rats to establish the effects of just the chemo drugs on DA release, beginning to dose female rats will introduce hormonal effects, which can play a part in the experiences of the women reporting cognitive issues after therapy.

All of the data collected in this project will assist in the development of ways to treat the cognitive decline experienced by cancer patients. There have been successes with the use of methylphenidate and erythropoietin (*14-17*); however this work would open up more opportunities to find other, more suitable treatments.

5.3 CAGED COMPOUNDS

5.3.1 Summary of Findings

While caged compounds have been used in brain slices (*18-20*), utilizing caged compounds paired with FSCV opens up many opportunities to evaluate DA responses in real time to the photorelease of different compounds. We have shown that our instrumentation can successfully release glutamate bound to the *p*-hydroxyphenacyl photoprotecting group.

5.3.2 Future Research Ideas

The effects of photoreleasing pHP-glu on DA release and uptake in brain slices, while quantifying the amount of 4-HPA byproduct is produced by the light exposure to quantify the amount of glutamate released. After characterizing the immediate effects of releasing glutamate on DA release and uptake, GABA could be used since it has already been synthesized with the pHP protecting group.

Applying the use of caged compounds in brain slices of neurological disease states could also provide valuable information about the response to glutamate and GABA. It would be especially helpful in evaluation of the response of the DA system to glutamate and GABA photorelease in FXS since it is hypothesized that glutamate may play a role in the phenotypical problems associated with the syndrome.

The synthesis of other compounds utilizing the pHP “cage” would also allow for many other experiments to be performed to investigate the real time DA response.

5.4 REFERENCES

1. Baranek, G. T., Danko, C. D., Skinner, M. L., Bailey, D. B., Jr., Hatton, D. D., Roberts, J. E., and Mirrett, P. L. (2005) Video analysis of sensory-motor features in infants with fragile X syndrome at 9-12 months of age, *J Autism Dev Disord 35*, 645-656.

2. Einfeld, S. L., Tonge, B. J., and Florio, T. (1994) Behavioural and emotional disturbance in fragile X syndrome, *Am J Med Genet 51*, 386-391.

3. Jinnah, H. A., Gage, F. H., and Friedmann, T. (1991) Amphetamine-induced behavioral-phenotype in a hypoxanthine guanine phosphoribosyltransferase deficient mouse model of Lesch-Nyhan Syndrome, *Behavioral Neuroscience 105*, 1004-1012.

4. Rebec, G. V., and Segal, D. S. (1980) Apparent tolerance to some aspects of amphetamine stereotypy with long-term treatment, *Pharmacology Biochemistry and Behavior 13*, 793-797.

5. Salvatore, M. F., Apparsundaram, S., and Gerhardt, G. A. (2003) Decreased plasma membrane expression of striatal dopamine transporter in aging, *Neurobiol. Aging 24*, 1147-1154.

6. Yamamoto, M., Ozawa, H., Saito, T., Hatta, S., Riederer, P., and Takahata, N. (1997) Ca2+/CaM-sensitive adenylyl cyclase activity is decreased in the Alzheimer's brain: possible relation to type I adenylyl cyclase, *J. Neural Transm. 104*, 721-732.

7. Putney, J. W. (1990) Capacitative calcium entry revisited, *Cell Calcium 11*, 611-624.

8. Regehr, W. G., and Tank, D. W. (1991) Selective FURA-2 loading of presynaptic terminals and nerve-cell processes by local perfusion in mammalian brain slice, *Journal of Neuroscience Methods 37*, 111-119.

9. Chang, S., Bray, S. M., Li, Z. G., Zarnescu, D. C., He, C., Jin, P., and Warren, S. T. (2008) Identification of small molecules rescuing fragile X syndrome phenotypes in Drosophila, *Nature Chemical Biology 4*, 256-263.

10. Jim, H. S. L., Donovan, K. A., Small, B. J., Andrykowski, M. A., Munster, P. N., and Jacobsen, P. B. (2009) Cognitive Functioning in Breast Cancer Survivors: A Controlled Comparison, *Cancer 115*, 1776-1783.

11. Kannarkat, G., Lasher, E. E., and Schiff, D. (2007) Neurologic complications of chemotherapy agents, *Curr Opin Neurol 20*, 719-725.

12. Marin, A. P., Sanchez, A. R., Arranz, E. E., Aunon, P. Z., and Baron, M. G. (2009) Adjuvant Chemotherapy for Breast Cancer and Cognitive Impairment, *Southern Medical Journal 102*, 929-934.

13. Mustafa, S., Walker, A., Bennett, G., and Wigmore, P. M. (2008) 5-Fluorouracil chemotherapy affects spatial working memory and newborn neurons in the adult rat hippocampus, *Eur J Neurosci 28*, 323-330.

14. Meyers, C. A., Weitzner, M. A., Valentine, A. D., and Levin, V. A. (1998) Methylphenidate therapy improves cognition, mood, and function of brain tumor patients, *Journal of Clinical Oncology 16*, 2522-2527.

15. Rozans, M., Dreisbach, A., Lertora, J. J., and Kahn, M. J. (2002) Palliative uses of methylphenidate in patients with cancer: a review, *J Clin Oncol 20*, 335-339.

16. Sood, A., Barton, D. L., and Loprinzi, C. L. (2006) Use of methylphenidate in patients with cancer, *Am J Hosp Palliat Care 23*, 35-40.

17. Yamamoto, M., Koshimura, K., Kawaguchi, M., Sohmiya, M., Murakami, Y., and Kato, Y. (2000) Stimulating effect of erythropoietin on the release of dopamine and acetylcholine from the rat brain slice, *Neurosci. Lett. 292*, 131-133.

18. Kandler, K., Givens, R., and Katz, L. C. (1997) Photostimulation with Caged Glutamate, In *In Imaging Neurons: A Laboratory Manual* (Yuste, R., Lanni, F., and Konnerth, A., Eds.), Cold Spring Harbor Laboratory Press.

19. Lee, T. H., Gee, K. R., Davidson, C., and Ellinwood, E. H. (2002) Direct, real-time assessment of dopamine release autoinhibition in the rat caudate-putamen, *Neuroscience 112*, 647-654.

20. Lee, T. H., Gee, K. R., Ellinwood, E. H., and Seidler, F. J. (1996) Combining 'caged-dopamine' photolysis with fast-scan cyclic voltammetry to assess dopamine clearance and release autoinhibition in vitro, *Journal of Neuroscience Methods 67*, 221-231.

FIN.